UTILIZATION OF MICROALGAE IN GREEN CONTEXT: ADSORPTIVE REMOVAL OF IONIC CONTAMINANTS FROM AQUEOUS MEDIA AND PRODUCTION OF MICROALGAL BIOPLASTICS

by

Beste Özgümüş

B.S., Chemistry, Boğaziçi University, 2012

Submitted to the Institute for Graduate Studies in
Science and Engineering in partial fulfillment of
the requirements for the degree of
Master of Science

Graduate Program in Chemistry

Boğaziçi University

2019

ACKNOWLEDGEMENTS

First of all, I would like to express my gratitude to my thesis supervisor Assist. Prof. M. Fırat İLKER for giving me a chance to work with him and for his insightful guidance. I am grateful to him for his undepletable amount of patience, empathy and tolerance.

I am also very grateful to Prof. Loredana MARINIELLO for giving me an opportunity to train in her laboratory at University of Naples Federico II, for her valuable supervision, assistance and for trust in me. Thanks to her I have discovered my passion for bioplastics.

I would like to thank Assoc. Prof. Turgay ÇAKMAK for welcoming me in his laboratory and introducing me the art of microalgae cultivation. I am grateful for his guidance, friendship and patience. I am also grateful to my thesis committee member Assoc. Prof. Başak KAYITMAZER for reading and reviewing my thesis.

I would like thank Prof. Raffaele PORTA, Prof. Prospero DI PIERRO, Marilena ESPOSITO, Mohammed SABBAH for their friendship, helpful discussions and contributions to my studies; Asmaa AL-ASMAR, Maria FENDERICO, Manar ABDALRAZEQ, Harun AKSOY, Tuğba DAYIOĞLU, Mohammed AL-HADDAD for their endless support and friendship. I would like to express my special thanks to Prof. C. Valeria L. GIOSAFATTO for encouragement, support, friendship and guidance.

Additionally, I would like to acknowledge Boğaziçi University Research Fund (Grant Number 19B05P3) for the financial support for my research.

Last but least, I would like to thank my wonderful family, without them nothing would be possible.

ABSTRACT

UTILIZATION OF MICROALGAE IN GREEN CONTEXT: ADSORPTIVE REMOVAL OF IONIC CONTAMINANTS FROM AQUEOUS MEDIA AND PRODUCTION OF MICROALGAL BIOPLASTICS

Microalgae are known for their remarkable growth rates and adaptation capabilities. In this study, microalgae were used as environmentally friendly materials for two different applications. The first part is focused on removal of dyes from aqueous media using microalgae as adsorbents. Nile blue, methylene blue, eriochrome black t, and congo red are used as model charged contaminants. Seven microalgae species were used either immobilized in hydrogels or in free forms. Two of best cationic dye adsorbing species, *Chlorella* and *Scenedesmus* were selected for further experiments. Effects of growth period and Ca^{2+} deprivation on dye removal was studied. In kinetic experiments employing *Chlorella*, pseudo-first order, pseudo-second order and intraparticle diffusion models were employed for the interpretation of resulting data. Langmuir, Freundlich and Temkin models were used to fit resulting adsorption isotherms. Moreover, FT-IR analysis was conducted on these microalgae before and after dye adsorption.

In the second part, a type of cyanobacteria *Spirulina*-based biodegradable plastic films were prepared in different formulations by casting method. Films were characterized by tensile tests and zeta potential measurements. *Spirulina* was used in *Spirulina*/PVA blends in the absence or presence of several concentrations of microbial Transglutaminase as crosslinker. *Spirulina* was also tested as the single matrix with several concentrations of plasticizer and the enzyme. Additionally, proteins were extracted from *Spirulina* and films were prepared using this extract, modified or not modified with microbial Transglutaminase.

ÖZET

MİKROALGLERİN YEŞİL UYGULAMALAR KAPSAMINDA KULLANIMI: İYONİK KİRLETİCİLERİN SUDAN EMME YOLUYLA ARITILMASI VE MİKROALG BAZLI BİYOPLASTİK ÜRETİMİ

Mikroalgler yüksek büyüme hızları ve dikkate değer adapte olabilme yetenekleri ile bilinirler. Bu çalışmada mikroalgler çevresel uygulamalar bağlamında değerlendirilmiştir. Çalışmanın ilk kısmında, çeşitli mikroalg biyo-emiciler sudan kirletici boya arıtma testlerinde kullanılmıştır. Nil mavisi, metilen mavi, eriokrom siyahi t indikatörü ve kongo kırmızısı örnek iyonik kirleticiler olarak seçilmiştir. 7 mikroalg türü kalsiyum aljinat jelleri içinde ya da serbest şekilde kullanılmıştır. Katyonik boyayı en iyi emen türlerden ikisi, *Chlorella* ve *Scenedesmus* seçilerek büyüme periyodu ve Ca^{2+} eksikliğinin boya emme kapasiteleri üzerindeki etkileri çalışılmıştır. *Chlorella* kullanılarak psödo birinci derece, psödo ikinci derece kinetik modelleri ve parçacık içi difüzyon modeli çalışılmıştır. *Chlorella* ve *Scenedesmus* boya emme izotermlerinin Langmuir, Freundlich ve Temkin modellerine uygunluğu incelenmiştir. Bu iki mikroalg türünün boya emmeden önce ve sonra FT-IR analizleri yapılmıştır.

İkinci kısımda dökme metoduyla, farklı formülasyonlarda, bir siyanobakteri olan Spirulina bazlı biyo-bozunabilirliğe sahip plastik filmler hazırlanmıştır. Filmler çekme testleri ve zeta potansiyel ölçümleri ile karakterize edilmiştir. Spirulina çeşitli konsantrasyonlarda mikrobiyel Tranzglutaminaz çapraz bağlayıcı varlığında veya yokluğunda Spirulina/PVA karışımlarında kullanılmıştır. Ayrıca çeşitli plastifiyan ve enzim konsantrasyonlarında Spirulina tek bileşen olarak da kullanılmıştır. Buna ek olarak, Spirulina'nın proteinleri ekstre edilerek mikrobiyal Tranzglutaminaz ile modifiye edilmiş ya da edilmemiş filmler hazırlanmıştır.

TABLE OF CONTENTS

LIST OF FIGURES

LIST OF TABLES

LIST OF SYMBOLS

b_T	Temkin heat of adsorption
k_1	Pseudo-first order rate constant
k_2	Pseudo-second order rate constant
K_F	Freundlich adsorption capacity
k_i	Intraparticle diffusion parameter
K_L	Langmuir equilibrium constant
K_T	Temkin isotherm constant
n_F	Freundlich adsorbent/adsorbate affinity
q	Adsorption capacity
q_e	Adsorption capacity at equilibrium
q_t	Maximum adsorption capacity
q_t	Adsorption capacity at time t
R_L	Langmuir separation factor

LIST OF ACRONYMS/ABBREVIATIONS

ATR	Attenuated Total Reflection
bioPE	Biobased Polyethylene
bioPET	Biobased Poly(ethylene terephthalate)
BBM	Bold's Basal Medium
CA	Cellulose acetate
CR	Congo red
E	Young's Modulus
EBT	Eriochrome black t
EDTA	Ethylenediaminetetraacetic acid
FFS	Film forming suspension
FT-IR	Fourier Transform Infrared Spectroscopy
MB	Methylene blue
mTG	Microbial Transglutaminase
NB	Nile blue
PBS	Poly(butylene succinate)
PCL	Polycaprolactone
PHA	Polyhydroxyalkanoates
PLA	Poly(lactic acid)
PVA	Poly(vinyl alcohol)
SDS-PAGE	Sodium dodecyl sulfate polyacrylamide gel electrophoresis
SPE	*Spirulina* protein extract
TS	Tensile Strength
UTS	Ultimate Tensile Strength
WWTP	Wastewater Treatment Plant

1. INTRODUCTION

As a result of ever-growing rate of industrial production of goods, we face a multifaceted problem of environmental pollution and its adverse effects on human health and ecosystems. Every year thousands of new synthetic compounds enter in global market. Only in EU, between 2009 and 2018 more than 82,000 new entries have been registered [1].

The problem becomes more alarming when we consider that a large number of pollutants are very resistant to natural degradation pathways and can travel long distances. Furthermore, some of them, even when they are present at low concentrations, are known to accumulate in biological organisms, passing from generation to generation, from bottom to the top of the food chain. An increasing number of scientific reports suggest a correlation between certain pollutants and various health problems such as chronic diseases, many types of cancer, developmental problems, learning disabilities, immunological, behavioral, neurological and reproductive disorders, lower IQ, defects in visual recognition memory, short-term memory and motor performance, undesired genetic mutations in humans, animals and other organisms [2–11].

Chemical contamination in aquatic environments is a serious problem given the mobility and high solvation capacity of water. Chemicals can enter in aquatic environments by atmospheric deposition, weathering or by direct discharge of agricultural, domestic, or industrial waste products, also via wastewater treatment plants (WWTPs). Especially discharges from municipal and industrial WWTPs are a major source of aquatic chemical contamination in industrialized countries, revealing a growing need for superior yet economical treatment techniques [12]. Water can transport these contaminants to long distances through underground reservoirs and surface water currents. Recently microplastics and polyfluorinated chemicals found in snow and seawater in Antarctica clearly demonstrates ability of water to disperse contaminants to even the most remote, pristine habitats [13].

Microalgae and cyanobacteria are photosynthetic microorganisms that are found in every aquatic environment. They are photosynthetically more efficient than plants and contain high amounts of protein, lipids, carbohydrates, pigments, antioxidants and vitamins [14]. They are adaptable to different nutrient regimes and environmental conditions accumulating higher amounts of carbohydrates, lipids or other compounds under stress [15]. Because of many valuable chemical products that can be extracted from microalgae and cyanobacteria, together with desirable growth rates, they are cultivated for several commercial uses such as food supplements, animal feed, cosmetics, pharmaceuticals, food additives and biodiesel [14–18]. Recently application fields of microalgae and cyanobacteria extended to water treatment [19] and plastics [20].

As environmentally friendly products they have several advantages over plants. First, cultivation of microalgae or cyanobacteria does not require arable land or high freshwater consumption [21]. They can be cultivated in large open ponds under the sunlight or in suitable closed bioreactors. In addition, saline water or wastewater can be utilized as nutrient source [15]. Currently, efforts are being made to increase economic viability of microalgae and cyanobacteria commercialization by process optimization [21], biorefinery concept [22–24] utilization of residual biomass [25] or simply by using wastewater as nutrient source [22, 26, 27]. Therefore, it is expected that the cost of cultivation will diminish in near future.

This dissertation consists of the investigation of two of environmental applications of certain common types of microalgae: In one part environmentally friendly, economical and natural materials to be used in water remediation as adsorbents for removal of dissolved pollutants with diverse chemical structures; in the other part biodegradable film preparation from several formulations and characterization of produced films.

First part of the thesis is focused on utilization of microalgae for water remediation, focusing on the removal of water-soluble dyes that have distinct chemical structures and ionic characters encompassing all three possibilities, anionic, cationic and zwitterionic. Dyes are selected as models for ionic non-biodegradable contaminants. Due to their charge and polarity these contaminants have higher solubilities in water

and difficult to eliminate from aqueous media. Some of water-soluble pollutants have been known to be degraded by microbial action or through advanced water treatment techniques. However, some other pollutants, like dyes are recalcitrant, they resist microbial degradation, or degradation by light or oxidants, consequently they can stay intact in water for very long periods [12]. Furthermore, degradation of several azo dyes results in more toxic chemicals [28].

Second part will be focused on production and characterization of *Spirulina*-based biodegradable plastic films employing a convenient protein extraction technique without the use of organic solvents. Bioplastics production capacities are constantly increasing, global production increased from 1.58 million tons in 2013 to around 2.11 million tons in 2018 and furthermore, it is projected that it will reach to approximately 2.62 million tons in 2023 with a notable expansion in the share of biodegradable plastics over non-biodegradable ones [29–31]. Biopolymers as a convenient source for bioplastic production are renewable, abundant and rather easily biodegradable while they are suitable for further chemical functionalization or blend preparation [32].

Arthrospira, or conventionally called *Spirulina*, is an edible cyanobacterial genus that is remarkable with its high protein content. It has been commercially exploited for many decades in food, feed and cosmetics industries, owing to its suitability for large scale production. Today *Spirulina*, regarded as healthy food, is even added in food formulations such as pasta, ice cream, yogurt and biscuits [33, 34]. Furthermore, it has been employed for environmental applications like biogas production [35] and bioremediation [19]. High protein content of *Spirulina* makes it a good candidate for protein-based biodegradable films. In this study *Spirulina*-based films has been developed using either neat *Spirulina* or *Spirulina* protein extract in the presence or absence of microbial Transglutaminase, an isopeptide bond forming enzyme used for crosslinking proteins. Resulting films were characterized by tensile tests and additionally for *Spirulina* protein extract Z-average and zeta potential measurements were carried out.

1.1. Microalgae

1.1.1. Definition

Microalgae are eukaryotic microorganisms living in aquatic bodies that can utilize sunlight to produce biomass. Cyanobacteria, even though represent a diverse class of microorganisms, are conventionally called prokaryotic microalgae or "blue-green algae". Despite physiological differences both class of microorganisms can use sunlight, synthesize and accumulate commercially relevant biomolecules, adaptable to changes in environmental conditions, capable of photoautotrophic, heterotrophic and mixotrophic cultivation. Here in this study the term microalgae has been used for both microalgae and cyanobacteria unless specified otherwise, since the scope of this text is merely elaborating environmental applications of them.

1.1.2. Cultivation

One of the advantages of microalgae production is the adaptability of these microorganisms to a variety of conditions. They can be grown phototrophically, heterotrophically and mixotrophically. Photo-autotrophic cultivation requires simple and generally cheap macro and micronutrients. Wastewater, seawater or brackish water can be utilized for cultivation with the benefit of reducing costs. Considering diminishing water supply and increasing population, the fact that microalgae don't necessarily require freshwater is becoming more and more important.

Another advantage of microalgae cultivation is the high specific growth rate. They grow rapidly compared to higher plants with an average doubling time as 26 hours [36]. Under favorable conditions some strains achieve even shorter times down to 3.5 hours [24].

Moreover, microalgae can survive in various environmental conditions and nutrient regimes. They have the ability to modify metabolism in response to different environmental conditions and stress. They adapt to extreme conditions by accumulat-

ing polyols, lipids and carbohydrates [37–39]; recycling micronutrients [37] or thickening cell wall [38].

1.1.3. Applications

For many decades microalgae are commercially exploited in food, feed, cosmetic industries. Some species like *Chlorella* and *Spirulina* are completely edible and they are sold as food supplements in the market because of their high protein, lipid, mineral and vitamin content. Apart from human consumption, they are also utilized as animal feed in aquaculture. Some microalgae species produce pigments that have high market value [19]. In addition to the nutritional value of their content, several studies indicate immunoregulatory, anticancer, anti-inflammatory and antibiotic activity [40].

Recently application areas of microalgae are being expanded into biofuel production [24], water remediation [19] and bioplastic production [41, 42]. Studies focused on biofuel have brought about many advancements towards higher volume productions and commercialization of *Spirulina*. For the near future, expectations are towards a decrease in cultivation costs, which can stimulate expansion to other possible application areas.

1.2. Water Remediation by Adsorption

Adsorption technique is inexpensive, simple and effective way of removing pollutants from aqueous media. It is superior to other techniques in simplicity of design, ease of operation, cost effectiveness, insensitivity to toxic chemicals and lack of secondary pollution. In addition, safe operation of adsorption technique makes it available for use in several different settings, not limited to WWTPs [28]. Because of their recalcitrant nature, removal of dyes at low concentrations (and other recalcitrant polar pollutants) by conventional methods is not yet economically viable [43]. Therefore, eliminating these compounds from aquatic environments by sorption method is expected to provide an effective, economical and rapid way.

1.2.1. Types of Adsorbents Used in Water Remediation

Conventionally one of the most commonly used adsorbent and the most effective one is activated carbon. It is produced by pyrolysis followed by chemical activation to introduce functional groups on the surface upon which contaminants are adsorbed. Pyrolysis occurs at very high temperatures and hence the production of activated carbon is rather an energy consuming process. As much as it is an effective technique for removing variety of contaminants, its effectiveness has limits in removing polar contaminants [18]. Consequently, the search for novel and environmentally friendly adsorbent materials is in progress, especially when the need for large scale rehabilitation methodologies for water bodies is considered.

Natural macromolecules such as starch, chitin, chitosan, alginate are promising because they are abundant and possess plenty of functional groups such as carbonyl, hydroxyl, carboxyl, amine and amide that can interact favorably with adsorbates, therefore they have been tested for their sorption characteristics in many studies [44]. For example, considerable number of studies has been conducted on chitosan for its adsorptive capacity [45]. Depending on pH, chitosan can be polycationic and is able to interact by electrostatic interactions with anionic compounds. It can also bind to metal ions or electron deficient organic compounds to some extent depending on conditions employed [46]. Functional polysaccharides are used in many industrial product formulations (medicine, cosmetics, textile, paints) however one main disadvantage of their large-scale use is the rather high cost.

Another approach however is to use bio-based adsorbents as whole, that is without extracting biomacromolecules. Plants, algae, microalgae, bacteria and fungi contain many biomacromolecules that are rich in functional groups like carbonyl, hydroxyl, carboxyl, amine, amide therefore many sites to accommodate adsorbates. Among these microalgae some attract great attention because they are non-pathogenic, photosynthetic microorganisms with high growth rates and high photosynthetic efficiency [47]. In addition, they are rich in carbon compounds producing variety of biomacromolecules [15].

Also, noteworthy that microalgae production generally requires very simple and cheap compounds.

1.2.2. Microalgae as Novel Biosorbents

Microalgae, either living or dead, have been studied extensively for toxic heavy metal removal from water and has been proven to be an effective method for cationic compounds. Soeder et al. [48] reported Coelastrum proboscideum absorbs lead from 1.0 ppm solution with 100% removal yield in 20 hours at 23°C and about 90% after only 1.5 hours at 30°C. Metal ions not only adsorbed on cell walls but also can be accumulated inside the cells. Metal intake in cells are slow and specific to living cells. On the other hand, adsoption on cell wall is fast and doesn't require a living organism [19].

Microalgae have also been proven to be effective for dye removal from aqueous media. Many acidic and basic dyes were tested for their removal capacity. For example, Spirogyra rhizopus was able to remove Acid Blue 290, 1.36 times of its dry biomass whereas *Spirulina platensis*, was able to remove Acid Blue 9 1.45 times of its dry biomass [49, 50].

Several functional groups such as carboxyl, hydroxyl, phosphate, sulfate, amino, sulfhydryl on cell walls of microalgae account for high adsorption capacity. Coexistence of these groups makes cell walls of microalgae amphoteric in nature providing enough sites for both anions and cations to be attached [19, 51–53]. Because the structural diversity of micropollutant molecules is ever increasing, and the current thesis work focus on the investigation of microalgae species as promising biosorbents for the removal of diverse chemical structures.

1.2.3. Microalgae Cell Wall

Although large number of studies have been conducted on microalgae, composition and structure of microalgal cell wall has been almost unexplored compared to those of close relatives macroalgae. Keeping in mind the changeability of microalgal

cell wall it can be generalized that in eukaryotic microalgae the cell wall is generally consists of a microfibrillar layer of cellulose, sandwiched between amorphous layers of polysaccharide. Biochemical composition roughly contain: 25-30% cellulose, 15-25% hemicellulose, 35% pectin and 5-10% glycoproteins. It may be silicified or calcified, and it may be strengthened with plates and scales. Some species may contain a complex hydrocarbon layer of algaenan to increase cell wall resistance against lysis [54,55]. Cell wall composition and morphology may depend on species, strain, pH and temperature of the environment, growth media and life cycle [55].

For dye adsorption cell wall composition is of utmost importance. Therefore, factors that may alter the cell wall and affect dye adsorption is essential in this context.

Hanifzadeh et al. [37] showed Ca^{2+} deprivation showed no adverse effect on growth of *Chlorella sorokiniana*, conversely, lipids and carbohydrates were in significantly higher quantities, reaching 30% increase in biomass productivity in Ca^{2+} depleted medium. They obtained significantly higher number of cells, larger cell size and cell dry weight compared to nutrient replete control. Authors conclude that this phenomenon can be explained by less rigid and more permeable cell wall in the absence of Ca^{2+}.

Cell wall composition and thickness also change during life cycle. As young cells grow and proliferate the cell wall thickens. In fact, cell wall thickness changes drastically in growth phase. For example, newly formed daughter cells of *Chlorella vulgaris* possess 2 nm thin electron-dense unilaminar layer. The thickness reaches 17-21 nm upon maturation. Furthermore, the composition of cell wall is not constant during life cycle. Young cells have a more flexible cell wall composing from mostly hemicelluloses. The rigid microfibrillar chitosan-like layer is formed after maturation [56].

Motivated by above findings, in this dissertation work, dye adsorption performances of various microalgae have also been studied for the effect of Ca^{2+} deprivation and different growth periods, since these factors will result in cell walls of different

compositions. However, examination of cell wall compositions is beyond the scope of this study.

1.3. Bio-based Plastics

1.3.1. Classification

The term bioplastic is ambiguous because not all bio-based plastics are biodegradable and not all petroleum-based plastics are non-biodegradable. Therefore, a classification is needed to avoid misconception. Generally biodegradable plastics consist of three groups. Agro-polymers is one group and examples are starch, pectin, proteins, lignocellulosic products and chitosan. This group is characterized by high biodegradation rates. The second group is biopolyesters that are synthesized from bio-based monomers like those of PLA and PHA. The third group is biodegradable polymers that are synthesized from petroleum-based monomers like those of PCL and PVA [57]. Despite biodegradability under favorable conditions, petroleum-based bioplastics are not renewable consequentially not sustainable. There is another group that is bio-based non-degradable polymers. Polymers like bioPET, bioPE are identical to conventional petroleum derived ones however the monomers come from renewable sources. This group of polymers share the same fate of petroleum derived ones as they are non-degradable and contribute to plastic waste accumulation in the world [31].

1.3.2. Biopolymer-Based Plastics

Cellulose-based plastics are in the market for a while. In fact, cellulose acetate (CA) was first prepared in 1865 although biodegradable CA plastics have been in market since 1991. Most applications of CA have been replaced by petroleum-based plastics however it persists as a bio-based plastic [58]. Chitosan has remarkable mechanical and antibacterial properties and is mostly used in pharmaceutical, biomedical applications due to its excellent compatibility and ability to form complexes [59]. Starch is another biopolymer that is used in plastic applications, usually as a component of biodegradable or compostable blends from which packaging films, foams and disposable items

are produced. According to Nova Institute report [29] the annual production of starch was 428,000 tons in 2016. Protein-based plastics have been used as early as 1930 to produce car parts [60]. They were replaced by petroleum-based plastics however, in the last decades protein-based materials once again attracted attention as edible films and sheets, microencapsulating agents, adhesives, wound dressings and various bionanocomposites because of their excellent film forming and O_2, CO_2 barrier properties [61, 62].

1.3.3. *Spirulina*-Based Plastics

High protein content of *Spirulina* (55-70 %) [63] makes it a good candidate for protein-based biodegradable films. Only few studies exist about *Spirulina*-based plastics. It has been used mainly as a component of composite materials and blends for food packaging and biomedical applications [64–66]. Zeller et al. [20] used neat *Spirulina* as the single matrix and in a blend with polyethylene (PE) to produce compression molded plastics. Compared to neat *Spirulina*/PE blends have shown poor mechanical properties and performed unsatisfactorily. This is not surprising considering the incompatibility of two matrices. In another study Zhu et al. [41] demonstrated the effect of compatibilizer in poly(butylene succinate) (PBS)/*Spirulina* blends. In the presence of the compatibilizer maleic anhydride-grafted PBS *Spirulina*/PBS blends exhibited better cohesion and higher tensile strength. 50% *Spirulina* loaded samples exhibited 69.1% increase in tensile strength without change in elongation at break. Moreira et al. [42] developed *Spirulina* protein concentrate based nanofibers by free surface electrospinning methodology however in order to form uniform nanofibers blending with another polymer is necessary since high conductivity of protein solutions may create aggregates.

1.3.4. Microbial Transglutaminase Treatments on Proteins

Microbial transglutaminase (mTG) belongs to Transglutaminases family which are able to catalyze bond formation between Lys ε-amino and Gln γ-carboxamide groups in proteins. These inter- and intramolecular crosslinks alter physicochemical

properties of protein network which may results better mechanical and barrier properties in resulting films depending on the substrate. Microbial transglutaminase has broader substrate specificity and function in a wide range of pH and temperature [67]. Previous studies showed use of mTG yielded 2-fold increase in TS and 10-fold increase in elongation at break of whey protein/pectin blend films compared to control, as well as 36% decrease in both H_2O vapor and O_2 permeability [68]. Bitter vetch protein films modified by mTG demonstrated 700-fold decreased O_2 and 50-fold decreased CO_2 permeability together with increased TS [69].

2. AIM OF THE STUDY

The aim of this study was to investigate potential of microalgae as materials in water remediation and bioplastic production. The first focus was contaminant removal from aqueous media by adsorption method, in which the ultimate goal was to identify those biosorbents with high affinity towards all types of water-soluble organic molecules that represent different charge characters such as cationic, anionic or zwitterionic.

Adsorption method is an economical, easy and rapid way of contaminant removal. Production of commonly used adsorbent activated carbon is a very energy consuming process. Cell wall of microalgae have many functional groups which provide suitable sites for adsorption. Therefore, using biosorbents like microalgae offer a more environmental method. This is an initial investigation in the quest for a cheap natural adsorbent that can be used in removal of wide set of structurally different chemical contaminants from water. Nile blue, methylene blue, eriochrome black t and congo red, all synthetic organic molecules with different structures, are chosen as model charged, recalcitrant contaminants with different charge characters such as cationic, anionic or zwitterionic. Owing to light absorption in the visible range and high molar absorptivities, dyes can be quantified rapidly and economically by means of spectrophotometers.

Initially, adsorption capacities of various microalgae have been compared either in immobilized or free form. Then, *Chlorella* and *Scenedesmus* were selected for further experiments which include the effect of growth period and Ca^{2+} deprivation on dye removal capacity. Moreover, adsorptions were characterized by kinetic and equilibrium studies. FT-IR analysis was provided to determine which functional groups involved in adsorption process.

Another objective of this study was to prepare *Spirulina*-based biodegradable films. *Spirulina* is a very good candidate for protein-based films because of its high growth rate, high protein content and biocompatibility. It has been used in blend and as the single component. It was examined if *Spirulina* is a substrate of microbial

Transglutaminase and whether enzyme modification enhanced mechanical properties. Furthermore, proteins extracted from *Spirulina* were used to develop films modified or not with the enzyme.

3. EXPERIMENTAL

3.1. Materials and Methods

Sodium alginate, methylene blue and congo red were purchased from Fisher Scientific, $CaCl_2$ Anhydrous was purchased from J.T.Baker, nile blue (hydrogen sulfate) and eriochrome black t (C.I.14645) were purchased from Merck KGaA, all other chemicals were purchased from Sigma Aldrich and Cabot Norit® SA2 steam activated carbon was used.

Isolab RC-22/25 mm 0.22 μm syringe filters were used to filter activated carbon. Orbital Shaker was MRC BT-350 Shaking Water Bath and centrifuge was Ohaus FC5706 (6000 rpm = 4427 g) Deionized water was obtained from Elix® (10)UV Water Purification System Type 2 water system.

For all dye solutions stock solutions are prepared at 544 mg/L concentration. Stock phosphate solution was prepared by mixing 30.50 ml 0.2 M Na_2HPO_4 and 19.50 ml 0.2 M KH_2PO_4 and adjusting the final volume to 100 ml.

The microalgae species used in Sections 4.2 and 4.3 were kindly provided by Professor Turgay Çakmak; *Chlorella vulgaris* strain TMCC6 (*Chlorella*-M) and *Scenedesmus* sp. which were used in Sections 4.4, 4.6, 4.7 and 4.8 were cultivated in Professor Turgay Çakmak's laboratory in Istanbul Medeniyet University under his supervision. Another strain of *Chlorella vulgaris* strain CCAP 211/11B (*Chlorella*-L) which was used in Sections 4.5, 4.6 and 4.7 was kindly provided by Professor Melek Türker Saçan and it was grown in our laboratory.

The second part of the study, preparation of Spirulina-based bioplastic films, was conducted in Biotechnology Biochemistry and Enzimology (BBE) Research Group laboratories at University of Naples Federico II under the supervision of Professor Loredana Mariniello.

Microbial Transglutaminase is purchased from Ajinomoto Co. under the trade-name Activa® WM and derived from the culture of Streptoverticillium sp. The specific activity of the enzyme was 92 units/g. Estimation of enzymatic activity was carried out by a colorimetric hydroxamate assay [70]. *Spirulina* sp. was kindly supplied by ATI Biotech (Naples, Italy) under the trade name Italga.

3.2. Cultivation of Microalgae

Chlorella and *Scenedesmus* species were grown in Bold's Basal Medium (BBM) whose composition is given in Figure 3.1 [71]. The media volume didn't exceed 500 ml in 1000 ml Erlenmeyer flasks. The cultures were cultivated under continuous light and aerated with an air pump. The temperature was maintained at 25^0C. During the cultivation optical cell density was monitored on a daily basis at 680 nm with ultraviolet/visible (UV/Vis) spectrophotometer (UV-2600, Shimadzu, Kyoto, Japan). For the tests in Section 4.4 unmodified BBM (control) and Ca^{2+} free BBM were used. The samples were collected right after the start of culture, on 5^{th}, 10^{th} and 15^{th} day. For the rest of the tests all species were cultivated at exponential or linear growth phases. All glassware, culture media and air hoses were autoclaved before use, the flasks were properly plugged with cotton. Cultivation set-up is as shown in Figure 3.2. Harvested microalgae were centrifuged at 5000 rpm, washed twice with distilled water, lyophilized and stored at 4^0C until use. Microscope images were taken using Nikon Eclipse LV150N at 20x magnification.

3.3. Preparation of Hydrogels

3.3.1. Preparation of Neat Calcium Alginate Hydrogels

2% (w/w) sodium alginate was added to deionized water at room temperature under constant stirring and left overnight to achieve complete hydration. Then the solution was added dropwise into 0.1%, 0.5%, 1.0%, 2.0%, 4.0% and 10.0% $CaCl_2$ (w/w) solutions depending on desired crosslinking density with constant stirring. Upon addition of sodium alginate into $CaCl_2$ solutions beads formed immediately. After 15

Component	*Stock Solution* ($g \cdot L^{-1}$ dH_2O)	*Quantity Used*	*Concentration in Final Medium (M)*
Macronutrients			
$NaNO_3$	25.00	10 mL	2.94×10^{-3}
$CaCl_2 \cdot 2H_2O$	2.50	10 mL	1.70×10^{-4}
$MgSO_4 \cdot 7H_2O$	7.50	10 mL	3.04×10^{-4}
K_2HPO_4	7.50	10 mL	4.31×10^{-4}
KH_2PO_4	17.50	10 mL	1.29×10^{-3}
NaCl	2.50	10 mL	4.28×10^{-4}
Alkaline EDTA Solution		1 mL	
EDTA	50.00		1.71×10^{-4}
KOH	31.00		5.53×10^{-4}
Acidified Iron Solution		1 mL	
$FeSO_4 \cdot 7H_2O$	4.98		1.79×10^{-5}
H_2SO_4		1 mL	
Boron Solution		1 mL	
H_3BO_3	11.42		1.85×10^{-4}
Trace Metals Solution		1 mL	
$ZnSO_4 \cdot 7H_2O$	8.82		3.07×10^{-5}
$MnCl_2 \cdot 4H_2O$	1.44		7.28×10^{-6}
MoO_3	0.71		4.93×10^{-6}
$CuSO_4 \cdot 5H_2O$	1.57		6.29×10^{-6}
$Co(NO_3)_2 \cdot 6H_2O$	0.49		1.68×10^{-6}

Figure 3.1. Composition of Bold's Basal Medium (BBM).

minutes the beads were sieved out. The beads were washed with either deionized water or phosphate buffer diluted by 1% from stock solution, for 15 minutes to remove excess Ca^{2+} ions. Washed hydrogels were sieved out and freeze dried. Nile blue (NB) dye adsorption tests were carried out in 1% diluted phosphate buffer. To study the effect of buffer amount in the solution, in Section 4.1.1 some tests were carried out in 25% diluted phosphate buffer.

3.3.2. Preparation of Calcium Alginate/Microalgae Composite Hydrogels

Exactly 5 mg of each microalgae were added to 2% (w/w) sodium alginate solutions under constant stirring and the hydrogels were prepared as described in Section 3.3.1. The $CaCl_2$ solution concentration was 2.0% (w/w). All composite hydrogels were washed only with 1% diluted phosphate buffer to remove excess Ca^{2+} ions. The

microalgae species were *Chlorella*, *Dunaliella*, *Anabaena*, *Haematococcus*, *Scenedesmus*, *Phaeodactylum*, *Spirulina*.

Figure 3.2. Image of cultivation set-up.

3.4. Dye Adsorption Tests

All tests were done in batch mode, in 50 ml Falcon tubes under constant shaking at 150 rpm for predetermined periods. At the end of each period, final concentrations were analyzed by UV/Vis spectrophotometer using Shimadzu UV-1700 PharmaSpec. Maximum absorption wavelengths were 635 nm for NB, 664 nm for methylene blue (MB), 613 nm for eriochrome black t (EBT) and 497 nm for congo red (CR). Before studying with each dye, calibration curves are prepared from known concentrations and during the readings care was taken not to exceed absorbances in calibration curve ranges, the analyte solutions were diluted if necessary. Dye solutions were freshly prepared by diluting stock solutions to desired concentrations. All solutions contained phosphate buffer diluted by 1% from stock solution. The tests were conducted at room

temperature and were carried out in triplicates except the tests in Sections 4.1, 4.2 and 4.4. q (mg/g) is defined as adsorption capacity and it is given by

$$q = \frac{V\ (C_{initial} - C_{final})}{m} \tag{3.1}$$

where V (L) is volume of the dye solution, m (g) is the mass of the adsorbent, $C_{initial}$ and C_{final} (mg/L) are initial and final dye solution concentrations [43]. Removal yield (%) is given by

$$\text{Removal yield} = \frac{(C_{initial} - C_{final})}{C_{initial}} \times 100 \tag{3.2}$$

3.4.1. Hydrogel Dye Adsorption Tests

The tests were carried out either with neat calcium alginate hydrogels or with microalgae composite hydrogels for which 80 mg of dried hydrogels were weighted. In composite hydrogels the weight of microalgae was 5 mg. NB was used as an example of organic cationic dye for the dye adsorption tests and initial concentration was 10.75 mg/L for each sample. At the end of predetermined periods the hydrogels were removed easily from the solutions using a proper size sieve.

3.4.2. Free Microalgae Dye Adsorption Tests

At the end of each predetermined period, tubes were centrifuged at 6000 rpm for 10 minutes and supernatants were analyzed for final concentrations by spectrophotometer at corresponding maximum absorption wavelengths. Because of its small size centrifugation was not enough to separate activated carbon from solution therefore samples containing activated carbon as adsorbent were additionally passed through syringe filters of 0.22 μm porosity.

EBT forms complex with divalent cations and change color. In order to avoid color change caused by these cations, before spectrophotometric measurements 18 ml

of supernatant was transferred into 2 ml of 1% (w/w) Na_2EDTA solution as chelating agent.

For microalgae comparison tests 5 mg of dry pulverized microalgae was added in 40 ml of 10.75 mg/L NB solutions. The amounts kept identical to hydrogel dye adsorption tests for comparison purposes. In growth condition comparison tests 10 mg of dried microalgae and 10 ml of 6.8 mg/L NB solutions were used.

Growth condition comparison tests were conducted with two selected species, *Scenedesmus* sp. and *Chlorella vulgaris* that were grown in Prof. Turgay Çakmak's Laboratories at Medeniyet University, labeled simply as *Scenedesmus* and *Chlorella*-M. respectively.

For each set of measurements blank biosorbents were prepared at exactly the same conditions. These samples were used as reference in UV/Vis measurements to avoid any interference from suspended compounds.

3.5. Kinetic Studies

Another strain of *Chlorella vulgaris* strain CCAP 211/11B (*Chlorella*-L) that was grown in our laboratory was used to conduct kinetic studies. 300 mg of dried *Chlorella*-L was added into 300 ml of 20 mg/L dye solutions in Erlenmeyer flasks. The flasks were placed on orbital shaker at 150 rpm. After predetermined periods 3.5 ml samples were collected, centrifuged and transferred into another tube.

Two frequently used kinetic models to describe adsorption kinetics, Lagergren's pseudo-first order model and pseudo-second order model were employed. Additionally, intraparticle diffusion model was used.

Linear form of Lagergren's pseudo-first order rate expression [72] is given by

$$\log(q_{e,exp} - q_t) = \log q_{e,cal} - \frac{k_1}{2.303} t \tag{3.3}$$

where q_t, $q_{e,exp}$ and $q_{e,cal}$ (mg/g) are adsorption capacity at time t (min), experimental equilibrium adsorption capacity and calculated equilibrium adsorption capacity, respectively; and k_1 (min^{-1}) is the pseudo-first order rate constant.

Linear form of pseudo-second order rate expression [72] is given by

$$\frac{t}{q_t} = \frac{1}{k_2\, q_e^2} + t\frac{1}{q_e}. \tag{3.4}$$

where k_2 (g/mg min) is the pseudo-second order rate constant.

Intraparticle diffusion model expression is given by

$$k_i = \frac{q_t}{t^{\frac{1}{2}}} \tag{3.5}$$

where k_i (mg/g min^{-1}) is the intraparticle diffusion rate parameter, each step of intraparticle diffusion is specified with numbers. For intraparticle diffusion model to be valid, the above equation should give a straight line for each step of intraparticle diffusion [73].

3.6. Equilibrium Studies

Equilibrium studies were carried out with 20 mg dried adsorbent in 20 ml of MB, EBT and CR dye solutions. The initial concentrations were in the range of 3.4 - 544 mg/L. For convenience, initial concentrations are specified as multiple of X where X equals to 6.8 mg/L. The final concentrations were analyzed as described in Section 3.4.2, all samples were incubated long enough to reach equilibrium. The adsorbents were *Scendesmus*, *Chlorella*-M, *Chlorella*-L and activated carbon. Langmuir, Freundlich and Temkin models were studied as isotherm models. Coefficients were calculated from linearized forms of original equations. q_e is taken as experimental equilibrium adsorption capacity and used throughout equilibrium studies.

Linear form of Langmuir model [74] is given by

$$\frac{C_{final}}{q_e} = \frac{1}{q_{max}\, K_L} + \frac{C_{final}}{q_{max}} \tag{3.6}$$

where K_L (L/mg) is the Langmuir equilibrium constant and q_{max} (mg/L) is the maximum adsorption capacity which is calculated from linear form of the equation. Langmuir separation factor (R_L) [75] is defined by

$$R_L = \frac{1}{K_L\, C_{initial}}. \tag{3.7}$$

Linear form of Freundlich model [74] is given by

$$\ln q_e = \ln K_F + \frac{1}{n_F} \ln C_{final} \tag{3.8}$$

where K_F (L/g) is Freundlich adsorption capacity and n_F is the dimensionless affinity between the adsorbent and adsorbate.

Linearized Temkin isotherm model [76] is expressed as

$$q_e = \frac{RT}{b_T} \ln K_T + \frac{RT}{b_T} \ln C_{final} \tag{3.9}$$

where b_T (kJ/mol) is heat of adsorption and K_T (L/mg) is Temkin isotherm constant.

3.7. FT-IR Analysis

FT-IR analyses were conducted with an ATR-FT-IR equipment. Before analyses samples were collected at the end of isotherm studies, rinsed with deionized water, freeze dried and stored at 4^0C until the analysis. The analysis was carried out using Thermo Scientific Nicolet 380 FT-IR instrument equipped with a diamond probe and OMNIC^{TM} software. The range between 4000 cm^{-1}-400 cm^{-1} was scanned. Number of scans for each sample were 32 and data spacing was 0.482 cm^{-1}.

3.8. *Spirulina* Protein Extraction Procedure

Proteins were extracted as described by Safi et al. [77] with minor modifications. *Spirulina* was pulverized and suspended in deionized H_2O so that the ratio was 1:50 (w/v). The pH was measured to be 7.45. *Spirulina* suspension was sonicated for 40 minutes in an ice bath during which 2 minutes sonication and 6 minutes rest cycles were repeated. Then the pH of the suspension was stabilized to 12.00 using 1 N NaOH and kept under constant stirring for 1 hour, followed by centrifugation at 15,000 g for 20 minutes at 20^0C. The pellet obtained from pH 12 was stored at 4^0C. Supernatant was collected and pH was adjusted to 3.00 using 1 N HCl. After 10 minutes the mixture was centrifuged at 15,000 g for 20 minutes at 20^0C. Pellet (*Spirulina* protein extract) was collected, dried in climatic chamber at 25^0C and 45% relative humidity for 48 hours. The supernatant from pH 3 was also saved and kept at 4^0C for further analysis.

3.9. Film Preparation

3.9.1. *Spirulina*/PVA Blend Films

10% aqueous solution of PVA was prepared by heating it to 95^0C for 2 hours. *Spirulina* suspension was prepared by suspending 10% (w/w) *Spirulina* in deionized water, sonicating for 10 minutes in ice bath and heating to 55^0C for 4 hours. Glycerol and Activa® aqueous stock solutions were 10% (w/w). The film forming suspensions (FFSs) were prepared as indicated in Table 3.1. Activa® solution was added so that the final concentrations of mTG correspond to 18, 36, 72 and 145U/g Protein. All FFSs were incubated at 37^0C for 2 hours before casting. The films were casted on Petri dishes and dried in climatic chamber (25^0C, 45% relative humidity) overnight.

3.9.2. *Spirulina* Films

Spirulina suspension was prepared as described in Section 3.9.1. Sorbitol (SOR) and Activa® solutions were 10% (w/w). Compositions of FFSs are given in Table 3.2. The FFSs are incubated, casted and dried as described in Section 3.9.1.

Table 3.1. Composition of film forming suspensions of Spirulina/PVA blends.

Composition	**Sample**	**PVA**	***Spirulina***	**Glycerol**	**Activa®**	**Final Volume**
PVA	P	5.6 g	(-)	(-)	(-)	15 ml
PVA + GLY	PG	5.6 g	(-)	1.875 ml	(-)	15 ml
PVA + SP + GLY	PSG	5.6 g	6.250 ml	1.875 ml	(-)	15 ml
PVA + SP + GLY + mTG (18U)	PSGT1	5.6 g	6.250 ml	1.875 ml	0.781 ml	15 ml
PVA + SP + GLY + mTG (36U)	PSGT2	5.6 g	6.250 ml	1.875 ml	1.562 ml	15 ml
PVA + SP + GLY + mTG (72U)	PSGT4	5.6 g	6.250 ml	1.875 ml	3.125 ml	15 ml
PVA + SP + GLY + mTG (145U)	PSGT8	5.6 g	6.250 ml	1.875 ml	6.250 ml	15 ml

3.9.3. *Spirulina* Protein Extract Films

2% (w/w) SPE stock solution was prepared using deionized water, adjusting pH to 7.00 and stirring overnight for a complete hydration. Half of this solution was saved without any treatment (SPE-U). The other half was heated to 70^0C for 1 hour (SPE-H) as indicated by Chronakis [63]. While another 2% SPE was prepared by adjusting pH to 12.0 and stirring 2 hours. After 2 hours pH was brought to 7.0 (SPE-P). For each FFS 30 ml of 2% protein solutions were taken, 1.20 ml of 20% (w/w) SOR (40% with respect to SPE) was added. For enzyme treated films, 0.87 ml of 10% w/w Activa®

Table 3.2. Composition of film forming suspensions of *Spirulina* films.

Composition	**Sample**	***Spirulina***	**Sorbitol**	**Activa®**	**Final Volume**
SP + 30% SOR	S30	6.250 ml	1.875 ml	(-)	15 ml
SP + 30% SOR + mTG (36 U)	S30-mTG1	6.250 ml	1.875 ml	1.562	15 ml
SP + 30% SOR + mTG (72 U)	S30-mTG2	6.250 ml	1.875 ml	3.125	15 ml
SP + 40% SOR	S40	6.250 ml	2.500 ml	(-)	15 ml
SP + 40% SOR + mTG (36 U)	S40-mTG1	6.250 ml	2.500 ml	1.562	15 ml
SP + 40% SOR + mTG (72 U)	S40-mTG2	6.250 ml	2.500 ml	3.125	15 ml
SP + 50% SOR	S50	6.250 ml	3.125 ml	(-)	15 ml
SP + 50% SOR + mTG (36 U)	S50-mTG1	6.250 ml	3.125 ml	1.562	15 ml
SP + 50% SOR + mTG (72 U)	S50-mTG2	6.250 ml	3.125 ml	3.125	15 ml

solution was added (corresponding to 20U/g protein) to the mixtures. Final volumes were adjusted to 50 ml by deionized water and all FFSs were incubated at 37^0C for 2 hours before casting. The films were casted on Petri dishes and dried in climatic chamber (25^0C, 45% relative humidity) for 48 hours.

3.10. Kjeldahl Protein Quantification

Kjeldahl protein determination was carried out using Velp Scientifica DK6 Heating Digester equipped with a UDK 126A distillation unit. 1 g of dry biomass was used for each sample.

The titration was performed using 0.1 N HCl. Nitrogen to Protein conversion factor was taken as 6.25 [78].

3.11. Zeta potential and Particle Size Measurements

Zeta potential and hydrodynamic diameter called Z-Average were determined with Malvern® Zetasizer Nano-ZSP with automatic titrator unit (MPT-2). The device uses a helium-neon laser of 4 mW output power operating at the fixed wavelength of 633 nm. Temperature was set at 25°C, applied voltage was 200 mV and duration of each analysis was approximately 10 min. The measurements were carried out as triplicates and results were reported as mean ± standard deviation. Before titration, *Spirulina* was sonicated and pH was adjusted to 12.00.

3.12. Sodium Dodecyl Sulfate Polyacrylamide Gel Electrophoresis (SDS-PAGE)

SDS-PAGE was performed as described by Laemmli [79]. The samples (either mTG modified or not) were incubated at 37^0C for 2 hours prior to analysis. Sample buffer (pH 6.8, containing 15 mM of Tris–HCl, 0.5% (w/v) of SDS, 2.5% (v/v) of glycerol, 200 mM of β-mercaptoethanol, and 0.003% (w/v) of bromophenol blue) were added to samples in 1:4 (v/v) ratio (25 μl sample buffer for 100 μl sample), vortexed and incubated 5 minutes at 100^0C. The buffered samples were, then, loaded so that all the wells contain 25 μg of protein. Electrophoresis was conducted at 80 V for 2-3 hours and the proteins were stained with Coomassie Brilliant Blue R250. Bio-Rad Precision Protein Standards were used as molecular weight markers. Bio-Rad 4-20% gradient polyacrylamide precast gels were used except for film forming suspensions in Figure 5.5 which was freshly prepared 12% polyacrylamide gel.

3.13. Tensile Tests

Tensile tests were performed using Instron universal testing instrument model no. 5543A. Film tensile strength (TS), ultimate tensile strength (UTS), elongation

at break and Young's modulus (E) were measured according to the ASTM D882-97 (1997) using Test Method A, the static weighing, constant rate-of-grip separation test. The initial grip separation was 40 mm, and the crosshead speed was 10 mm/min in tension mode.

Film samples strips (10−11 mm wide and 50 mm long), obtained by sharp scissors, were conditioned for at least 2 hours at 54% relative humidty and 25°C by placing them into a desiccator over a saturated solution of $Mg(NO_3)_2.6\ H_2O$ before being tested. For each film type ten strips were used. Thickness of each strip was measured separately from at least 3 different points using Electronic digital micrometer DC-516 (sensitivity 0.001 mm). Film thickness results were reported as a mean of these measurements.

4. REMOVAL OF DYES FROM AQUEOUS MEDIA USING MICROALGAE

4.1. Calcium Alginate Dye Adsorption Optimization

4.1.1. The Effect of Buffer on Dye Adsorption

Before studying microalgae, optimal conditions for nile blue (NB) dye adsorption of calcium alginate hydrogels have been studied as control. The employment of gels was primarily due to the ease of recollection of millimeter size gels using proper sieves, even in large scale use. Alginate gel is one of the most conveniently prepared hydrogels. In addition, they provide a suitable matrix in the search of composite hydrogels carrying multiple adsorbents. Since dye adsorption tests were performed in buffered solutions, the effect of buffer wash which is carried out prior to dye adsorption process and the effect of buffer concentration used during the tests were examined. During hydrogel formation, free Ca^{2+} ions may stay in the matrix, removing these free cations effectively is important for following dye adsorption tests as they hinder dye-adsorbent contact. For that purpose, two hydrogels were washed with deionized water (A1, A25) and other two with buffer solution diluted by 1% from stock solution (A1-BW, A25-BW). The subsequent dye adsorption tests were carried out in either 1% diluted buffer (A1, A1-BW) or 25% diluted buffer (A25, A25-BW).

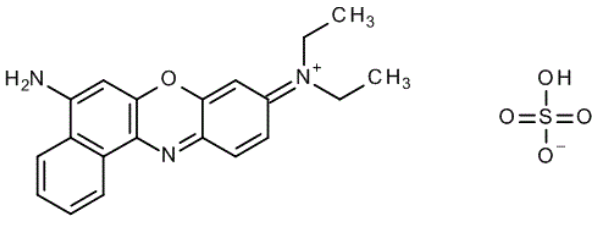

Figure 4.1. Chemical structure of nile blue.

The results of dye adsorption tests are presented in Figure 4.2. The gels washed with deionized water exhibit a delayed NB dye adsorption compared to buffer washed

ones. It is likely that, deionized water was insufficient in excess Ca^{2+} ion removal and presence of remaining free Ca^{2+} ions may impede NB adsorption onto gels. However possibly pointing out to selective ion exchange, at the end of 3-day duration similar dye adsorption values were obtained.

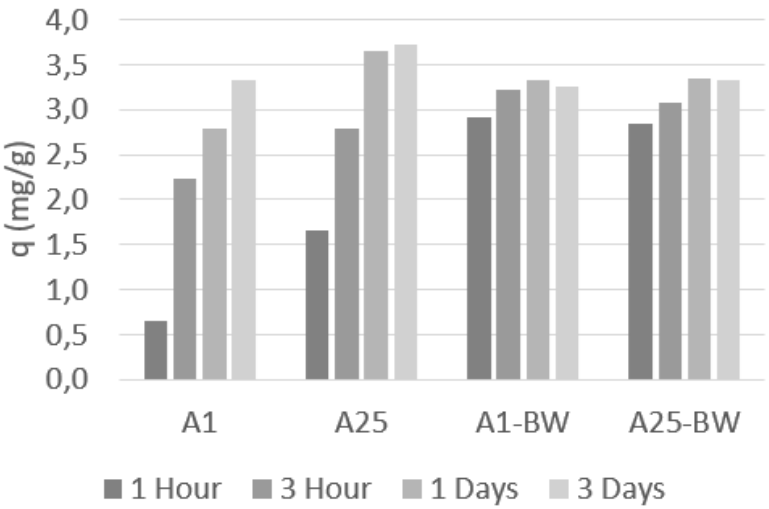

Figure 4.2. The effect of buffer on NB adsorption on calcium alginate gels. A1=1% diluted buffer, A25=25% diluted buffer, BW=buffer wash.

The buffer concentration used during dye adsorption process seems to have no effect on gels subjected to buffer wash previously. For gels washed with deionized water on the other hand, difference in the observed adsorption capacities may arise from the presence free Ca^{2+} ions. Phosphate anions may facilitate the ion exchange between free Ca^{2+} and NB.

4.1.2. The Effect of $CaCl_2$ Concentration on Dye Adsorption

Ca^{2+} ions form physical crosslinks with alginate during hydrogel formation. The concentration of Ca^{2+} ions effect crosslinking density and swelling behavior of the hydrogel, which is expected to enhance penetration and adsorption of dyes within the gel. Therefore, optimal concentration of Ca^{2+} ions for dye adsorption purposes was studied. The effect of $CaCl_2$ concentration as crosslinking agent on NB adsorption of the subjected gel is given in Figure 4.3. Sodium alginate solution has been added in

$CaCl_2$ solution with concentrations ranging from 0.1% (A-0.1) to 10.0% (A-10.0). The highest dye adsorption capacity was obtained with A-0.1 however the beads fractured after 1 hour, pointing to insufficient crosslinking resulting in poor mechanical properties. $CaCl_2$ concentrations of 0.5%, 1.0% and 2.0% had similar effect on the ultimate dye adsorption capacities. 4.0% $CaCl_2$ solution resulted in a delayed dye adsorption. The reason could be that rather densely crosslinked surface hindered penetration of dye molecules, along with the fact that higher amounts of Ca^{2+} cations keep the cationic dye away from the gel through electrostatic repulsion. When even higher amounts of crosslinking were induced, as in the case of 10.0% $CaCl_2$, results demonstrated clear negative effect on dye adsorption capacity

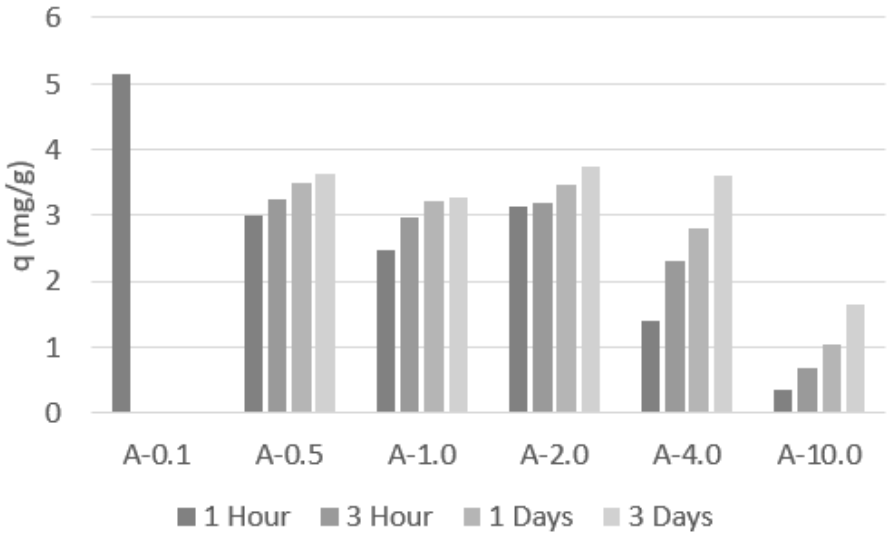

Figure 4.3. The effect of crosslink density on nile blue adsorption of calcium alginate gels. A=calcium alginate gel, numbers indicate the concentration of $CaCl_2$.

4.2. Dye Adsorption Tests of Calcium Alginate/Microalgae Composite Gels

In order to compare dye removal performances of structurally different types of microalgae, 7 different microalgae species and, to provide a comparison to a standard product, a suitable type of activated carbon were immobilized separately in calcium alginate hydrogels. A neat calcium alginate hydrogel was also prepared as control.

Hydrogel preparation was optimized according to the results of Section 4.1. NB removal yields of these hydrogels are given in Table 4.1.

Table 4.1. Nile blue removal yields (%) of various microalgae and activated carbon immobilized in calcium alginate. A=calcium alginate gel.

Adsorbent	**1 Hour**	**3 Hours**	**1 Day**	**3 Days**
A-Activated carbon	51.3	56.3	60.9	62.7
A-Chlorella	24.3	43.3	50.3	56.5
A-Dunaliella	21.0	47.3	55.9	63.3
A-Anabaena	50.5	53.8	56.9	54.6
A-Haematococcus	14.1	45.0	52.0	59.0
A-Scenedesmus	23.2	49.4	56.1	64.3
A-Phaeodactylum	47.1	54.5	58.7	62.4
A-Spirulina	20.6	43.1	49.2	56.5
A-Empty	27.7	49.1	55.8	62.3

It is notable that at the end of 1 hour Anabaena and Phaeodactylum loaded gels (A-Anabaena and A-Phaeodactylum) could remove NB molecules almost as much as activated carbon loaded gel (A-Activated carbon), whereas gels loaded with other types of microalgae and the blank gel showed a delayed dye adsorption. At the end of 3 days dye removal yields were in the range of 55-64%. Surprisingly dye removal of activated carbon loaded gel was limited to 63%. In control experiments performed, neat activated carbon, free from any gel coverage was able to remove the cationic dye, NB, in 95-100% range. Clearly immobilization in calcium alginate hindered an efficient dye/adsorbent contact to occur and yield unsatisfactory results. From one point of view this result was unexpected for cationic dye adsorption performances, because the swollen high surface area and anionic nature of alginate was expected to hold higher amounts of cationic dye due to ionic attraction, however possibly higher amounts of cationic calcium ions on gels could be counteracting, finally rendering alginate hydrogels poorer adsorbents compared to activated carbon or most of the microalgae studied. Consequently, in

the rest of the adsorption studies, microalgae were tested in free form rather than immobilized in alginate gels.

4.3. Dye Adsorption of Various Free Microalgae

Same set of microalgae species used in Section 4.2 were employed, in their free form. The aim of this section is to compare cationic dye removal performances of microalgae among each other and select best performing species for further studies with other types of dyes. Mass of microalgae utilized, initial dye concentration, volume of solutions was identical to those in the experiments of previous section. NB removal yields of these microalgae species and activated carbon are presented in Figure 4.4.

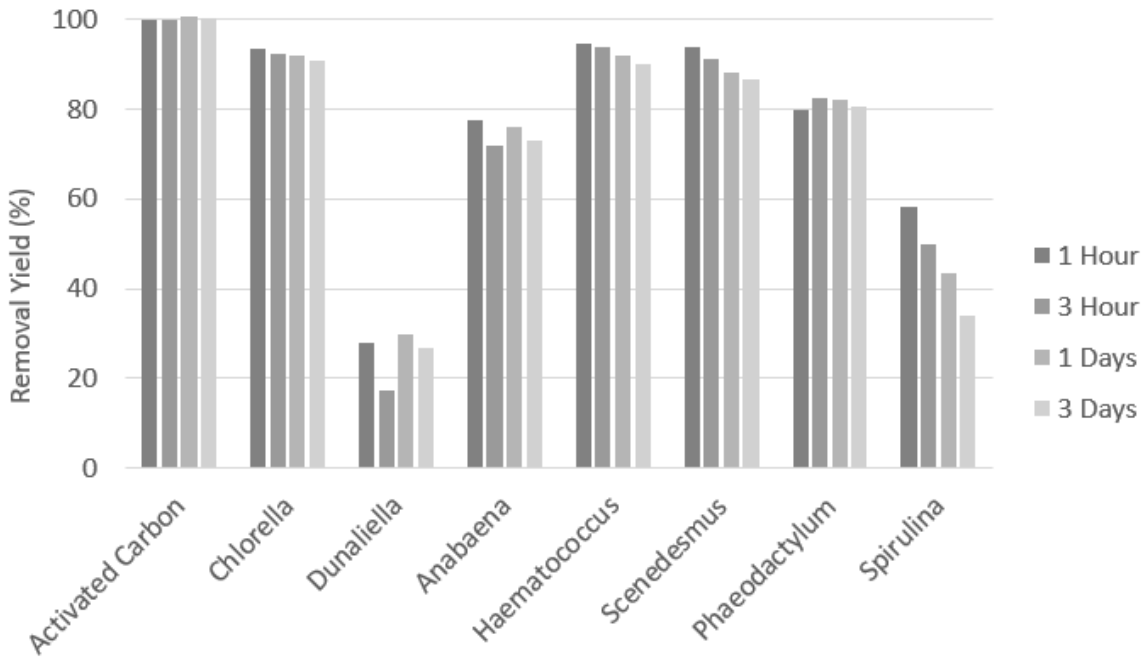

Figure 4.4. Nile blue removal yields (%) of various microalgae and activated carbon in free form.

Generally, dye removal yields of free microalgae were much higher than that of immobilized ones. *Chlorella*, *Scenedesmus*, *Haematococcus* were able to remove 93%, 94%, 95% of dye molecules in 1 hour, respectively. *Dunaliella* have the lowest dye removal yield which could be expected since this species is known to lack a rigid cell

wall. *Chlorella*, *Haematococcus*, *Scenedesmus* and *Spirulina* reached maximum dye removal yields in 1 hour followed by a slight decrease at longer durations. Presumably, decomposition of these microalgae may cause a slight decrease in their dye removal yields.

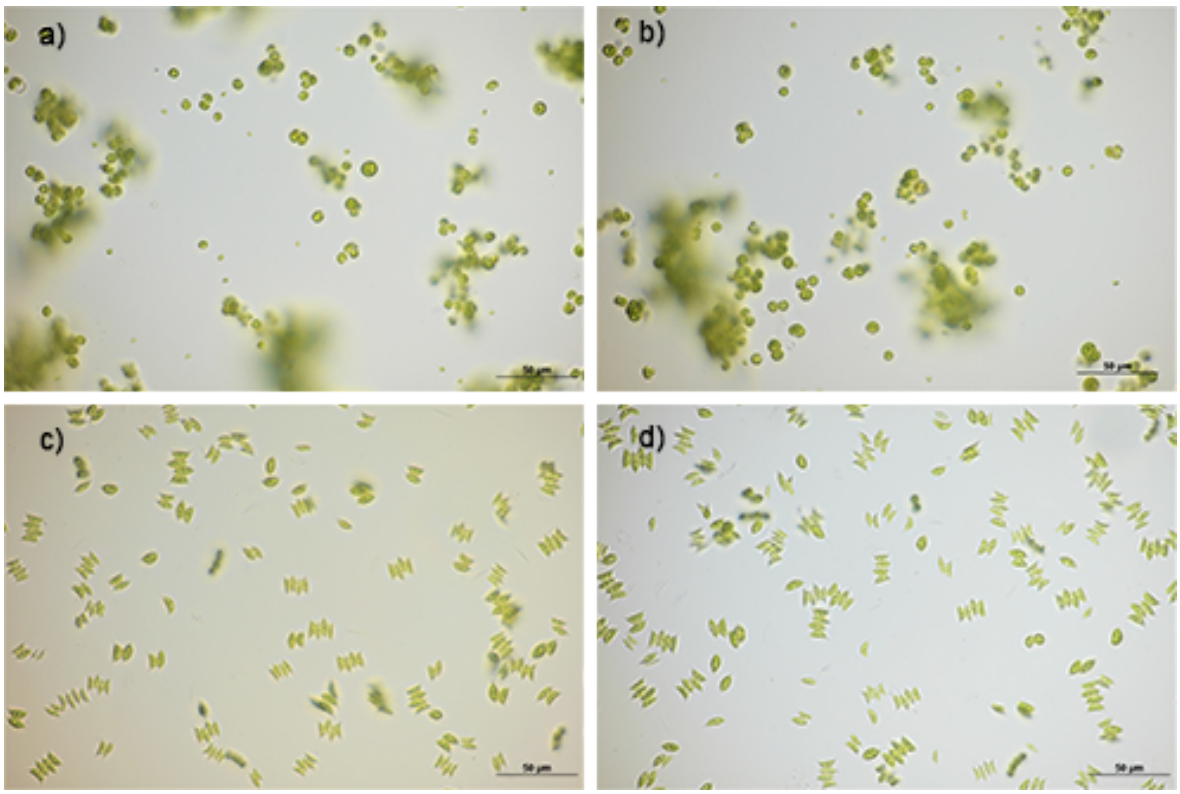

Figure 4.5. Microscope images of 15th day of the cultures. a) *Chlorella*-M control b) *Chlorella*-M under Ca^{2+} deprivation c) *Scenedesmus* control d) *Scenedesmus* under Ca^{2+} deprivation.

4.4. The Effect of Growth Period and Ca^{2+} Deprivation on Resulting Dye Adsorption Capacities

Two of the best cationic dye adsorbing species in previous section, *Chlorella* (*Chlorella*-M hereinafter) and *Scenedesmus*, were selected for further analysis. These species are also two of the most conveniently produced ones. In an attempt to improve dye removal efficiency, microalgae were harvested on 5th, 10th and 15th days from the start of cultures and used as adsorbents in dye removal tests. By this approach, it

was expected to investigate whether dye adsorption capacity of selected microalgae increases as the cultures grow older and number of mature cells increase. It is reported that mature cells are expected to have thicker cell walls [70] which in turn may increase dye adsorption capacities.

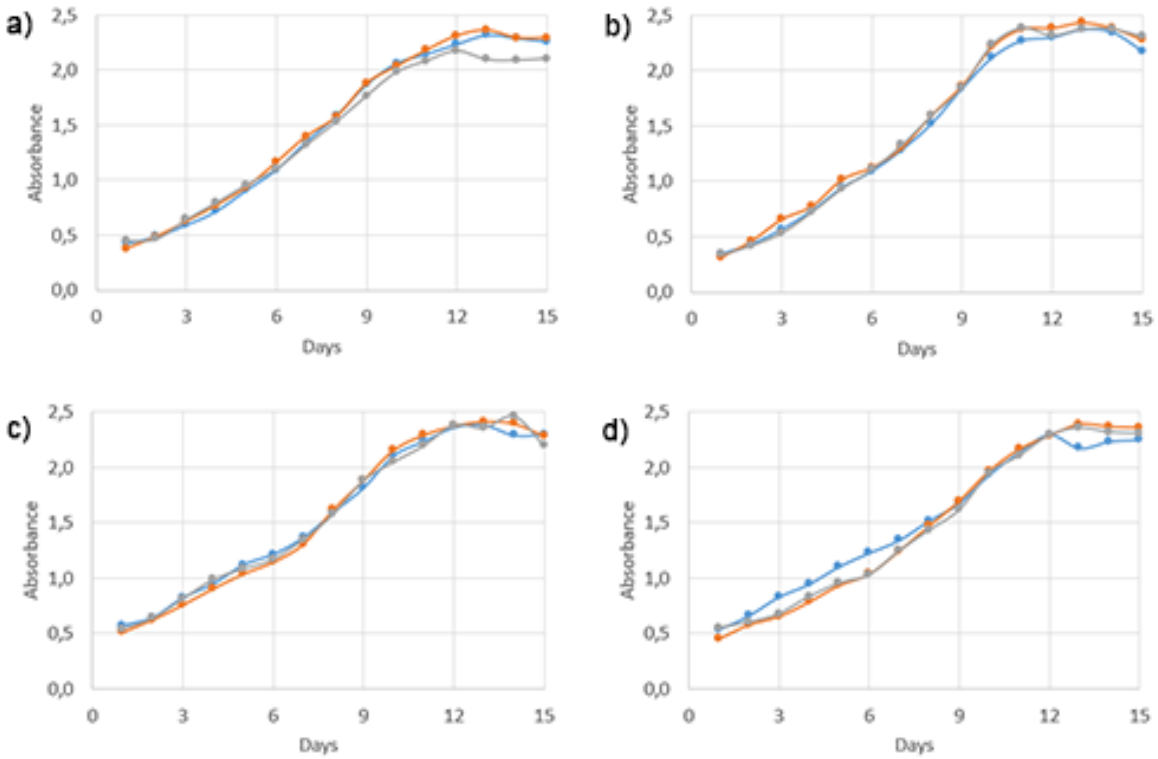

Figure 4.6. Optical density plots. Absorbance at 680 nm against culture day. a) *Chlorella*-M control b) *Chlorella*-M under Ca^{2+} deprivation c) *Scenedesmus* control d) *Scenedesmus* under Ca^{2+} deprivation.

Additionally, the effect of Ca^{2+} deprivation on dye adsorption capacity was studied. As indicated in Section 1.2.3 Ca^{2+} deprivation may have positive effect on cell wall flexibility and permeability [37] which may also increase dye adsorption capacity.

Hence *Chlorella*-M and *Scenedesmus* were grown in either BBM or Ca^{2+} free BBM to examine the effect of Ca^{2+}. Microscope images on 15^{th} day of cultures were given in Figure 4.5. No visual difference in morphology or cell size can be detected between control and Ca^{2+} deprived microalgae.

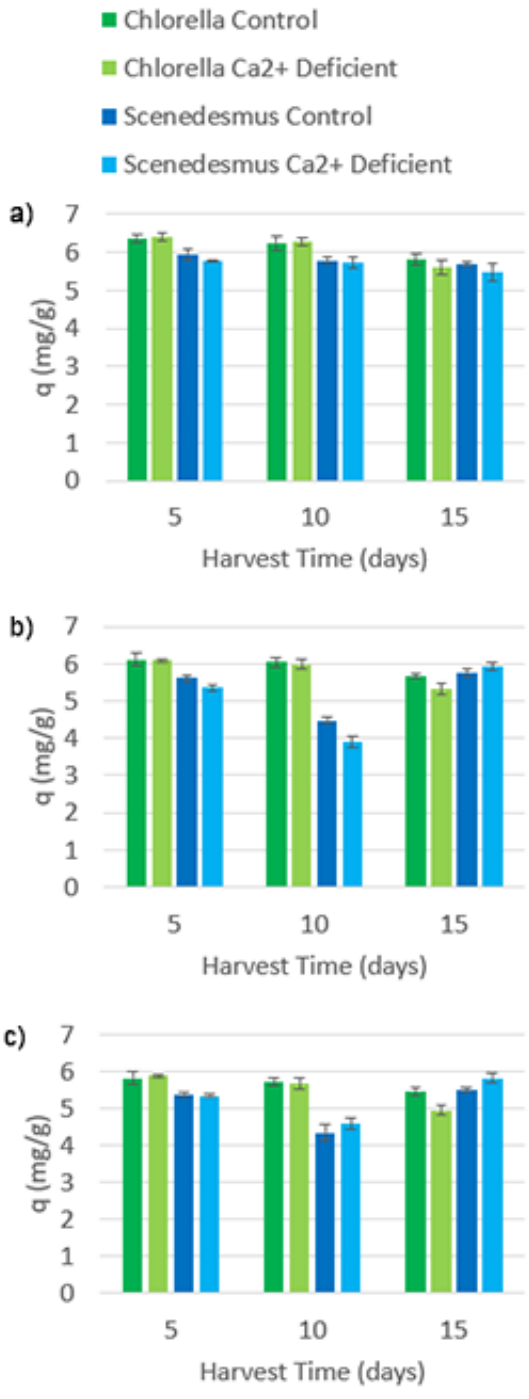

Figure 4.7. Dye adsorption capacities of *Chlorella*-M and *Scenedesmus* grown in control and under Ca^{2+} deprivation harvested in 5^{th}, 10^{th}, 15^{th} days a) 1-hour dye adsorption b) 1-day dye adsorption c) 3-day dye adsorption.

The microalgae were harvested on 5^{th}, 10^{th} and 15^{th} days of the cultures. Optical density against culture day plots are given in Figure 4.6. Optical density is defined by light absorbance value at 680 nm and plotting optical density values against time provides an easy way of monitoring microalgae growth. It should be kept in mind that it is not a quantitative method for obtaining biomass density. 680 nm is associated with chlorophyll's light absorbance. In Figure 4.6 it can be observed that 5^{th} and 10^{th} day represent the exponential or linear growth phases whereas 15^{th} days represents the stationary phase or the start of decline of the culture. Also, no difference can be seen between control and Ca^{2+} deprived microalgae.

The results of NB adsorption tests are given in Figure 4.7. The adsorbents were added in NB dye solution for 1-hour, 1-day and 3-day durations. 1-hour duration adsorption capacities of both microalgae exhibit no difference between Ca^{2+} deprived samples and control. Maximum dye adsorption capacities were observed for these samples. For *Chlorella*-M harvested on the 15^{th} day a slight difference between Ca^{2+} deprived samples and control was observed in longer dye adsorption durations. Meanwhile *Scenedesmus* showed a significant difference for samples harvested on the 10^{th} day for 1-day dye adsorption duration. The effect of Ca^{2+} deprivation is complex however it can be concluded that in our hands it did not improve dye removal efficiency at a considerable extent.

For samples harvested on the 5^{th} and the 10^{th} day, *Chlorella*-M outperformed *Scenedesmus* in each dye adsorption duration. For 15^{th} day harvested samples dye adsorption of *Chlorella*-M showed a decline, especially more pronounced for Ca^{2+} deprived samples. As in our previous assumption, this slight release of adsorbed dye could be due to a slow and partial degradation of microalgae bodies, which then would be expected to be more pronounced in Ca^{2+} deprived more permeable cell walls. As a general trend, dye adsorption capacities decreased for longer dye adsorption durations, and best results were obtained within 1-hour duration.

1-hour duration NB dye removal yields of *Chlorella*-M and *Scenedesmus* cultivated in control BBM is given in Figure 4.8 in comparison with activated carbon.

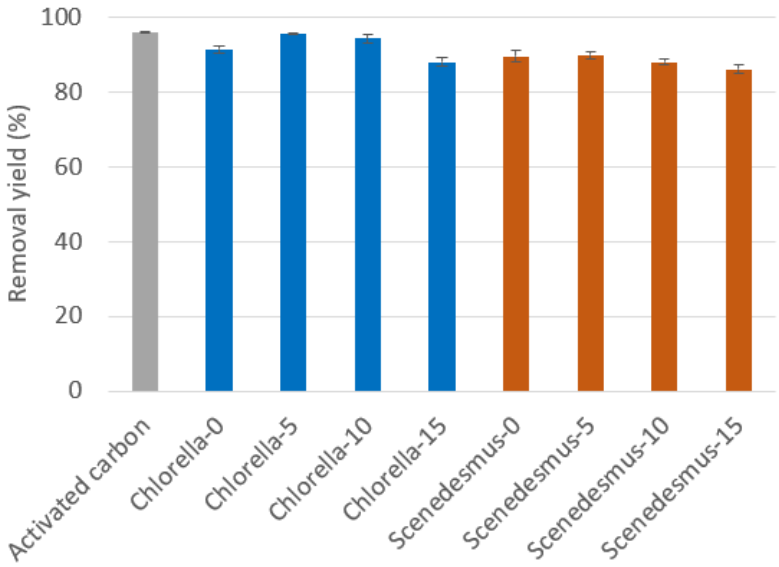

Figure 4.8. 1-hour nile blue removal yields (%) of activated carbon, *Chlorella*-M and *Scenedesmus* grown in control BBM and harvested on 0^{th}, 5^{th}, 10^{th} and 15^{th} days.

Samples were also collected immediately after the start of a new culture (*Chlorella*-0, *Scenedesmus*-0). The numbers next to *Chlorella*-M and *Scenedesmus* represent day of harvest from start of the cultures. For example, *Chlorella*-5 represents *Chlorella*-M harvested on the 5^{th} day.

There was a small decrease in removal yields for the 15^{th} day harvested samples therefore it is deduced that harvesting both microalgae in exponential or linear growth phases are slightly better for dye removal purposes. *Chlorella*-M harvested on 5^{th} day and 10^{th} day (exponential or linear growth phases) removed 96% and 94% of NB respectively, in the range of dye removal yield of activated carbon. Therefore, the rest of the study was conducted with microalgae harvested during exponential or linear growth phases.

4.5. Kinetic Studies

Encouraged by satisfying cationic dye removal performances of *Chlorella*, we have started a more conveniently available culture in our laboratory. This culture has been

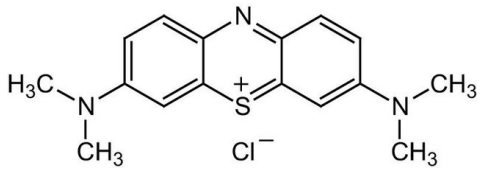

Figure 4.9. Chemical structure of methylene blue.

denominated *Chlorella*-L, its dye adsorption properties were measured to be in the same order with the previously studied strain of *Chlorella* (*Chlorella*-M) and consequently kinetic studies has been conducted with it. Another cationic dye methylene blue (MB) (Figure 4.9), an anionic dye eriochrome black t (EBT) (Figure 4.10) and a zwitterionic dye congo red (CR) (Figure 4.11) were used for kinetic studies, in which CR carries multiple cationic and anionic sites, with an excess anionic charge expected due to strong acidic nature of sulfonates. Pseudo-first order and pseudo second order are frequently used to model adsorption kinetics. Calculated rate constants (k_1, k_2), calculated and experimental equilibrium adsorption capacities ($q_{e,cal}$, $q_{e,exp}$) are summarized in Table 4.2. The time dependent change in adsorption capacities are presented in Figure 4.12.

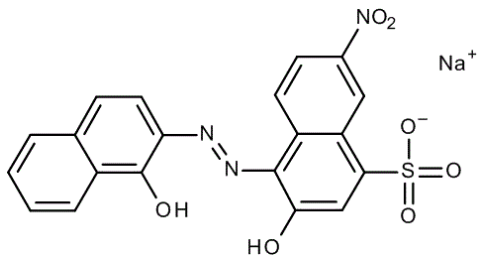

Figure 4.10. Chemical structure of eriochrome black t.

Coefficients of determination (R^2) indicate all adsorptions on *Chlorella*-L follow pseudo-second order kinetics. Calculated equilibrium adsorption capacities agree reasonably well with calculated values. This result is in good agreement with literature [72, 80, 81]. Linearized pseudo-second order plots of MB, EBT and CR are given in Figure 4.13. On the other hand, pseudo-first order model estimations of equilibrium adsorption capacities disagree with experimental data. Furthermore, coefficients of determination confirm the observed disagreement with pseudo-first order kinetics. Ho

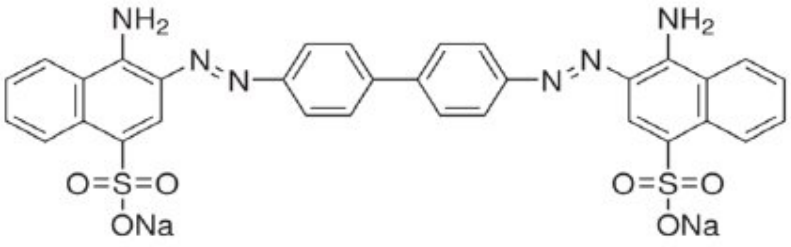

Figure 4.11. Chemical structure of congo red.

and McKay [72] stated that pseudo-first order kinetics are valid for initial 20 minutes of adsorptions. Consequently, it was expected that cationic MB adsorption on *Chlorella*-L could follow pseudo-first order kinetic model rather than pseudo-second order since it reached a plateau in 10 minutes. Whereas, anionic EBT and zwitterionic CR reached plateaus in 120 minutes and 90 minutes, respectively, thus follow pseudo-second order as anticipated.

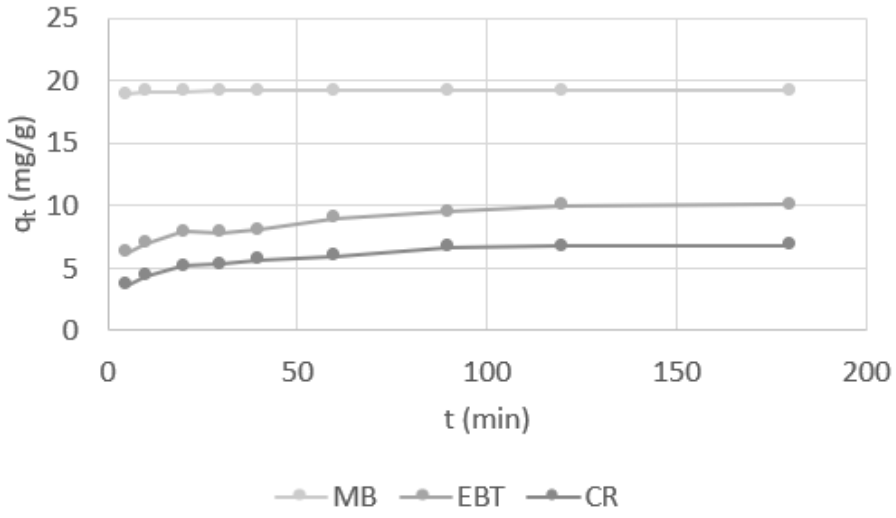

Figure 4.12. Time dependent change of adsorption capacities of *Chlorella*-L.

Despite not being a kinetic model, intraparticle diffusion model was selected to elaborate the adsorption steps. This model assumes that adsorption takes place in 3 steps. First, dye molecule migrates to exterior surface of adsorbent, then moves within the pores and finally is adsorbed on the surface of the material. As the third step is

Table 4.2. Pseudo-first order and pseudo-second order rate constants and maximum adsorption capacities.

Adsorbate	**Pseudo First Order**			**Pseudo Second Order**			**Experimental**
	k_1	$q_{e,cal}$	$\mathbf{R^2}$	k_2	$q_{e,cal}$	$\mathbf{R^2}$	$q_{e,exp}$
MB	0.044	0.957	0.534	2.096	19.157	1.000	19.166
EBT	0.033	5.521	0.886	0.013	10.406	0.998	10.049
CR	0.158	336.124	0.688	0.018	7.102	0.998	6.789

expected to happen fast, it is not the rate determining step. According to this theory, second step represents the main resistance to mass transfer and therefore it is the rate determining step. If the adsorption process can be explained by intraparticle diffusion model the plot of q_t against $t^{1/2}$ should give straight line or several straight lines in case the material is porous. The number and characteristics of these straight lines give information about the porosity of the adsorbent [73]. Intraparticle diffusion model coefficients of *Chlorella*-L is listed in Table 4.3.

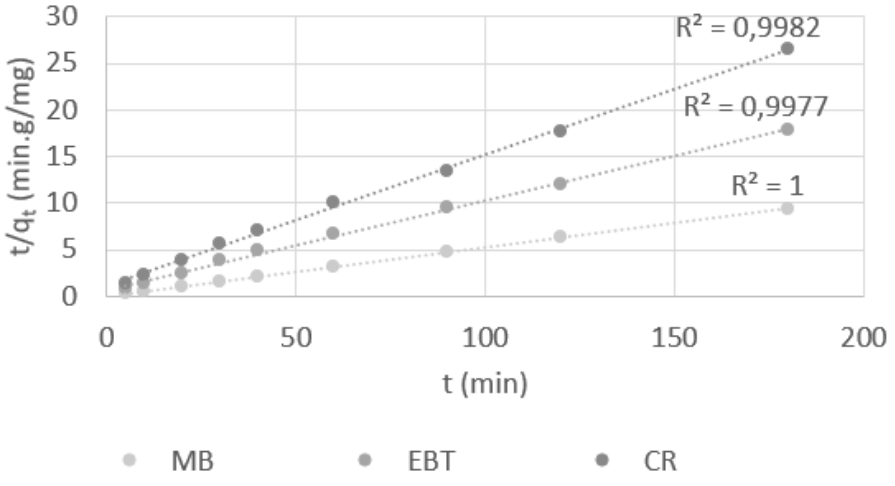

Figure 4.13. Linearized pseudo-second order plots of *Chlorella*-L.

The plot of q_t against $t^{1/2}$ did not result in a straight line for cationic MB which indicates intraparticle diffusion is not applicable. Since cationic MB adsorption was very rapid, it is possible that monitoring MB adsorption requires more frequent sam-

pling. Hence, possibility of MB adsorption following intraparticle diffusion model is not ruled out.

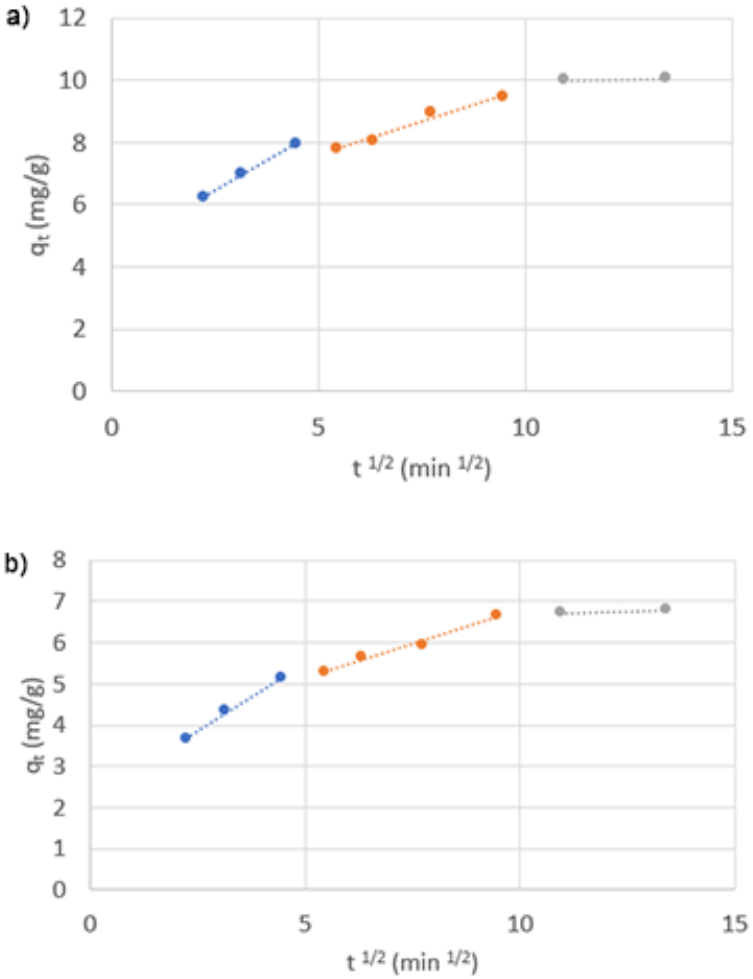

Figure 4.14. Intraparticle diffusion model of a) EBT b) CR on *Chlorella*-L.

The plots of q_t against $t^{1/2}$ of anionic dye EBT and zwitterionic CR is presented in Figure 4.14. Both dyes resulted in 3 straight lines implying 3 steps of intraparticle diffusion occurring during the adsorption of these dyes on *Chlorella*-L. Intraparticle diffusion constant (k_i) is not a rate constant, yet, it provides a means of comparison. For the first and second step, k values of EBT are higher than that of CR. Given larger and more rigid structure of CR it would not be surprising that it is transferred slower through the matrix.

Table 4.3. Intrapaticle diffusion model coefficients.

Adsorbate	**1st Step**			**2nd Step**			**3rd Step**		
	$k_{i,1}$	θ_1	$\mathbf{R^2}$	$k_{i,2}$	θ_2	$\mathbf{R^2}$	$k_{i,3}$	θ_3	$\mathbf{R^2}$
MB	(-)	(-)	(-)	(-)	(-)	(-)	(-)	(-)	(-)
EBT	0.765	4.523	0.999	0.437	5.397	0.973	0.018	9.803	1.000
CR	0.659	2.202	0.998	0.333	3.462	0.983	0.028	6.412	1.000

Plazinski et al. [82] proved that applicability of pseudo-second order kinetic model is not dependent on rate determining step, that it can be valid for diffusion-controlled adsorptions (like EBT and CR on *Chlorella*-L) as well as adsorptions whose slowest step is the third step.

4.6. Equilibrium Studies

In Section 4.3 cationic dye NB removal yields of various free microalgae and activated carbon were compared. In this section removal yields of 2 different strains of *Chlorella vulgaris* (*Chlorella*-M, *Chlorella*-L), *Scenedesmus* in comparison to a suitable type of activated carbon were studied for the removal of a cationic dye MB, an anionic dye EBT, and a zwitterionic dye CR in 3.4 - 544 mg/L (0.5 - 80X) initial concentration range in aqueous solutions. Results are given in Figure 4.15. Different adsorption patterns observed for dilute and concentrated initial dye concentrations. For concentrated solutions *Scenedesmus* showed the lowest adsorption capacities for each dye however for CR it exhibited better dye removal compared to *Chlorella*-L up to 5X (X = 6.8 mg/L) initial concentration.

Surprisingly MB removal yields of both *Chlorella* strains were higher than that of activated carbon at elevated concentrations of dye, even though for dilute concentrations of dye activated carbon outperformed *Chlorella* by a small difference, roughly less than 6% difference. In other words, while activated catbon is capable of removing 100% of MB dye, *Chlorella* (*Chlorella*-M or *Chlorella*-L) behaves as if few percent of

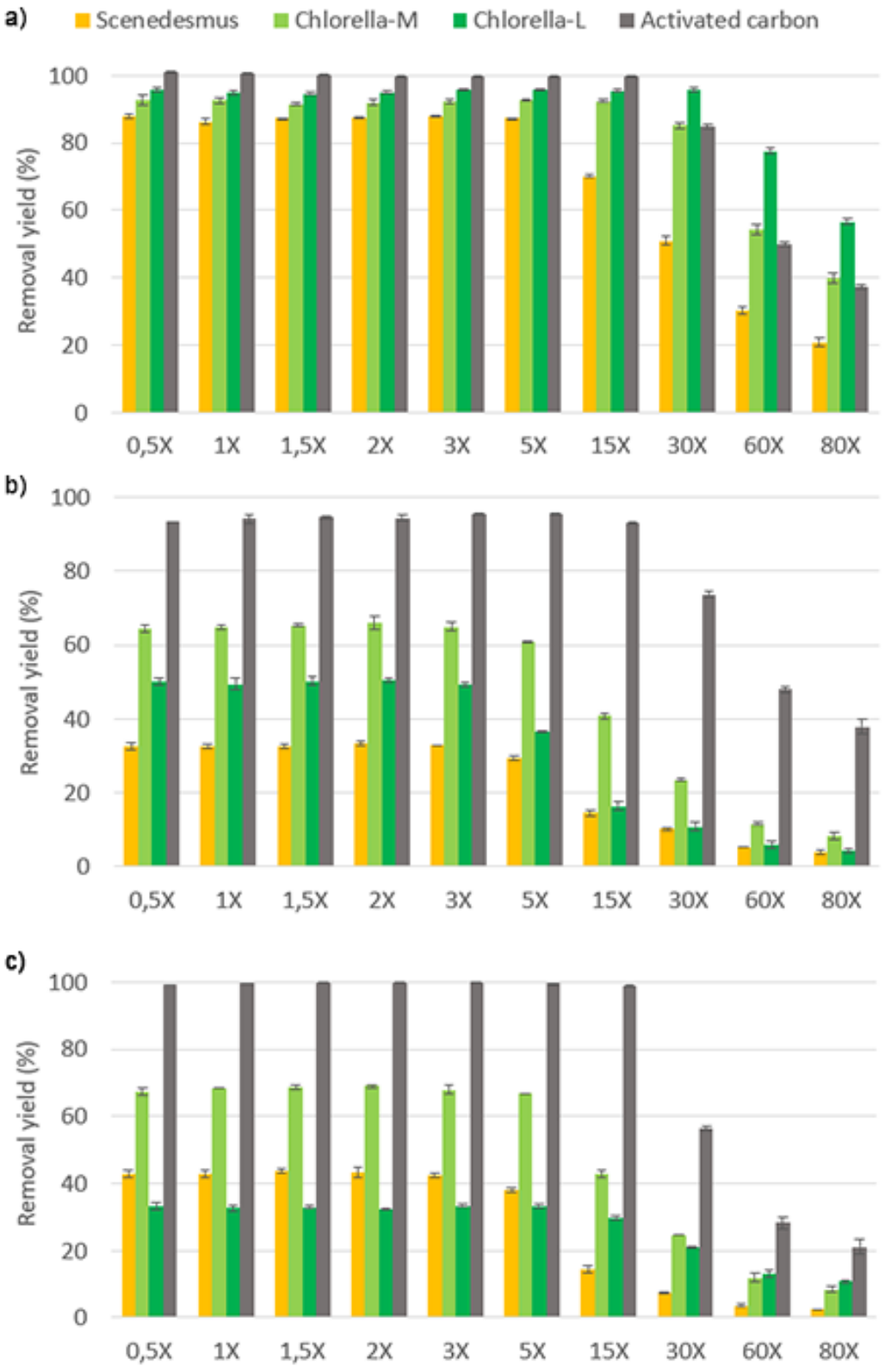

Figure 4.15. *Scenedesmus*, *Chlorella*-M, *Chlorella*-L and activated carbon removal yields (%) of a) MB b) EBT c) CR (X = 6.8 mg/L)

the cationic dye always remain in the solution, possibly in a dynamic equilibrium. Nevertheless, both strains have remarkably high cationic dye removal yields, approaching activated carbon. This fact is in line with Section 4.3. On the other hand, for anionic dye EBT and zwitterionic dye CR, activated carbon proved to be a better adsorbent.

4.7. Isotherm Models

Isotherms of MB, EBT and CR adsorptions on *Scenedesmus*, *Chlorella*-M, *Chlorella*-L and activated carbon were derived from equilibrium studies and given in Figure 4.16. Isotherm models were employed to obtain an insight about the mechanisms of adsorption processes. Three frequently used isotherm models Langmuir, Freundlich and Temkin were employed. Isotherm coefficients were calculated according to these models and listed in Table 4.4.

Langmuir model assumes a monolayer coverage of the adsorbate and equal affinities for all adsorption sites, as opposed to a three-dimensional multi layered structure with diverse affinities. Despite oversimplicity, according to high coefficients of determination ($R^2 > 0.99$), Langmuir model prediction suited best within the range of concentrations studied. Moreover, calculated q_{max} values generally agreed well with the experimental data. The Langmuir constant K_L reflects the affinity between adsorbent and adsorbate. High K_L values of activated carbon for MB and CR explained well the high removal yields, although for MB both *Chlorella* strains have higher q_{max} values compared to activated carbon.

Freundlich isotherm is frequently used to model heavy metal and dye adsorptions. It assumes multilayer adsorption without an equilibrium condition. Freundlich isotherm model assumes higher affinity binding sites are occupied first and binding affinity decreasing with increasing number of occupied sites [74]. n_F is related to the intensity of adsorption. It is accepted that when n_F is between 1 and 10, adsorption is favorable. [83] Table 4.4 reveals all n_F values are in this range therefore Freundlich model assumes a favorable adsorption for each adsorbent and adsorbate.

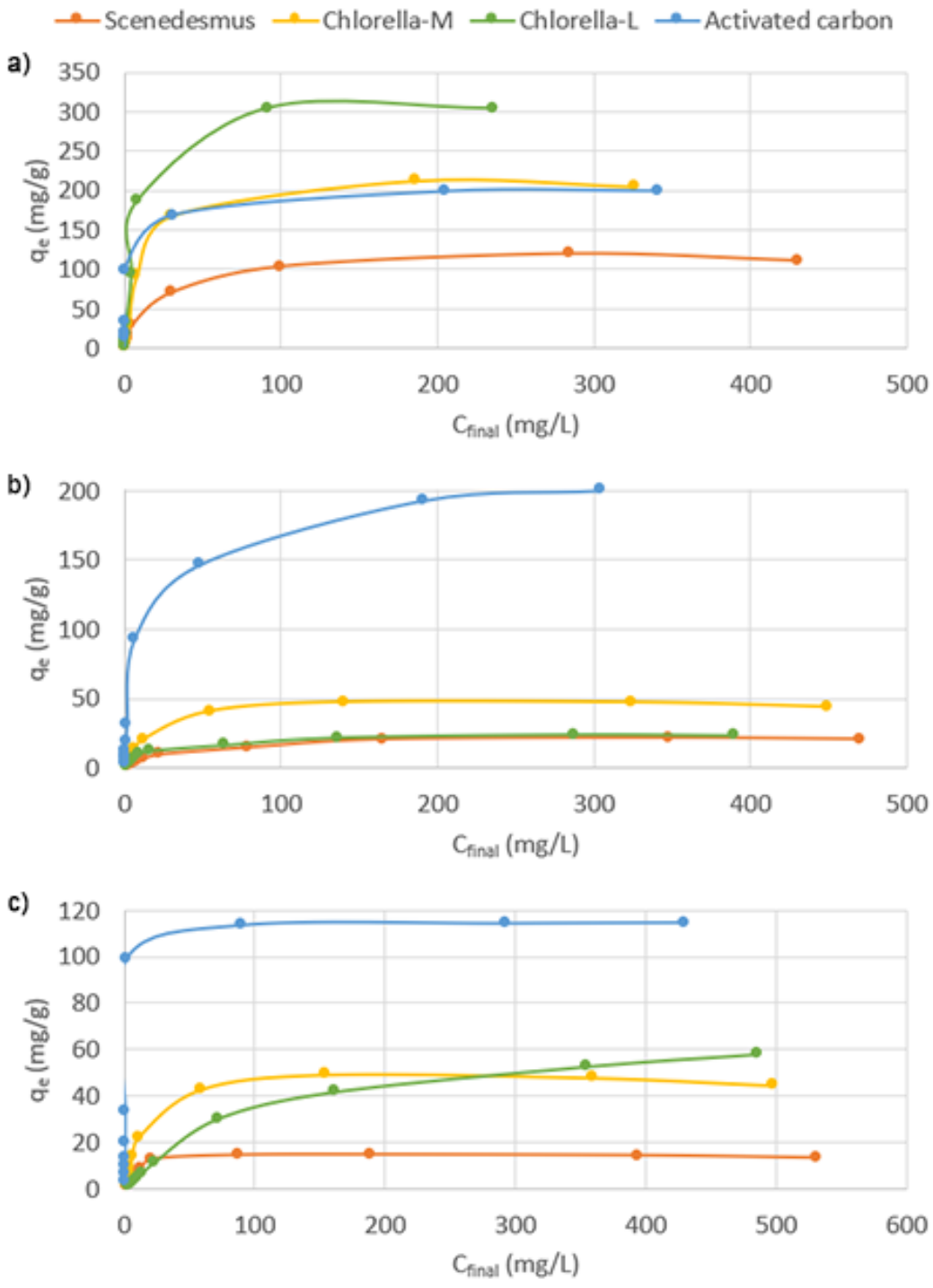

Figure 4.16. Isotherms of a) MB b) EBT c) CR

Table 4.4. Langmuir, Freundlich and Temkin isotherm coefficients of *Scenedesmus*, *Chlorella*-M, *Chlorella*-L and activated carbon for MB, EBT and CR.

		Scenedesmus			***Chlorella*-M**			***Chlorella*-L**			**Activated Carbon**		
Langmuir		q_{max} **(mg/L)**	K_L **(L/mg)**	$\mathbf{R^2}$	q_{max} **(mg/L)**	K_L **(L/mg)**	$\mathbf{R^2}$	q_{max} **(mg/L)**	K_L **(L/mg)**	$\mathbf{R^2}$	q_{max} **(mg/L)**	K_L **(L/mg)**	$\mathbf{R^2}$
	MB	118	0.07	0.997	217	0.07	0.998	323	0.08	0.997	200	4.17	1.000
	EBT	23	0.03	0.997	47	0.07	0.998	25	0.05	0.998	204	0.10	0.999
	CR	14	0.14	0.996	47	0.07	0.996	75	0.01	0.993	115	2.35	1.000
Freundlich		***Scenedesmus***			***Chlorella*-M**			***Chlorella*-L**			**Activated Carbon**		
		n_F	K_F **(L/g)**	$\mathbf{R^2}$	n_F	K_F **(L/g)**	$\mathbf{R^2}$	n_F	K_F **(L/g)**	$\mathbf{R^2}$	n_F	K_F **(L/g)**	$\mathbf{R^2}$
	MB	1.9	8.00	0.920	1.7	12.25	0,970	1.5	18.15	0.899	4.4	64.04	0.770
	EBT	1.9	1.28	0.908	2.1	3.82	0,878	2.3	2.49	0.875	1.9	16.24	0.906
	CR	2.9	2.34	0.740	2.2	4.08	0,864	1.5	1.12	0.960	6.1	50.92	0.793
Temkin		***Scenedesmus***			***Chlorella*-M**			***Chlorella*-L**			**Activated Carbon**		
		b_T **(kJ/mol)**	K_T **(L/mg)**	$\mathbf{R^2}$	b_T **(kJ/mol)**	K_T **(L/mg)**	$\mathbf{R^2}$	b_T **(kJ/mol)**	K_T **(L/mg)**	$\mathbf{R^2}$	b_T **(kJ/mol)**	K_T **(L/mg)**	$\mathbf{R^2}$
	MB	133	1.46	0.975	73	1.93	0.953	50	2.70	0.944	136	256.15	0.936
	EBT	594	0.44	0.978	292	0.90	0.948	581	0.87	0.986	86	3.53	0.988
	CR	1053	1.79	0.827	291	0.96	0.939	213	0.21	0.952	216	144.94	0.902

However, coefficients of determination indicate Freundlich model is unable to describe the obtained experimental data.

Worth mentioning that Freundlich model is valid for low concentrations. Up to 5 X initial concentrations all adsorbents gave coefficients of determination higher than 0.98 for linear fitted Freundlich model and diverge from linearity as concentrations increase. It has been suggested that Freundlich model may not be suitable for concentrated solutions [84].

Temkin model is used to predict binding energies. There are two Temkin constants; K_T Temkin isotherm constant and b_T (kJ/mol) heat of adsorption [76]. Although b_T doesn't give exact enthalpies, it provides a useful tool to compare binding energies and hence affinities between adsorbate and adsorbent. Calculated b_T values are very close for MB adsorption on *Scenedesmus* and on activated carbon; for EBT adsorption on *Scenedesmus* and *Chlorella*-L; for CR adsorption on *Chlorella*-L and activated carbon which suggests same type of binding sites may be responsible of adsorption process. Nonetheless, relatively low coefficients of determination indicate applicability of Temkin model is not appropriate for these adsorbent/adsorbate pairs.

4.8. FT-IR Spectra Comparisons of Neat and Dye Adsorbed Microalgae

FT-IR spectroscopy may provide useful information about functional groups involved in adsorption. Adsorbents used for FT-IR analysis were *Chlorella*-M and *Scenedesmus* and adsorbents after dye adsorption are labeled with MB, EBT or CR. For example, *Chlorella*-MB represents MB adsorbed *Chlorella*, so MB is expected to be bound on *Chlorella* surface.

FT-IR spectra of neat *Chlorella* and neat *Scenedesmus* (in other words before dye adsorption) are presented in Figure 4.17 and Figure 4.18, respectively. In FT-IR spectra of *Chlorella* and *Scenedesmus* almost all peaks fall within the same ranges, which indicate presence of similar structural components. Assignments of major bands for both species are as follows. The broad bands between 3600-3000 cm^{-1} were attributed

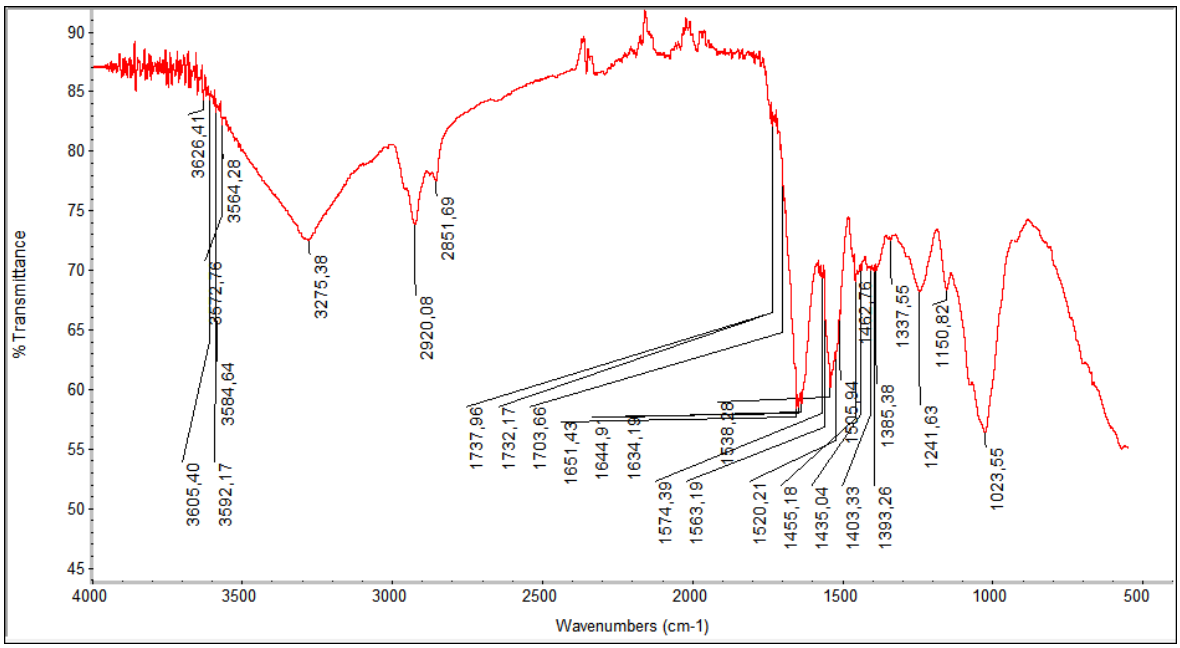

Figure 4.17. FT-IR Spectrum of neat *Chlorella*.

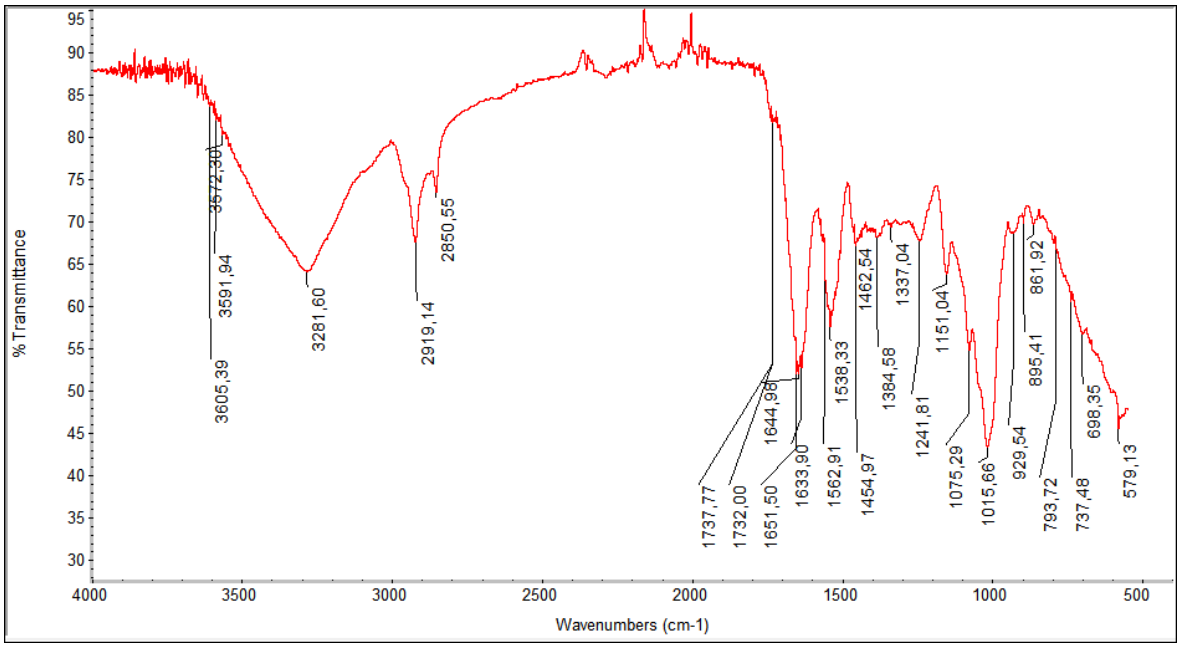

Figure 4.18. FT-IR Spectrum of neat *Scenedesmus*.

to O-H and N-H stretching, which are present in many biological components such as carbohydrates, proteins, nucleic acids. Bands at 2918, 2921 and 2850 cm^{-1} belong to asymmetric and symmetric stretching of sp^3 CH bonds, which are mostly present in lipids and carbohydrates. Peaks around 1732 cm^{-1} were assigned to C=O stretching bands of ester groups of *Scenedesmus* and *Chlorella*, respectively, most probably arising from lipids. Characteristic of proteins, amide I bands from C=O stretching and amide II bands from C-N stretching in combination with N-H bending vibrations, were present as multiple bands between 1700-1615 cm^{-1} and 1570-1500 cm^{-1}. Peaks between 1460-1440 cm^{-1}, and at 1385 cm^{-1} were assigned to bending vibrations of sp^3 C-H bond respectively. Again, for both species, major band peaking at 1240 cm^{-1} was easily observable, and it can be assigned as phosphate groups' P=O asymmetric stretching vibration. Two peaks that appear as shoulders at 1150 cm^{-1} and 1075 cm^{-1}, and the broad band with peaks at 1023 cm^{-1} or 1016 cm^{-1}, for *Chlorella* and *Scenedesmus* respectively, are characteristics of C-O stretching vibrations rising most probably from polysaccharide structures. However the shoulder peak at 1075 cm^{-1} may result from an overlap of symmetric stretching of P=O bonds of nucleic acids and/or phospholipids with polysaccharides' C-O vibrations, where C-O vibrations are expected to obscure bands rising from P=O bonds of nucleic acids and/or phospholipids [85]. Upon adsorptions of dyes on both microalgae species, major apparent changes in corresponding IR spectra were observed in the region between 1750 cm^{-1} and 1000 cm^{-1}, hence this particular region is taken as the focus of comparative FT-IR analyses below.

4.8.1. FT-IR Analysis of *Chlorella*-MB

FT-IR spectrum of *Chlorella*-MB superimposed with neat *Chlorella* spectrum are given in Figure 4.19. After MB adsorption on *Chlorella*, major bands of MB appeared and few changes in certain bands of *Chlorella* were observed. Changes in certain bands of *Chlorella* may be indicative of adsorption related to intermolecular interactions, such as ionic bonding, affecting the electronic environment and hence vibration of corresponding bonds of functional groups involved in adsorption. Looking at frequencies lower than 1732 cm^{-1} where most shifting bands and additional bands were observed,

a minor peak at 1732 cm^{-1} shifted to 1727 cm^{-1}. Several other minor peaks at 1714, 1704, 1694, 1687 cm^{-1} disappeared or may be masked by slightly expanding amide I band. These changes indicate that there may be some minor involvement of carbonyl

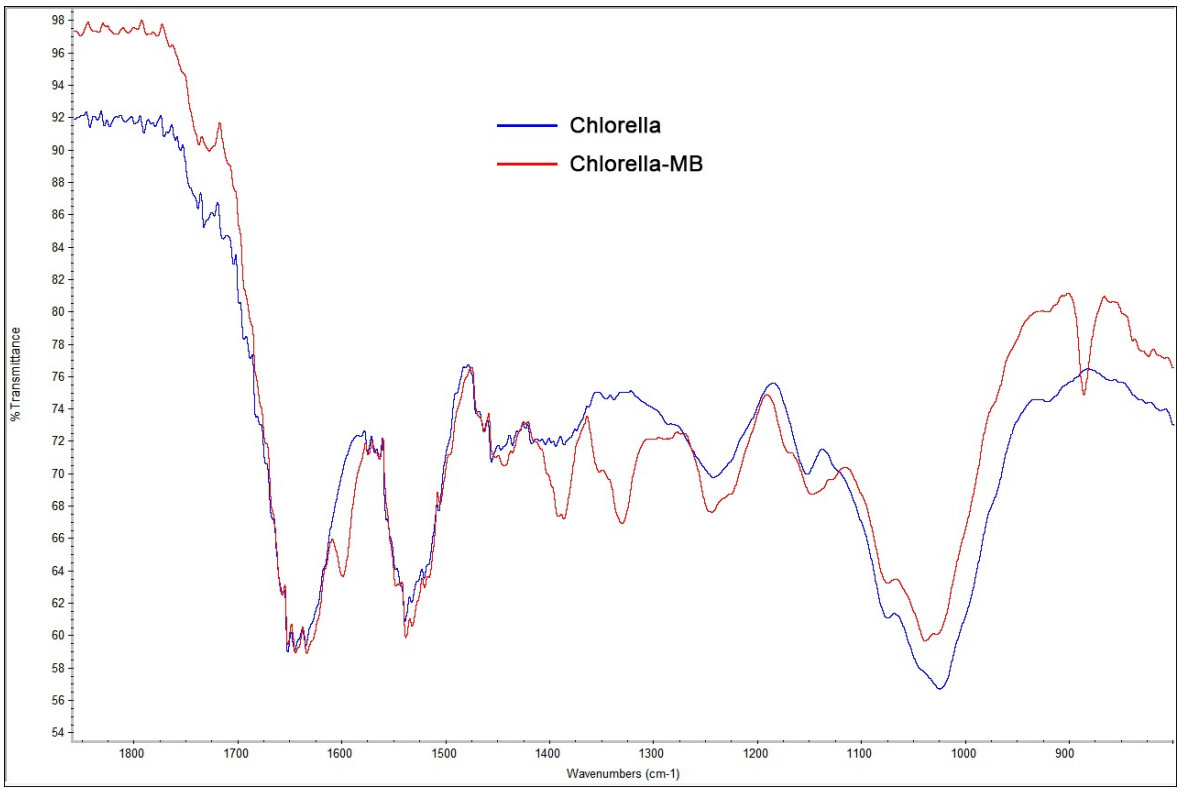

Figure 4.19. FT-IR spectra of *Chlorella* (Blue) and *Chlorella*-MB (Red).

group bearing functionalities, such as carboxylic acids in adsorption process of MB. However, disappearing bands are at very low intensities in comparison to much larger intensities of adsorbed MB bands, hence these very minor changes do not provide an explanation for the mechanism of adsorption. Changes in amide I and amide II bands are practically no detectable. The peaks at 1455 $cm^{-1}$and 1446 cm^{-1} which were attributed to asymmetric C-H bending, appear to have slight shifts to 1451 cm^{-1} and 1443 cm^{-1} caused by altered electron density upon adsorption on *Chlorella*. The broad band with a peak at 1242 cm^{-1}, which can be attributed to asymmetric stretching of P=O of nucleic acids or phospholipids, slightly changed in its appearance upon MB dye adsorption. This slight change in appearance can possibly be caused by the rise of rather low intensity peaks of MB dye as will be discussed in the next paragraph.

Peak at 1151 cm^{-1}, which we have assigned for C-O stretching, also had a shift to 1147 cm^{-1} upon MB adsorption, and two shoulder peaks appeared which can be assigned for MB peaks, as described in the next paragraph. May be the most noticeable change was observed near 1024 cm^{-1} which is attributed to C-O stretch of alkoxy groups in carbohydrates/polysaccharides. After MB adsorption, intensity of 1024 cm^{-1} peak decreased substantially, and a new peak appeared at 1038 cm^{-1}, as if part of the 1024 cm^{-1} vibrations shifted to higher frequency vibrations due to the intermolecular interactions involved in adsorption process. This change, together with the shift in 1151 cm^{-1}, indicate that it may be polysaccharides that are mostly involved in the adsorption process of the cationic dye MB.

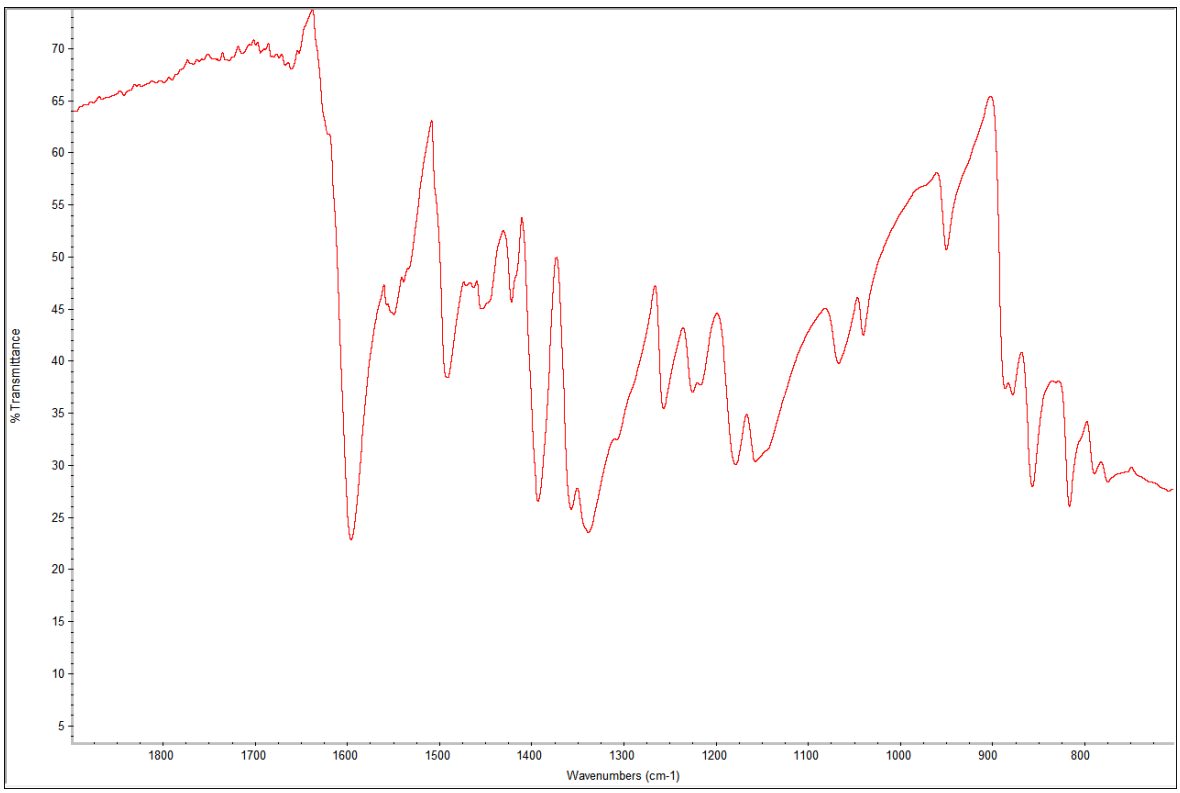

Figure 4.20. FT-IR spectrum of methylene blue (MB).

Then we focus on the appearance and shifts of MB bands upon adsorption on *Chlorella*. FT-IR spectrum of MB is given in Figure 4.20. A new peak at 1599 cm^{-1} appeared in *Chlorella*-MB spectrum. Likely, it is the conjugated C=C vibrations appearing at 1595 cm^{-1} [86] shifted to higher energy upon adsorption. In MB, an increased

electron density within the π-electron system upon ionic bonding could have caused this shift. The asymmetric C-H bending peaks also changed slightly; those peaks at 1455 cm^{-1} and 1446 cm^{-1} shifted to 1451 cm^{-1} and 1443 cm^{-1} with an apparent intensity increase observed for the peak at 1443 cm^{-1}. The peak at 1435 cm^{-1} was also present in neat *Chlorella* but its intensity increased.

There are two other bands appearing rising from MB vibrations, which masked the original peaks of *Chlorella* in the range of 1420-1270 cm^{-1}. Firstly, twin peaks appearing at 1390 cm^{-1} and 1385 cm^{-1} were assigned to symmetric C-H bending that were very weakly present in neat *Chlorella* at 1393 cm^{-1} and 1385 cm^{-1}. However, after adsorption on MB, intensity of these peaks increased considerably. In the original spectrum of MB only one peak appears at 1392 cm^{-1}, however upon adsorption a twin peak appearing at 1390 cm^{-1} and 1385 cm^{-1} may indicate that part of methyl groups are electronically affected through adsorption process. This may be a logical hypothesis because it is feasible that only one, out of two dimethyl amino group, would be involved on ionic adsorption.

Secondly, strong peaks appeared at 1351 cm^{-1} and 1330 cm^{-1} in *Chlorella*-MB spectrum were assigned to $C{=}S^{+}$ and tertiary amine C-N stretching, respectively [86], which originally appeared at 1356 cm^{-1} and 1338 cm^{-1}. Once again, these clear shifts point out to a change in electron density distribution of MB upon adsorption. Positive center of MB is distributed between dimethyl amino N and heterocyclic S atoms, through resonance. Hence it is logical to observe shifts in both positive centers. This result also points out to ionic nature of adsorption process. If covalent bonds were formed through these centers however, a much larger shift in the resulting spectrum would be expected.

MB peaks, which are originally at 1256 cm^{-1} and 1225 cm^{-1} and which can be assigned to C-H and heterocyclic C-C vibrations respectively, appeared as overlapped with the asymmetric phosphate band of *Chlorella*. The peak at 1256 cm^{-1} must have shifted to lower frequencies and was superimposed with asymmetric phosphate band. Once again, this observation can be explained by a change in the electronic environment

of amino methyl groups of MB, supporting the hypothesis of their involvement in an ionic adsorption process. Two shoulder peaks at 1169 cm^{-1} and 1127 cm^{-1} that appeared in *Chlorella*-MB spectrum can be assigned as bands belonging to MB that were originally at 1178 cm^{-1} and 1156 cm^{-1}, and are attributed to heterocyclic C-H/C-C and C-N vibrations, respectively [86].

4.8.2. FT-IR Analysis of *Scenedesmus*-MB

After adsorption of MB on *Scenedesmus*, similar changes with *Chlorella*-MB were observed in the *Scenedesmus*-MB spectrum (Figure 4.21). The minor peak at 1714 cm^{-1} disappeared and a slight shift in 1728 cm^{-1} peak to 1727 cm^{-1} was observed. As with *Chlorella*, these minor changes indicate a minor involvement of carbonyl group bearing functionalities nevertheless, considering much larger intensities of inherent MB peaks, carbonyl groups cannot be hold responsible of the adsorption of majority of MB molecules on *Scenedesmus*. Also, some minor changes were observed in amide II band's relative peak intensities. More specifically, the intensity of 1557 cm^{-1} peak increased whereas intensities of 1520 and 1516 cm^{-1} peaks were decreased.

Asymmetric P=O stretching band at 1242 cm^{-1} belonging to nucleic acids and/or phospholipids showed a slight shift to 1243 cm^{-1}, indicating a possible involvement of phosphate groups in adsorption, as in the case of *Chlorella*-MB. Worth mentioning, in the neat *Scenedesmus* spectrum there were two minor peaks at 1267 and 1212 cm^{-1} that disappeared after adsorption of MB, apparently they were buried under the phosphate peak due to a slight increase in intensities all over the range of the phosphate band. As a reasonable hypothesis it can be considered that not all but a part of phosphate groups were involved in adsorption leading to enlargement of the corresponding FT-IR band. The peak at 1151 cm^{-1}, which was assigned as C-O stretching of polysaccharides, showed a slight shift to 1149 cm^{-1}. Two peaks accompanying at the right- and left-hand side of this peak in *Chlorella*-MB are absent in *Scenedesmus*-MB. These two MB peaks are expected to be buried under inherent *Scenedesmus* peak at 1149 cm^{-1} since its intensity is larger than that of *Chlorella* and those MB peaks. However, in contrast to *Chlorella*, no change at the 1016 cm^{-1} peak was observed. Despite the slight shift from

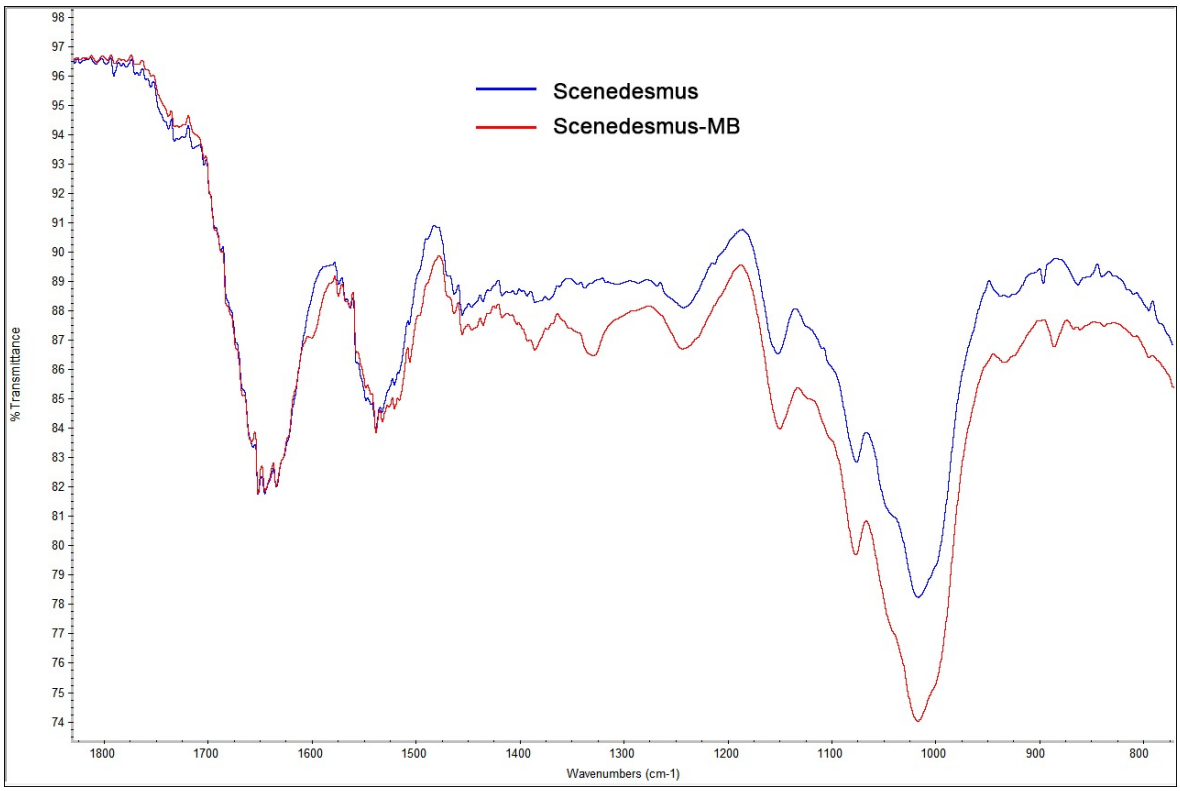

Figure 4.21. FT-IR spectra of *Scenedesmus* (Blue) and *Scenedesmus*-MB (Red).

1151 cm^{-1} to 1149 cm^{-1}, the lack of shift at 1016 cm^{-1} may indicate that C-O groups, hypothetically those of polysaccharides, were not apparently as involved in adsorption process as they were in the case of *Chlorella*.

After adsorption on *Scenedesmus*, four distinct MB peaks and typical shifts of these peaks were observed exactly as in the case of *Chlorella*. So corresponding discussion can be found in Section 4.8.1. This fact indicates that for both species MB is adsorbed through the same functionalities, namely ionic sites of the dye structure.

4.8.3. FT-IR Analysis of *Chlorella*-EBT

FT-IR spectrum of *Chlorella*-EBT superimposed with neat *Chlorella* spectrum are given in Figure 4.22 and spectrum of EBT is given in Figure 4.23. In comparison to MB, EBT yielded significantly less changes in FT-IR spectrum of *Chlorella*. Similar

to MB adsorption, EBT adsorption caused shifts and intensity changes of those minor carbonyl peaks indicating that carbonyl bearing functional groups may be involved in some part in adsorption process. These changes can be very minor. Then there was practically no change in amide peaks. Therefore, two apparent changes were observed in the spectra of *Chlorella* after EBT adsorption. First change was the shift of asymmetric phosphate stretching from 1242 cm^{-1} to 1237 cm^{-1}, which indicates phosphate group involvement in adsorption of EBT. Secondly, as in the case of MB, the intensity of the broad band near 1024 cm^{-1} decreased and another peak became more apparent at 1039 cm^{-1} upon EBT adsorption on *Chlorella*. Therefore, alkoxy groups, most probably those of polysaccharides, were important in EBT adsorption on *Chlorella*, as in the case of MB.

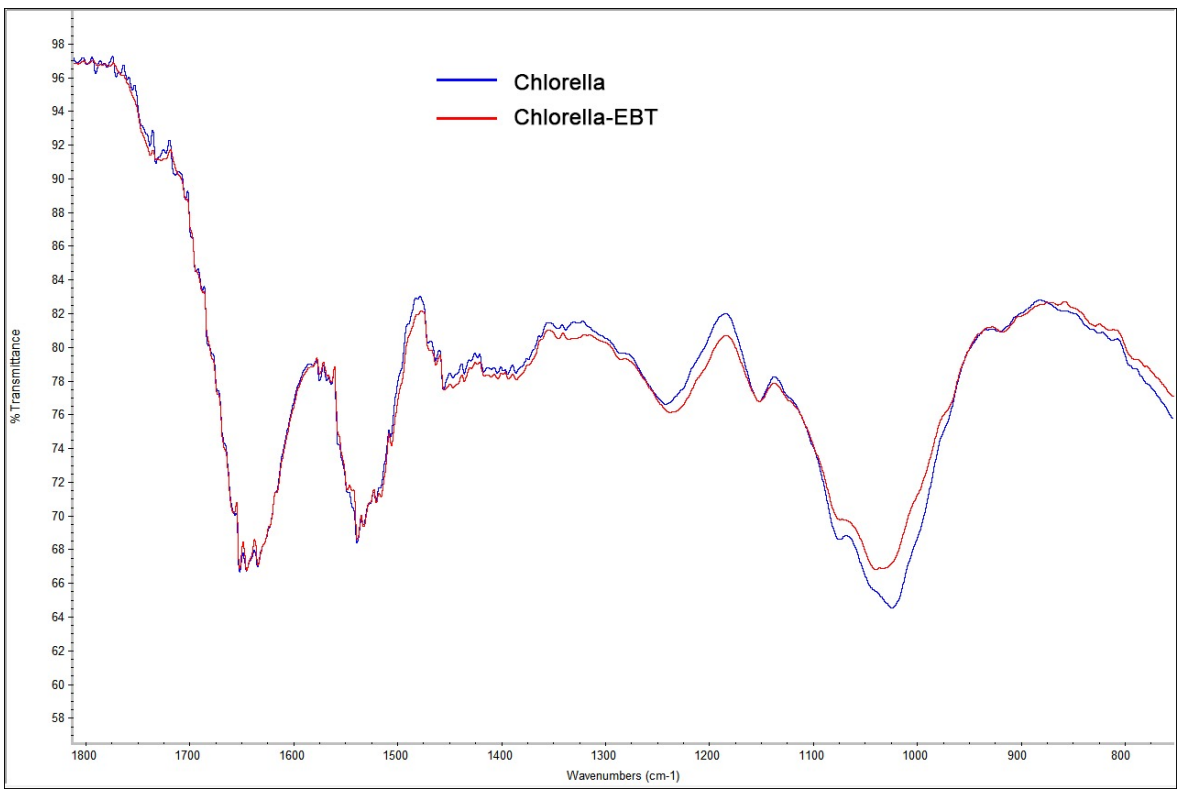

Figure 4.22. FT-IR spectra of *Chlorella* (Blue) and *Chlorella*-EBT (Red).

Surprisingly, none of EBT peaks were observed in *Chlorella*-EBT spectrum, or they were not intense enough to appear above *Chlorella* bands. Considering the amounts of EBT dye adsorbed on *Chlorella*, it was expected to observe EBT bands

along those of *Chlorella*. The absence of dye bands is observed both for EBT and CR adsorptions on both types of microalgae, and it will be discussed separately at the end of this section.

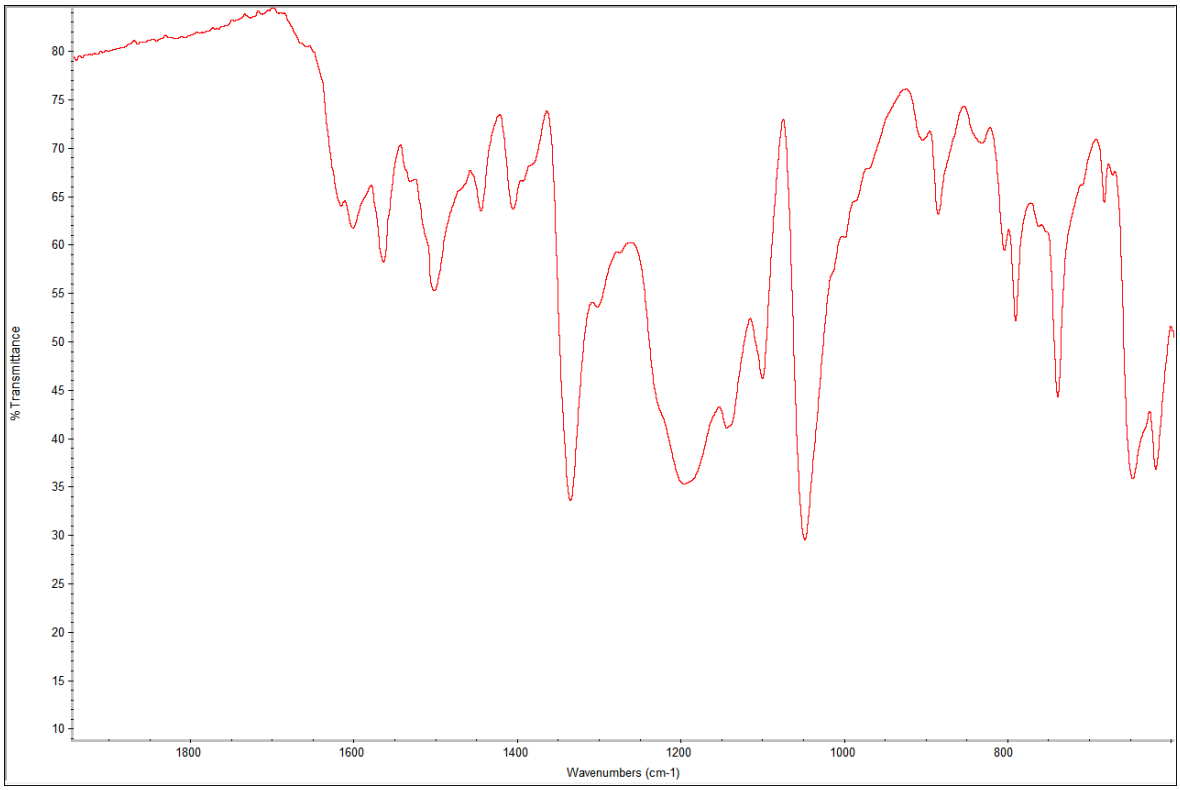

Figure 4.23. FT-IR spectrum of eriochrome black t (EBT).

4.8.4. FT-IR Analysis of *Scenedesmus*-EBT

FT-IR spectra of *Scenedesmus*-EBT and *Scenedesmus* are presented in Figure 4.24. EBT adsorption on *Scenedesmus* caused apparent changes in low intensity carbonyl peaks. The band between 1732-1723 cm^{-1} changed into a sharp peak at 1733 cm^{-1}; and the peak at 1714 cm^{-1} shifted to 1716 cm^{-1}. These changes indicate the role of carbonyl bearing functional groups in adsorption of EBT, however these changes can be considered very minor due to very low intensities of peaks at that region. Minor intensity decrease in amide II band was detected. Another minor change was observed as those peaks originally appearing at 1344 cm^{-1} and 1337 cm^{-1} in *Scenedesmus* were masked by the new peak at 1338 cm^{-1}, rising from the effect of NO_2 stretching of

EBT [87], which is also observable in *Chlorella*-EBT spectrum. As it was observed in *Chlorella*-EBT spectrum, a shift in asymmetric P=O stretching from 1242 cm^{-1} to 1239 cm^{-1} was apparent. In addition, as in the case of MB, shouldering peaks at 1267 and 1212 cm^{-1} disappeared after adsorption of EBT, explained as swollen phosphate band masking them. Lack of any change in 1151 cm^{-1} and 1075 cm^{-1} bands were con-

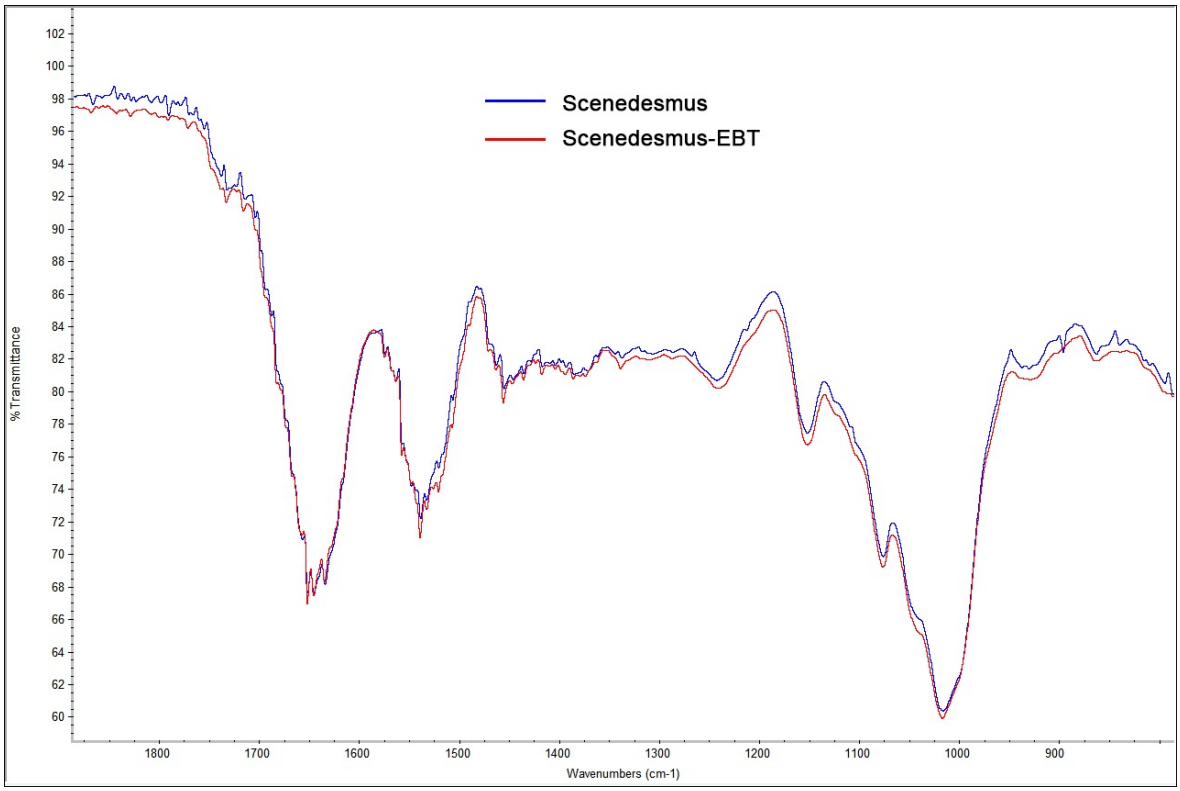

Figure 4.24. FT-IR spectra of *Scenedesmus* (Blue) and *Scenedesmus*-EBT (Red).

sistent with *Chlorella*-EBT spectral analysis result, but in contrast to *Chlorella* no change detected in 1016 cm^{-1} band either. Therefore, it can be deduced that, phosphate groups may be taking the most apparent role in the adsorption process of EBT on *Scenedesmus*, whereas polysaccharides are not as active as in the case of *Chlorella*.

4.8.5. FT-IR Analysis of *Chlorella*-CR

FT-IR spectra of *Chlorella*-CR and neat *Chlorella* are given in Figure 4.25 and spectrum of CR can be seen in Figure 4.26. Adsorption of CR on *Chlorella* did not

produce any but two apparent changes that are also observed in *Chlorella*-MB and *Chlorella*-EBT, and one very minor change on the corresponding spectrum. As in the case of *Chlorella*-EBT, the asymmetric P=O stretching peak at 1242 cm^{-1} shifted to 1236 cm^{-1}. And the original peak at 1024 cm^{-1} decreased in intensity to appear as twins with the peak at 1038 cm^{-1}. Then as a very minor change, the C-O peak at 1151 cm^{-1} shifted slightly to 1152 cm^{-1}. Both observations point out to the involvement of both phosphate groups and polysaccharides in CR adsorption process of *Chlorella*. As in the case of EBT, major FT-IR bands of CR were not observable, most probably buried under much intense *Chlorella* bands and this fact will be discussed at the end of this section.

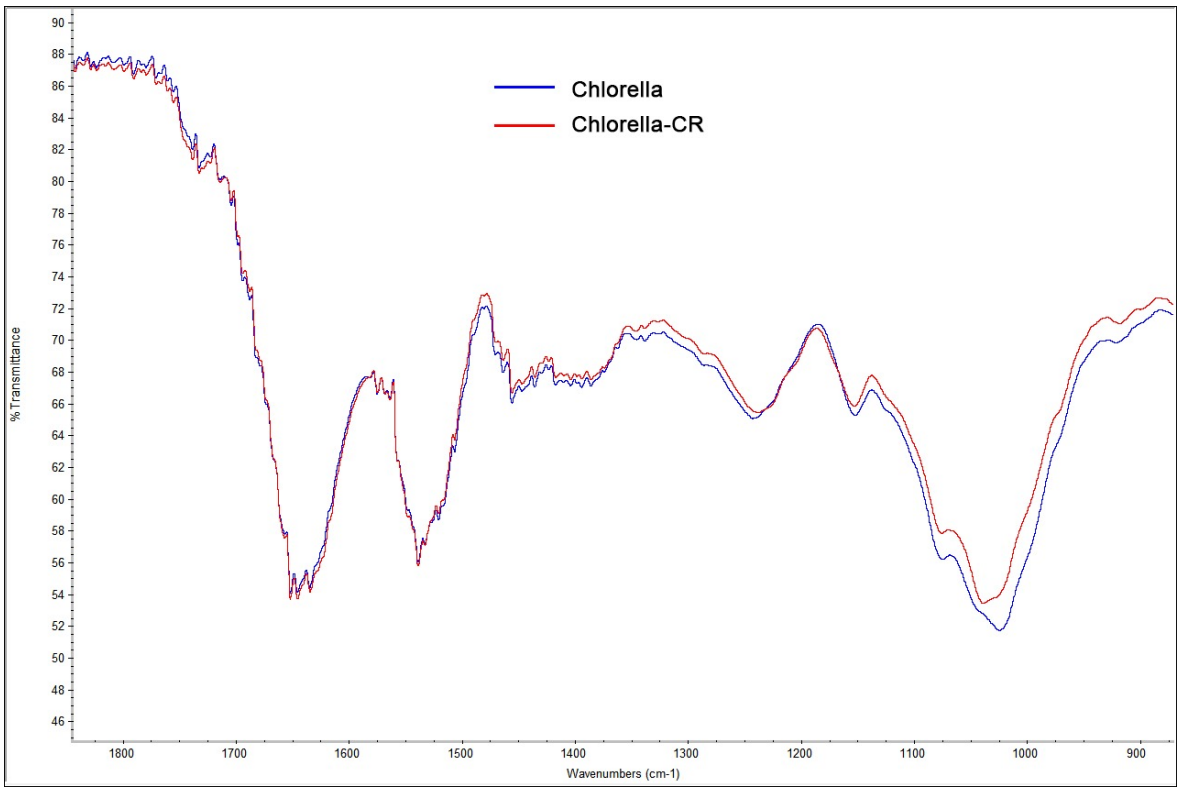

Figure 4.25. FT-IR spectra of *Chlorella* (Blue) and *Chlorella*-CR (Red).

4.8.6. FT-IR Analysis of *Scenedesmus*-CR

Adsorption of CR on *Scenedesmus* (Figure 4.27) did not yield any significant changes in the corresponding FT-IR spectrum, except shifts and intensity changes in

Figure 4.26. FT-IR spectrum of congo red (CR).

two particular regions. As a minor change in amide I band, the peak at 1656 cm^{-1} was shifted to 1658 cm^{-1} but no other shift was observed in any other carbonyl functionality. As another minor change in amide II band, no shift in peaks were observed, but the intensity of 1557 cm^{-1} peak increased whereas intensities of 1520 and 1516 cm^{-1} peaks were decreased. As the only major change, adsorption of CR on *Scenedesmus* caused a large shift in asymmetric P=O stretching from 1242 cm^{-1} to 1234 cm^{-1}, similar to but larger than the shift in *Chlorella*-CR spectrum, indicative of the important involvement of phosphate group bearing chemical structures, possibly phospholipids of cell membrane, and/or nucleic acids. Once again accompanying peaks at 1267 and 1212 cm^{-1} disappeared after adsorption of CR, being buried under the changing phosphate band. This phenomenon was observed in all spectra of *Scenedesmus* after dye adsorption.

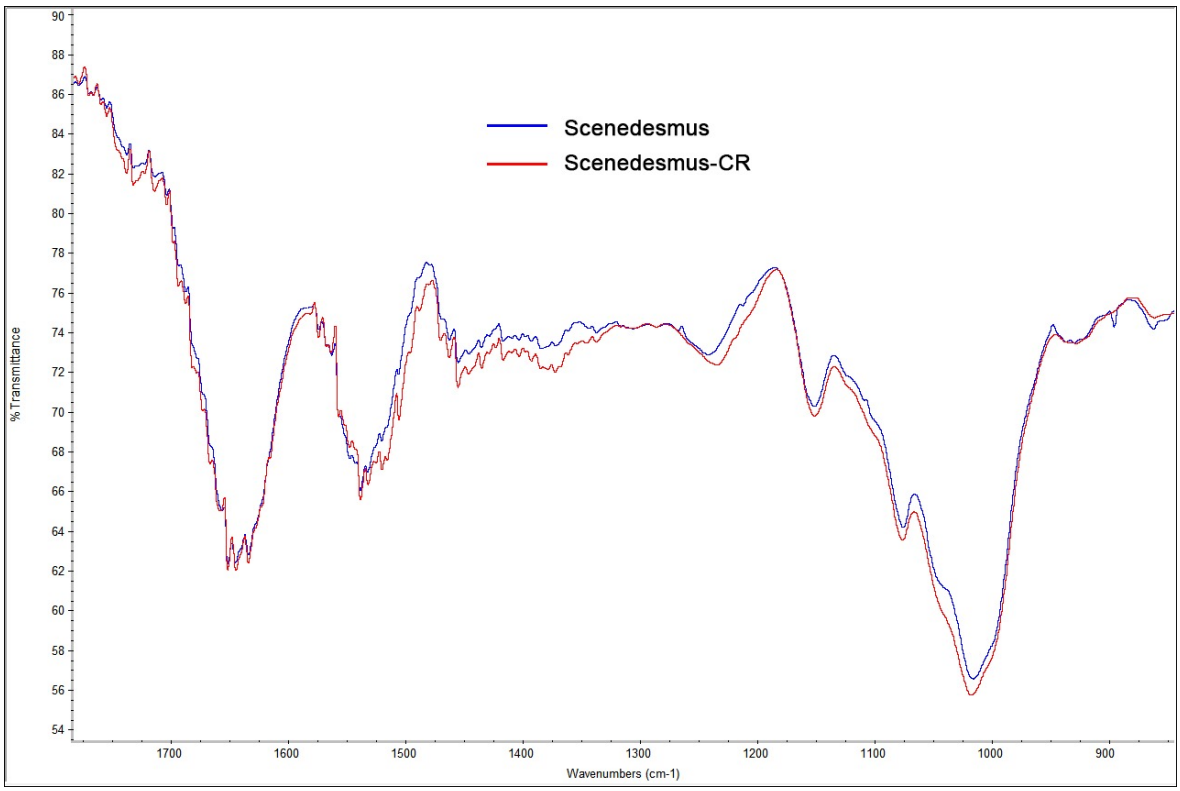

Figure 4.27. FT-IR spectra of *Scenedesmus* (Blue) and *Scenedesmus*-CR (Red).

4.8.7. Comparison of FT-IR Spectra and Conclusions

In all spectra some common changes occurred after adsorption process regardless of dye structure. First, the broad asymmetric P=O stretching band, in 1240 cm^{-1} region, exhibited a slight shift towards higher wavelengths after MB adsorption on *Chlorella* and *Scenedesmus* whereas, significant shifts towards lower wavelengths were observed with EBT and CR on both biosorbents, CR causing the highest shift. Phosphate groups are one of the major functionalities in biological materials, existing in nucleic acid structure and phospholipids which are important constituents of cell membrane. Therefore, it can be hypothesized that the cell membrane is exposed enough to play a significant role in adsorption of dye molecules. However, it is worth to discuss the fact that parallel to changes in asymmetric stretching of P=O a shift in symmetric stretching of P=O, which is expected around 1075 cm^{-1}, is not observable. This observation can be explained by symmetric P=O stretching vibration being buried under

the C-O vibrations of presumably polysaccharides in the same frequency range.

Minor peaks assigned to ester or carboxylic acid carbonyl groups also showed changes upon MB and EBT adsorptions. Considering that carbonyl group presence in the spectra is not significant, these changes are not sufficient to explain the adsorption process thoroughly.

Noticeably, in all *Chlorella* spectra a common change occurred, in the C-O vibration band with the highest absorbance peak around 1024 cm^{-1}, upon adsorption regardless of type of dye. But in the case of *Scenedesmus* no change was observed in that particular region, except one slight shift in a single peak at 1151 cm^{-1} in MB adsorption. Therefore, it can be deduced that, phosphate groups may be taking the most apparent role in the adsorption process of all three dyes on *Scenedesmus*, whereas polysaccharides are not as active as in the case of *Chlorella*.

Last noticeable point in the comparative analysis of IR spectra is the absence of dye peaks in the cases of EBT and CR dyes adsorbed on both *Chlorella* and *Scenedesmus*. When adsorbed dye amounts on microalgae are taken into consideration, because the adsorbed amounts of EBT and CR on *Chlorella* are sufficient to appear as FT-IR peaks, it was expected that EBT and CR peaks appear along with microalgae bands at least for *Chlorella*-EBT and *Chlorella*-CR. Their absence can only be explained by considering the rinsing step before the FT-IR analysis. All dye adsorbed *Chlorella* and *Scenedesmus* were rinsed with deionized water in order to eliminate free dye molecules present in the small amount of remaining supernatant. As a result of rinsing, EBT and CR adsorbed microalgae must have released some part of the adsorbed dye, hence on account of decreased amounts corresponding dye peaks do not appear, probably remaining hidden under the inherent peaks of biosorbents on the final spectra. This observation is another indication of the weaker binding, in other words lower affinities of EBT and CR dyes for both microalgae.

5. BIODEGRADABLE FILMS FROM SPIRULINA

This part of the study was conducted in Biotechnology Biochemistry and Enzimology (BBE) Research Group laboratories at University of Naples Federico II under the supervision of Professor Loredana Mariniello.

Rest of the study is focused on preparation and characterization of biodegradable films made out of the cyanobacteria (blue-green algae) *Spirulina*. Typical biochemical composition of *Spirulina* consists of 55-70 % proteins, 13-19 % carbohydrates, 6-8 % lipids, 7 % moisture, 7-14 % ash. High protein and low lipid content make *Spirulina* a good candidate for biopolymer-based films.

Spirulina was used in PVA blends or as the single matrix. In addition, proteins from *Spirulina* have been extracted from which films have been prepared in an attempt to improve mechanical properties. Furthermore, the films were modified with microbial Transglutaminase (mTG) to form intra-, intermolecular crosslinks between Lys ε-amino and Gln γ-carboxamide groups present in protein matrices. Due to these enzyme-induced crosslinks mechanical properties of resulting films are expected to be enhanced.

5.1. *Spirulina*/PVA Blend Films

In a study by Shi et al. [88] *Spirulina*/Poly(vinyl alcohol) (PVA) blends were prepared by casting method. PVA has excellent film forming properties, extensibility and regarded as a biodegradable polymer [89, 90] while, it is completely petroleum-based. Blending it with a suitable biobased matrix serves to reduce adverse impact on environment and increase biodegradation rate. Due to abundance of OH groups compatibility of these two matrices is expected. In this set of experiments the objective was to prepare *Spirulina*/PVA blends and modify the films by mTG. Detailed compositions of film forming suspensions (FFSs) of *Spirulina*/PVA blends are given in Table 3.1 in Section 3.9.1. Relative amounts of *Spirulina* and PVA are based on the study by Shi et al. [88] Neat PVA, plasticized PVA and plasticized PVA/*Spirulina* blend films were

Table 5.1. Tensile test results of PVA/*Spirulina* blend films.

Composition	**Sample**	**Thickness (mm)**	**Tensile Strength (MPa)**	**Elongation at Break (%)**	**Young's Modulus (MPa)**
PVA	P	0.02 ± 0.00	51.2 ± 4.7	21.8 ± 9.7	4163.7 ± 399.2
PVA + GLY	PG	0.09 ± 0.01	11.3 ± 3.6	384.0 ± 66.5	28.8 ± 3.8
PVA + SP + GLY	PSG	0.14 ± 0.01	7.9 ± 0.7	8.3 ± 1.0	271.6 ± 46.9
PVA + SP + GLY + mTG (18 U)	PSGT1	0.15 ± 0.01	8.5 ± 0.8	6.4 ± 1.5	394.1 ± 69.3
PVA + SP + GLY + mTG (36 U)	PSGT2	0.17 ± 0.02	5.4 ± 0.6	49.2 ± 31.2	118.9 ± 3.2
PVA + SP + GLY + mTG (72 U)	PSGT4	0.18 ± 0.02	6.3 ± 0.2	11.7 ± 3.8	253.5 ± 50.5
PVA + SP + GLY + mTG (145 U)	PSGT8	0.23 ± 0.04	4.4 ± 0.3	6.7 ± 1.9	234.0 ± 15.9
PVA + SP + GLY	REF	0.1	26	45	400

prepared by solution casting, after evaporation of water at room temperature. The blend films were also treated with several concentrations of mTG. Crude *Spirulina* was ultrasonically homogenized before addition in FFSs to ensure a thorough mixing of components. The results of tensile tests are given in Table 5.1. Tensile strength (TS) represents the resistance of the matrix to applied force; elongation at break is % ratio of increased length to initial length; and Young's modulus (E) which is calculated from initial slope of the strength/strain plot represents the stiffness of the matrix.

Glycerol, *Spirulina* and mTG caused thickening of resulting films. Thickening of mTG modified films is commonly observed in literature and it can be linked to enhancement of water holding capacity caused by mTG induced crosslinks [91,92]. Addition of *Spirulina* clearly caused a large decline in elongation at break and a decrease in mean tensile strength despite considerably large standard deviations in tensile strength values. *Spirulina* also significantly increased the stiffness of produced films. Modification with the lowest concentration of mTG (PSGT1, 18 u/g protein) reduced the extensibility, further increased the stiffness with only a slight increase in mean tensile strenght. However the effect of mTG to mechanical properties is complex, and it lacks a clear correlation between mTg amounts and mechanical properties. PSGT2 which was modified with 36 u/g protein mTG seems to be the best film forming one among all blends; having the highest extensibility, lowest stiffness and with 32% decrease in mean tensile strength compared to the blend film without enzyme modification (PSG). Nevertheless, mechanical properties of blends were poorer than neat PVA. Furthermore, the results of reference study couldn't have been reproduced.

5.2. *Spirulina* Films

Before coming to a judgement about rather unsatisfactory results of *Spirulina*/PVA blends, it is important to gain an insight about mechanical properties of *Spirulina* films as the single matrix. Hence, plastic films were prepared from ultrasonically homogenized *Spirulina* by casting method. Preliminary trials had shown that films casted in the absence of any plasticizer were too fragile to be peeled off from the surface of petri dishes. The films plasticized with glycerol were either too fragile or sticked on petri

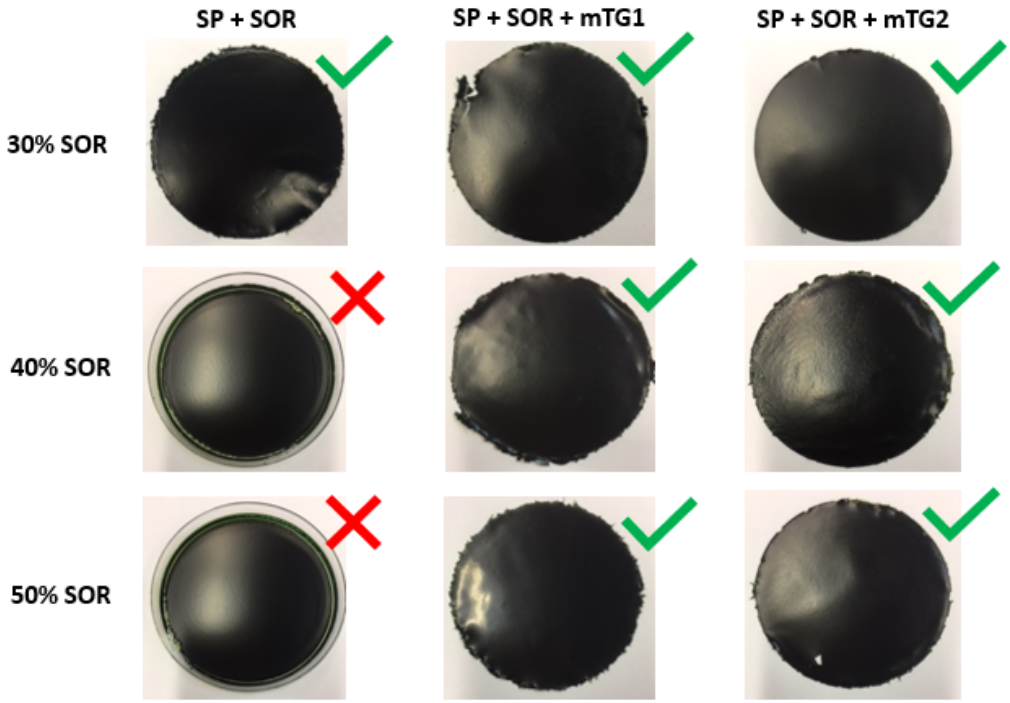

Figure 5.1. Images of sorbitol plasticized *Spirulina* films not modified and modified with two concentrations of mTG

dishes. Therefore, the films were plasticized with 30%, 40% or 50% sorbitol (SOR) to find the best plasticizer ratio and modified with two concentrations of microbial Transglutaminase (mTG). mTG concentration was either 36 u/g protein (mTG1) or 72 u/g protein (mTG2). Compositions of the film forming suspensions (FFSs) are presented in Table 3.2 in Section 3.9.2 and images of the films are given in Figure 5.1. *Spirulina* films casted with 30% (w/w) sorbitol were easily peeled off the surfaces. 40% and 50% (w/w) plasticized films were not peelable in the absence of mTG thus, they couldn't have been characterized by tensile tests.

The results of tensile tests are given in Figure 5.2. In general terms, tensile strength is the maximum stress applied to the sample which causes complete failure. However very weak and ductile samples deform extremely to release the stress and may break under much lower stress. In these cases, ultimate tensile strength (UTS) which is the maximum stress that the sample can withstand should be reported. The

films were very ductile elongating like a chewing gum before rupture so ultimate tensile strengths are also reported. According to tensile strength data enzyme modification significantly improves resistance of the matrix at the point of rupture except for the 50% plasticized films. However ultimate tensile strengths reveal that the maximum resistance of the films is not dependent on the amount of enzyme except for the film which contains 30% plasticizer and higher concentration of mTG (S30-mTG2). Tensile strength of S30-mTG2 equals to ultimate tensile strength; it has the highest resistance and stiffness and lowest extensibility among all films.

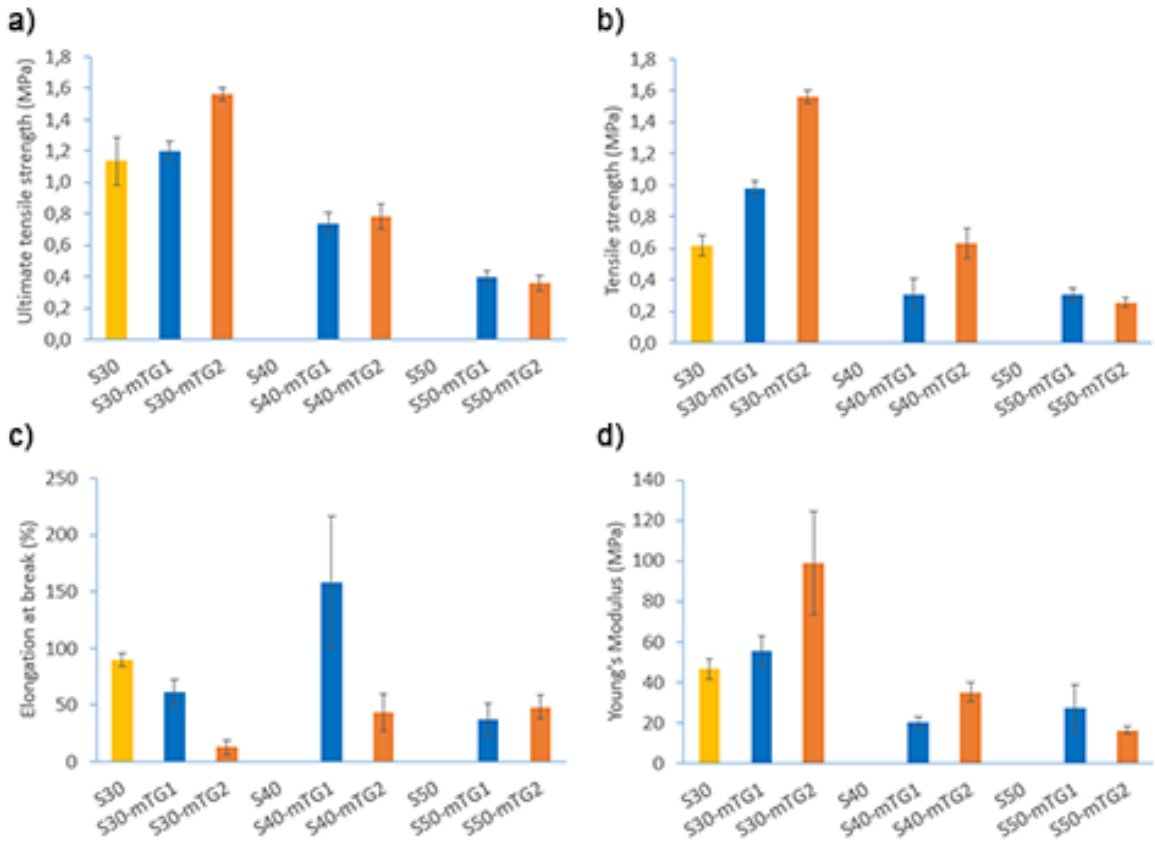

Figure 5.2. Tensile test results of neat *Spirulina* films a) ultimate tensile strength b) tensile strength c) elongation at break d) Young's modulus.

Unmodified *Spirulina* resulted in weak but flexible films (S30). For 30% and 40% plasticized films, mTG modification increased stiffness and reduced extensibility. The influence of mTG depends highly on the substrate, conformation of protein and incubation conditions [67, 68]. Results obtained by some studies [93, 94] are in accordance

with the results of *Spirulina* films such that mTG increased rigidity and reduced extensibility of the films. However, in many cases modification by enzyme was reported to enhance both resistance and extensibility concurrently [67], which is the desired outcome of mTG modification.

30% sorbitol seems to be the best amount of plasticizer, while higher amounts of sorbitol diminished tensile strength significantly. Since 30% plasticized *Spirulina* is already highly flexible, lower concentrations of sorbitol could be enough for a desired flexibility range.

5.3. Protein Extraction from *Spirulina* and Resulting Films

Weakness of ultrasonically homogenized neat *Spirulina* films may be attributed to presence of small molecules in the biological polymer matrix that weaken the interchain interactions. To eliminate such small molecules and overcome their possible adverse effects, proteins of *Spirulina* were extracted by a convenient acid/base extraction, for further film preparations.

5.3.1. Protein Quantification of the Extract

Protein content of the *Spirulina* protein extract (SPE) was quantified with Kjeldahl method. Kjeldahl detects Nitrogen mass which is then converted to protein amount. Kjeldahl method may give overestimated results because of the presence of non-protein Nitrogen. However, Safi et al. [95] reported that *Spirulina* protein extract obtained by a similar method gave accurate results with Kjeldahl.

An insoluble pellet, the precipitate obtained from pH 12 fraction and the supernatant from pH 3 were also stored to quantify unextracted protein amount. The images of the pellet from pH 12, the supernatant from pH 3 and *Spirulina* protein extract are given in Figure 5.3. The pellet from pH 12 fraction formed a fragile film upon drying that adhered to petri dish. *Spirulina* protein extract was very dark colored, which may be caused by oxidation in highly alkaline medium [96].

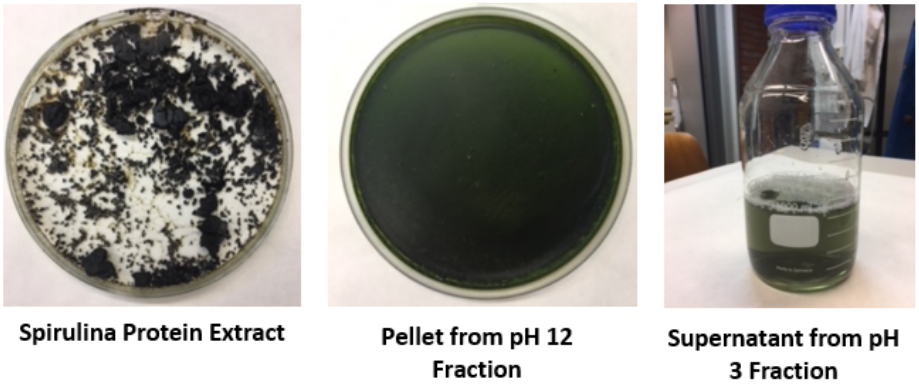

Figure 5.3. Fractions obtained from protein extraction procedure.

Table 5.2. Protein contents (%) by Kjeldahl method.

Sample	**Protein Content (%)**
Spirulina Protein Extract	67.2
Pellet from pH 12 Fraction	48.6
Neat *Spirulina*	63.5
Supernatant from pH 3 Fraction	0.33 g/L

The results of Kjeldahl protein quantification is given in Table 5.2. The Supernatant from pH 3 fraction contains very low amount of protein. This is not surprising considering that at pH 3 protein solubility is the lowest [96]. Supernatant is expected to contain low molecular weight water soluble compounds like low-molecular-weight peptides. On the other hand, results revealed that the fraction that is insoluble at pH 12 contains considerable amount of proteins. Most likely, these proteins are higher molecular-weight water insoluble proteins.

It may seem protein extraction resulted in a slight increase in protein content when protein content of neat *Spirulina* and SPE are compared. Nevertheless, from the results of Kjeldahl method it is deduced that polydispersity of proteins present in the extract is smaller than that of neat *Spirulina*.

Additionally, SPE is expected to contain water-soluble carbohydrates [97] and lipids because of emulsifying properties of *Spirulina* proteins [98].

5.3.2. Microbial Transglutaminase Activity of *Spirulina* Protein Extract

SDS-PAGE is a method for separating proteins on basis of molecular weights similar to chromatographic methods. During preparation of samples, proteins are denatured so that propagation speeds depend only on molecular weights of the proteins.

SDS-PAGE profiles of neat *Spirulina*, unmodified *Spirulina* protein extract (SPE) and SPE modified with various concentrations of mTG are given in Figure 5.4. A large portion of neat *Spirulina* bands are present in SPE. A slight shift in some bands was observed, which may be explained by partial hydrolysis resulted from highly alkaline medium during extraction. In literature it is reported that majority of proteins in *Spirulina* and SPE are , subunits of phycocyanin and allophycocyanin and molecular weights are in the range of 14-20 kDa [96,99]. In Figure 5.4 it is apparent that majority of proteins are in that particular range which is in accordance with literature.

mTG modification creates crosslinks and increases molecular weight of the proteins. Therefore, proteins modified with the enzyme cannot propagate in the gel. In Figure 5.4 it is seen that in the presence of mTG several bands disappeared from the gel and intensities of the bands diminish with increasing concentration of mTG. Observed disappearance of the bands proves SPE is a substrate for mTG. In addition, 20 u/g protein concentration of the enzyme seems to be the optimal concentration since higher concentrations did not create any observable difference.

5.3.3. Films Prepared from *Spirulina* Protein Extract

Films were prepared from *Spirulina* protein extract (SPE) as the single matrix, through solvent casting method in the presence or absence of the crosslinking agent mTG. SPE stock solutions were prepared in 3 ways, untreated, heat treated in an attempt to increase the strength of the matrix or pH treated to provide a better solvation.

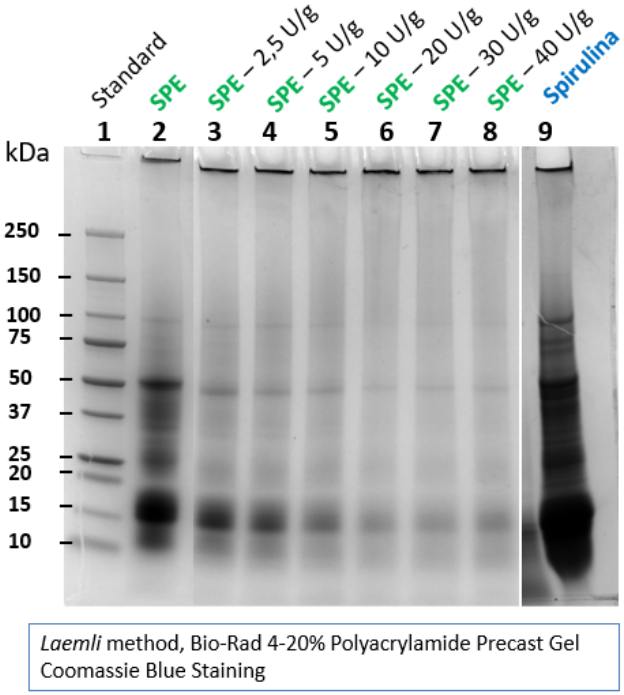

Figure 5.4. SDS-PAGE of neat *Spirulina*, unmodified SPE and SPE modified with increasing concentrations of mTG.

Chronakis [63] reported *Spirulina* platensis strain Pacifica undergoes heat-induced gelation between 40-80^{0}C and highest elastic modulus was obtained at 70^{0}C. Therefore, part of the stock SPE solution was heated to 70^{0}C for 1 hour and cooled back to room temperature before preparation of film forming suspensions (FFSs). This fraction was labeled as SPE-H. For a better solvation and mixing employing higher pH a part of SPE was dissolved by bringing the pH to 12.00 instead of 7.00. The solution at pH 12.00, was then brought to pH 7.00 and films were solution cast at this pH. This fraction was labeled as SPE-P. The untreated SPE stock solution which was dissolved at pH 7.00 without treatment of heat was labeled as SPE-U.

The film forming suspensions (FFSs) were prepared using the above described three different stock solutions. The resulting FFSs were incubated in the presence or absence of mTG. The SDS-PAGE profiles of three different stock solutions and resulting FFSs are given in Figure 5.5. SDS-PAGE was used to examine if heat treatment or

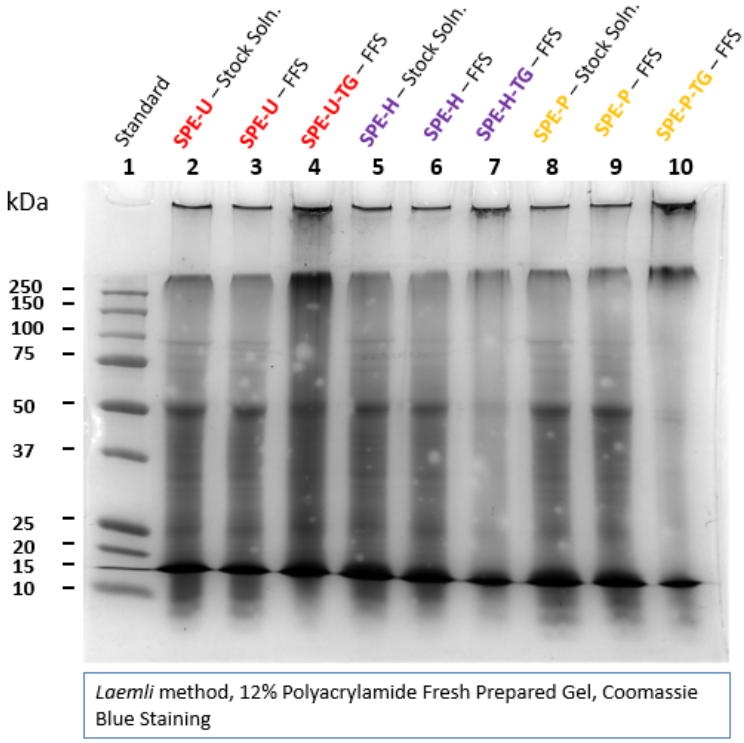

Figure 5.5. SDS-PAGE profiles of film forming suspensions and films prepared from SPE.

pH treatment caused any change in molecular weights. Figure 5.5 clearly show that there are no differences in molecular weight compositions of stock solutions or film forming suspensions. The enzyme modification changed protein profile of each film. Bands disappeared from mTG modified SPE-H and SPE-P as observed in Figure 5.4 however, SPE-U exhibit no clear distinct bands. It seems some part of enzyme modified proteins propagated in the gel, revealing suppressed crosslinking.

Images of the resulting films can be seen in Figure 5.6 and results of tensile tests are given in Figure 5.7. Tensile test results indicate mTG modification did not show any significant effect on tensile strength (TS) or Young's modulus (E) except for pH 12 solvated samples (SPE-P). However, on the contrary to the neat *Spirulina* films enzyme modification increased elongation at break significantly in all samples.

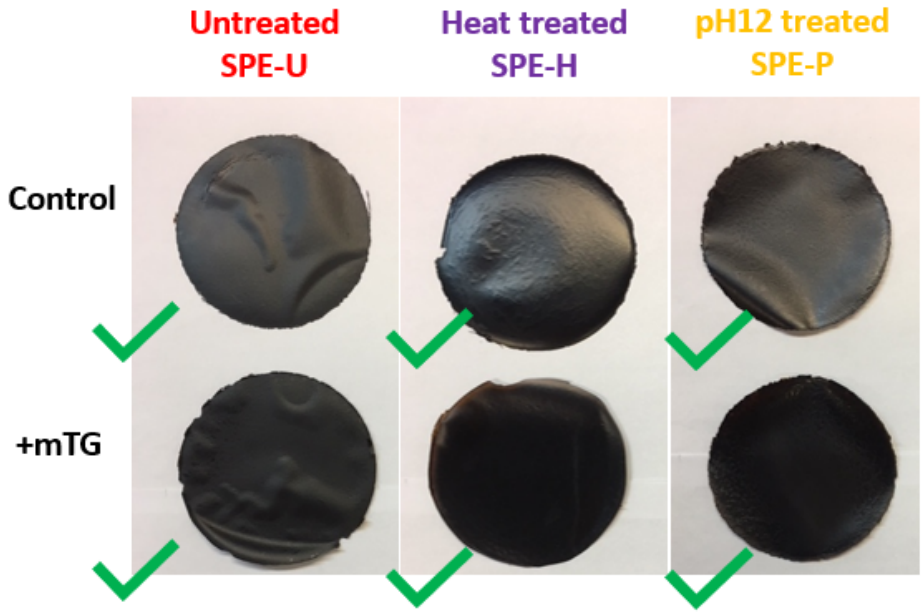

Figure 5.6. Images of films prepared from SPE with or without mTG.

Despite overlapping values, it is possible to argue heat treatment resulted in stronger films since mean tensile strenght of heat-treated film (SPE-H) increased by 26% with respect to that of untreated film (SPE-U). Furthermore, mTG modification resulted the highest elongation at break with heat-treated film. Mean elongation at break increased by 260% compared to that of untreated one.

Heat disrupts hydrogen bonds and interactions of hydrophobic groups, which naturally reside at inner compartments of the protein structure with respect to water that is at the outer region. Hydrophobic groups that are exposed to heat may interact among themselves to form hydrophobic physical crosslinks which may contribute to the gelation of the matrix. Chronakis [63] reported that at temperatures around 67^0C *Spirulina* protein extract undergoes heat induced denaturation. Heat-treatment of *Spirulina* protein extract may have provided new conformations suitable for enzymatic modification and consequently produced substantially more extensible matrix.

Compared to *Spirulina* films SPE films are stronger. It is suggested that by protein extraction small molecules were eliminated, and hence interaction of protein

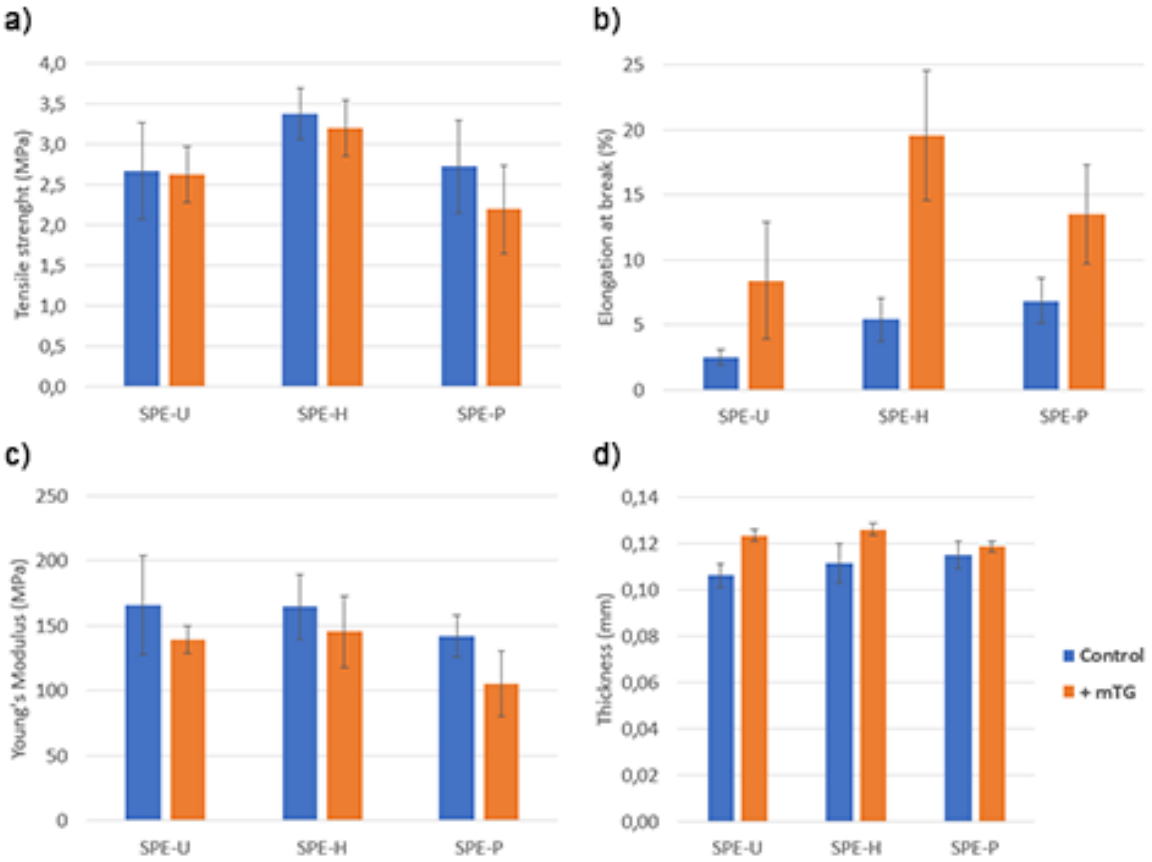

Figure 5.7. Tensile test results of the films prepared from SPE a) tensile strength b) elongation at break c) Young's modulus d) cross section thickness.

chains enhanced, which then improved mechanical properties. Conformations of the proteins in the extract are expected to be different than in crude *Spirulina* since alkaline extraction denatures proteins. It is well known that native proteins of *Spirulina* are highly structured [100]. With the natural arrangement of proteins, mTG may react increasing the rigidity of the matrix. Each treatment yields different rearrangement of proteins thus, enzyme modification works differently for each sample. mTG reacts favorably with heat-treated *Spirulina* protein extract increasing extensibility without compromising from tensile strength. Protein extraction followed by heat-treatment create favorable conditions for mTG catalyzed crosslinking reaction.

The films were further characterized by Z-Average and zeta potential measure-

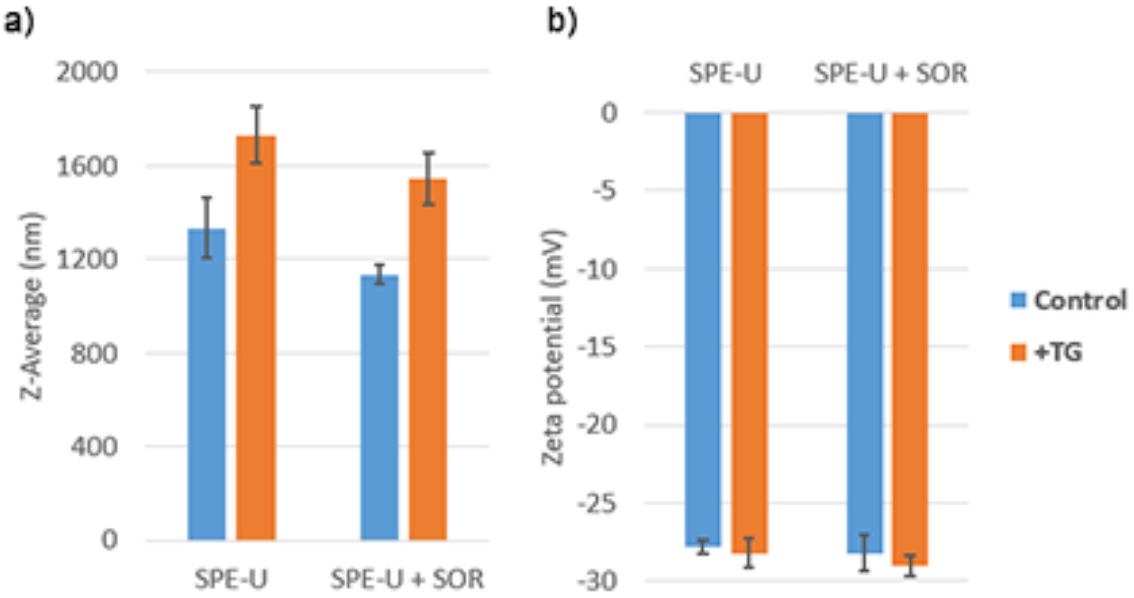

Figure 5.8. a) Z-Average and b) zeta potential measurements of SPE-U stock solution and SPE-U film forming suspension with/without mTG.

ments. Z-average is the intensity weighted mean hydrodynamic size of particles measured by dynamic light scattering technique. It is easy, non-destructive and provides a means for comparing particle sizes. Untreated SPE (SPE-U) stock solution was used for samples that are modified or not modified by mTG. Additionally, film forming suspension containing SPE-U was used for samples that are modified or not modified by mTG. Difference of film forming suspension is that they contain 30% (w/w) sorbitol with respect to proteins.

The results are given in Figure 5.8. From Z-average measurements it is seen that average particle size increased for the enzyme treated samples either in the presence or absence of sorbitol whereas, sorbitol only slightly diminished average particle size. It should be noted that particle sizes are in micrometers which indicates biomacromolecules are not completely soluble in aqueous media, they rather form hydrocolloids.

Zeta potential is the electrical potential difference between the bulk and slipping

plane of a charged particle in solution or suspension. Slipping plane is part of the electrical double layer and consists of the charged particle and bound ions (mostly oppositely charged) moving together with that particle. Since some biopolymers like proteins are polyelectrolytes, they exist as charged particles in solutions or suspensions. Some studies suggest there may be a correlation between zeta potential of FFSs and extensibility of the resulting films [101, 102].

Therefore, zeta potential of film forming suspension and stock solution of SPE-U was studied in the presence or absence of mTG and results are presented in Figure 5.8. The results show that zeta potential of control and enzyme modified samples were in the same range meaning that there is no correlation between increasing extensibility of mTG modified *Spirulina* protein extract and zeta potential values. As expected, addition of sorbitol did not have any effect on zeta potential.

It is generally accepted that if zeta potential magnitude is greater than 30 mV the particles repel one another and form stable colloids, whereas if magnitude of zeta potential is between 0 and 10 mV the colloid is very unstable. Unstable colloids tend to aggregate easily hence obtaining a thorough mixing may be challenging. At pH 7.00, zeta potential of neat *Spirulina* was in the range of -19 – 23 mV (data not shown). Compared with *Spirulina*, *Spirulina* protein extract is able to form slightly more stable particles since zeta potential was in the range of -27 – 30 mV.

6. CONCLUSION

In the first part of this study, several microalgae species were investigated for their potential as effective biosorbents that can ideally remove all variety of molecular structures of micropollutants. In the first steps of this rather extensive screening study, seven different types of microalgae which were originally obtained from various lakes in Anatolia, were tested and compared for their dye removal potentials. Initial tests were based on the removal of a model pollutant, a cationic dye nile blue (NB). Superior biosorbents for the cationic dye were then selected and employed for the investigation of their potential in the removal of three other dyes, one cationic, one representing an anionic structure, and the other a zwitterionic dye.

At the beginning of the study, in an attempt to find a suitable hydrogel matrix that can carry microalgae and also conveniently separable from water phase, a convenient candidate, calcium alginate hydrogels were employed. Various microalgae were immobilized in calcium alginate hydrogels and tested for their nile blue adsorption capacities in comparison with a suitable type of activated carbon for organic dye removal, encapsulated in alginate hydrogel. Immobilization resulted in delayed and moderate dye adsorption performances. When same species were used in neat form, without the alginate hydrogel, much superior adsorption performances were recorded for all adsorbents tested. Cationic dye removal percentages of *Chlorella*, *Scenedesmus* and *Haematococcus* were observed to be in the range of 93% to 95% within 1 hour. These successful results were close to that of activated carbon, which was observed to remove more than 99% of the cationic dye.

Chlorella and *Scenedesmus* were selected to study the effect of growth period and Ca^{2+} deprivation on dye adsorption performances. Ca^{2+} deprivation had no effect in *Chlorella* harvested on 5^{th} and 10^{th} day. On the other hand, it decreased adsorption capacity of *Chlorella* harvested on 15^{th} day for longer dye adsorption durations.

The effect of growth period on adsorption capacities was very limited. The sam-

ples harvested at exponential or linear phases exhibited slightly higher adsorption capacities. *Chlorella* harvested at these phases also showed better adsorption capacities than *Scenedesmus* while adsorption capacity of *Chlorella* decline for the samples harvested on 15^{th} day. Generally, best dye adsorption capacities were obtained during 1-hour dye adsorption duration.

Equilibrium studies revealed that both strains of *Chlorella* have higher adsorption capacities compared to *Scenedesmus* for cationic, anionic and zwitterionic dyes, even though anionic and zwitterionic dye removal yields were moderate for both in comparison to the activated carbon used. Surprisingly, compared to activated carbon, *Chlorella* showed higher adsorption capacities of the cationic dye methylene blue (MB) at elevated concentrations. All isotherm data agreed well with Langmuir model while both Langmuir and Freundlich indicate adsorptions were favorable within the concentration range.

Pseudo-second order adsorption behavior best described kinetic data of all dyes and predicted $q_{e,cal}$ values reasonably well. As expected, cationic dye (MB) adsorption was faster than anionic (EBT) and zwitterionic (CR) dye adsorption and it did not give linear plots of q_t against $t^{1/2}$. Whereas, intraparticle diffusion model was applicable to anionic and zwitterionic dyes.

FT-IR analyses indicated phosphate group involvement in adsorption of all three types of dye molecules on both *Chlorella* and *Scenedesmus*, which was more pronounced for EBT and CR. In *Chlorella* a common change was observed at 1024 cm^{-1} regardless of the type of dye. Consequently, alkoxy groups most probably those of polysaccharides were assumed to have taken important role in adsorption process onto *Chlorella*. However, this change was not observed in the case of *Scenedesmus*, hence polysaccharides were not as involved as in the case of *Chlorella*. The absence of inherent EBT and CR peaks on the spectra implies rather limited affinities of *Chlorella* and *Scenedesmus* for these dyes.

In the study of bioplastics, *Spirulina* was blended with PVA in order to reduce

PVA's negative impact on environment and increase biodegradability of PVA. The films were characterized by tensile tests. However, addition of *Spirulina* adversely affected mechanical properties causing a notable decline in extensibility and a slight decrease in mean tensile strength. The effect of microbial Transglutaminase (mTG) modification to mechanical properties lacked a general trend. Decrease in extensibility was not necessarily accompanied by increased resistance.

The single matrix *Spirulina* produced very weak, flexible but ductile films. 30% sorbitol was best plasticizer amount in improving mechanical properties. Modification with the enzyme increased stiffness however did not affect resistance of the matrix except higher amount of enzyme concentration in 30% plasticized sample. Consequently, native protein arrangement of *Spirulina* did not yield a suitable condition for enzyme modification. Additionally, it is suggested that small molecules present in *Spirulina* adversely affect favorable interactions between polymeric chains.

In order to change native protein conformation, eliminate small molecules, increase protein content and decrease polydispersity, proteins were extracted by a convenient acid/base extraction method. SDS-PAGE profile showed extracted proteins were substrate of mTG. *Spirulina* protein extract (SPE) was divided in three different fractions; untreated (SPE-U), heat-treated (SPE-H) and alkaline solubilized (SPE-P). Films were prepared using these fractions with or without mTG. Tensile test results exhibit favorable effect of the enzyme on extensibility of the matrices. Best results are obtained with heat-treated films. mTG modification increased mean elongation at break by 260% compared to that of control.

Z-average measurements showed enzyme modification increased average particle size in both plasticized and unplasticized *Spirulina* protein extract. No correlation was found between increased extensibility of enzyme modified samples and zeta potential values. However, compared to neat *Spirulina*, *Spirulina* protein extract particles were more stable having higher zeta potential values.

REFERENCES

1. European Chemicals Agency, *Registration statistics infograph*, 2019, `https://echa.europa.eu/registration-statistics-infograph#`, accessed on September 2019.

2. El-shahawi, M. S., A. Hamza, A. S. Bashammakh and W. T. Al-saggaf, "An overview on the accumulation , distribution , transformations , toxicity and analytical methods for the monitoring of persistent organic pollutants", *Talanta*, Vol. 80, No. 5, pp. 1587–1597, 2010.

3. Aggerbeck, M., A. Ambolet-Camoit, C. Ottolenghi, M. Kim, F. Letourneur, S. Jacques, C. Guguen-Guillouzo and R. Barouki, "Effects of combined persistant organic pollutants on global gene expression in human HepaRG cells: Enhanced down-regulation of metabolic pathways", *Toxicology Letters*, , No. 205, p. S41, 2011.

4. Huang, X., L. Lessner and D. O. Carpenter, "Exposure to persistent organic pollutants and hypertensive disease", Vol. 102, No. 1, pp. 101–106, 2006.

5. Smital, T., D. Epel, S. Britivić, S. KrČa, B. Pivčević, R. S. Klobučar and R. Žaja, "Inhibitors of the ABC transport proteins as emerging pollutants—determination and ecotoxicological relevance", *Toxicology Letters*, Vol. 164, pp. S43–S44, 2006.

6. Goldberg, M., "A systematic review of the relation between long-term exposure to ambient air pollution and chronic diseases", *Reviews on environmental health*, Vol. 23, No. 4, pp. 243–298, 2008.

7. Landrigan, P. J., C. B. Schechter, J. M. Lipton, M. C. Fahs and J. Schwartz, "Environmental pollutants and disease in American children: estimates of morbidity, mortality, and costs for lead poisoning, asthma, cancer, and developmental disabilities.", *Environmental health perspectives*, Vol. 110, No. 7, pp. 721–728, 2002.

8. Høyer, A. P., P. Grandjean, T. Jørgensen, J. W. Brock and H. B. Hartvig, "Organochlorine exposure and risk of breast cancer", *The Lancet*, Vol. 352, pp. 1816–1820, 1998.

9. Matés, J. M., J. A. Segura, F. J. Alonso and J. Márquez, "Free Radical Biology & Medicine Roles of dioxins and heavy metals in cancer and neurological diseases using ROS-mediated mechanisms", *Free Radical Biology and Medicine*, Vol. 49, No. 9, pp. 1328–1341, 2010.

10. Schettler, T., "Toxic Threats to Neurologic Development of Children", *Environmental Health Perspectives*, Vol. 109, No. 6, pp. 813–816, 2001.

11. Berghuis, S. A., K. N. J. A. V. Braeckel, P. J. J. Sauer and A. F. Bos, "Prenatal exposure to persistent organic pollutants and cognition and motor performance in adolescence", *Environment International*, Vol. 121, No. 8, pp. 13–22, 2018.

12. Reemtsma, T., S. Weiss, J. Mueller, M. Petrovic, S. González, D. Barcelo, F. Ventura and T. P. Knepper, "Polar pollutants entry into the water cycle by municipal wastewater: a European perspective", *Environmental science & technology*, Vol. 40, No. 17, pp. 5451–5458, 2006.

13. *Microplastics and persistent fluorinated chemicals in the Antarctic - Greenpeace Antarctic Report*, Greenpeace International, 2018.

14. Brown, L. M. and K. G. Zeiler, "Aquatic biomass and carbon dioxide trapping", *Energy Conversion and Management*, Vol. 34, No. 9-11, pp. 1005–1013, 1993.

15. Khan, M. I., J. H. Shin and J. D. Kim, "The promising future of microalgae: current status, challenges, and optimization of a sustainable and renewable industry for biofuels, feed, and other products", *Microbial cell factories*, Vol. 17, No. 1, p. 36, 2018.

16. Priyadarshani, I. and B. Rath, "Commercial and industrial applications of micro

algae – A review", *Journal of Algal Biomass Utilization*, Vol. 3, No. 4, pp. 89–100, 2012.

17. Spolaore, P., C. Joannis-cassan, E. Duran, A. Isambert, L. D. Génie and E. C. Paris, "Commercial Applications of Microalgae", *Journal of Bioscience and Bioengineering*, Vol. 101, No. 2, pp. 87–96, 2006.

18. Kovalova, L., D. R. Knappe, K. Lehnberg, C. Kazner and J. Hollender, "Removal of highly polar micropollutants from wastewater by powdered activated carbon", *Environmental Science and Pollution Research*, Vol. 20, No. 6, pp. 3607–3615, 2013.

19. Kumar, K. S., H.-u. Dahms, E.-j. Won, J.-s. Lee and K.-h. Shin, "Ecotoxicology and Environmental Safety Microalgae – A promising tool for heavy metal remediation", *Ecotoxicology and Environmental Safety*, Vol. 113, pp. 329–352, 2015.

20. Zeller, M. A., R. Hunt, A. Jones and S. Sharma, "Bioplastics and their thermoplastic blends from Spirulina and Chlorella microalgae", *Journal of Applied Polymer Science*, Vol. 130, No. 5, pp. 3263–3275, 2013.

21. Kothari, R., A. Pandey, S. Ahmad, A. Kumar, V. V. Pathak and V. V. Tyagi, "Microalgal cultivation for value-added products: a critical enviro-economical assessment", *3 Biotech*, Vol. 7, No. 4, p. 243, 2017.

22. de Carvalho, J. C., I. A. Borghetti, L. C. Cartas, A. L. Woiciechowski, V. T. Soccol and C. R. Soccol, "Biorefinery integration of microalgae production into cassava processing industry: Potential and perspectives", *Bioresource Technology*, Vol. 247, pp. 1165–1172, 2018.

23. Shah, M., R. Mahfuzur, Y. Liang, J. J. Cheng and M. Daroch, "Astaxanthin-producing green microalga Haematococcus pluvialis: from single cell to high value commercial products", *Frontiers in plant science*, Vol. 7, p. 531, 2016.

24. Chisti, Y., "Biodiesel from microalgae", *Biotechnology advances*, Vol. 25, No. 3, pp. 294–306, 2007.

25. Sumprasit, N., N. Wagle, N. Glanpracha and A. P. Annachhatre, "Biodiesel and biogas recovery from Spirulina platensis", *International Biodeterioration and Biodegradation*, Vol. 119, pp. 196–204, 2017.

26. Lu, Q., P. Han, F. Chen, T. Liu, J. Li, L. Leng, J. Li and W. Zhou, "A novel approach of using zeolite for ammonium toxicity mitigation and value-added Spirulina cultivation in wastewater", *Bioresource Technology*, Vol. 280, pp. 127–135, 2019.

27. Hultberg, M., O. Lind, G. Birgersson and H. Asp, "Use of the effluent from biogas production for cultivation of Spirulina", *Bioprocess and Biosystems Engineering*, Vol. 40, No. 4, pp. 625–631, 2017.

28. Pereira, L. and M. Alves, "Dyes—environmental impact and remediation", *Environmental protection strategies for sustainable development*, pp. 111–162, Springer, 2012.

29. *Bioplastic market data 2016: Global production capacities of bioplastics 2016-2021*, European Bioplastics e.V. & nova-Institute, 2016.

30. *Bioplastics market data 2017: Global production capacities of bioplastics 2017-2022*, European Bioplastics e.V. & nova-Institute, 2017.

31. *Bioplastics market data 2018: Global production capacities of bioplastics 2018-2023*, European Bioplastics e.V. & nova-Institute, 2018.

32. Imre, B., L. García, D. Puglia and F. Vilaplana, "Reactive compatibilization of plant polysaccharides and biobased polymers: Review on current strategies, expectations and reality", *Carbohydrate Polymers*, Vol. 209, pp. 20–37, 2019.

33. Caporgno, M. P. and A. Mathys, "Trends in microalgae incorporation into innovative food products with potential health benefits", *Frontiers in nutrition*, Vol. 5, No. 58, 2018.

34. Wu, Q., L. Liu, A. Miron, B. Klímová, D. Wan and K. Kuča, "The antioxidant, immunomodulatory, and anti-inflammatory activities of Spirulina: an overview", *Archives of Toxicology*, Vol. 90, No. 8, pp. 1817–1840, 2016.

35. Varol, A. and A. Ugurlu, "Biogas Production from Microalgae (Spirulina platensis) in a Two Stage Anaerobic System", *Waste and Biomass Valorization*, Vol. 7, No. 1, pp. 193–200, 2016.

36. Liu, J., J. Huang and F. Chen, "Microalgae as feedstocks for biodiesel production", *Biodiesel-Feedstocks and Processing Technologies*, IntechOpen, 2011.

37. Hanifzadeh, M., E. C. Garcia and S. Viamajala, "Production of lipid and carbohydrate from microalgae without compromising biomass productivities: Role of Ca and Mg", *Renewable energy*, Vol. 127, pp. 989–997, 2018.

38. Yap, B. H., S. A. Crawford, R. R. Dagastine, P. J. Scales and G. J. Martin, "Nitrogen deprivation of microalgae: effect on cell size, cell wall thickness, cell strength, and resistance to mechanical disruption", *Journal of industrial microbiology & biotechnology*, Vol. 43, No. 12, pp. 1671–1680, 2016.

39. Chen, M., H. Tang, H. Ma, T. C. Holland, K. Y. S. Ng and S. O. Salley, "Bioresource Technology Effect of nutrients on growth and lipid accumulation in the green algae Dunaliella tertiolecta", *Bioresource Technology*, Vol. 102, No. 2, pp. 1649–1655, 2011.

40. Karkos, P. D., S. C. Leong, C. D. Karkos, N. Sivaji and D. A. Assimakopoulos, "Spirulina in clinical practice: Evidence-based human applications", *Evidence-based Complementary and Alternative Medicine*, Vol. 2011, 2011.

41. Zhu, N., M. Ye, D. Shi and M. Chen, "Reactive compatibilization of biodegradable poly(butylene succinate)/Spirulina microalgae composites", *Macromolecular Research*, Vol. 25, No. 2, pp. 165–171, 2017.

42. Moreira, J. B., L. T. Lim, E. d. R. Zavareze, A. R. G. Dias, J. A. V. Costa and M. G. de Morais, "Microalgae protein heating in acid/basic solution for nanofibers production by free surface electrospinning", *Journal of Food Engineering*, Vol. 230, pp. 49–54, 2018.

43. Gadd, G. M., "Biosorption: critical review of scientific rationale , environmental importance and significance for pollution treatment", *Journal of Chemical Technology Biotechnology*, Vol. 84, No. 1, pp. 13–28, 2009.

44. Crini, G., "Recent developments in polysaccharide-based materials used as adsorbents in wastewater treatment", *Progress in polymer science*, Vol. 30, No. 1, pp. 38–70, 2005.

45. Tharanathan, R. N. and F. S. Kittur, "Chitin—the undisputed biomolecule of great potential", *Critical Reviews in Food Science and Nutrition*, Vol. 43, No. 1, pp. 61–87, 2003.

46. Desbrières, J. and E. Guibal, "Chitosan for wastewater treatment", *Polymer International*, Vol. 67, No. 1, pp. 7–14, 2017.

47. Singh, R. L. and R. P. Singh, *Advances in biological treatment of industrial waste water and their recycling for a sustainable future*, Springer, 2019.

48. Soeder, C. J., H.-D. Payer, K.-H. Runkel, J. Beine and E. Briele, "Sorption and concentration of toxic minerals by mass cultures of Chlorococcales", *Internationale Vereinigung für Theoretische und Angewandte Limnologie: Mitteilungen*, Vol. 21, No. 1, pp. 575–584, 1978.

49. Özer, A., G. Akkaya and M. Turabik, "Biosorption of acid blue 290 (AB 290)

and acid blue 324 (AB 324) dyes on Spirogyra rhizopus", *Journal of hazardous materials*, Vol. 135, No. 1-3, pp. 355–364, 2006.

50. Dotto, G. L., T. Cadaval and L. Pinto, "Use of Spirulina platensis micro and nanoparticles for the removal synthetic dyes from aqueous solutions by biosorption", *Process Biochemistry*, Vol. 47, No. 9, pp. 1335–1343, 2012.

51. Doshi, H., A. Ray, I. L. Kothari and B. Gami, "Spectroscopic and Scanning Electron Microscopy Studies of Bioaccumulation of Pollutants by Algae", *Current Microbiology*, Vol. 53, No. 2, pp. 148–157, 2006.

52. Aguirre, A.-M. and A. Bassi, "Investigation of biomass concentration, lipid production, and cellulose content in Chlorella vulgaris cultures using response surface methodology", *Biotechnology and bioengineering*, Vol. 110, No. 8, pp. 2114–2122, 2013.

53. Taylor, A. T. and S. E. Feller, "Structural studies of phycobiliproteins from Spirulina: Combining spectroscopy, thermodynamics, and molecular modeling in an undergraduate biochemistry experiment", *Journal of chemical education*, Vol. 79, No. 12, p. 1467, 2002.

54. Passos, F., E. Uggetti, H. Carrère and I. Ferrer, "Algal biomass: physical pretreatments", *Pretreatment of Biomass*, pp. 195–226, Elsevier, 2015.

55. Domozych, D. S., M. Ciancia, J. U. Fangel, M. D. Mikkelsen, P. Ulvskov and W. G. T. Willats, "The cell walls of green algae: a journey through evolution and diversity", *Frontiers in plant science*, Vol. 3, No. May, pp. 1–7, 2012.

56. Safi, C., B. Zebib, O. Merah, P.-Y. Pontalier and C. Vaca-Garcia, "Morphology, composition, production, processing and applications of Chlorella vulgaris: A review", *Renewable and Sustainable Energy Reviews*, Vol. 35, pp. 265–278, 2014.

57. Kumar, S. and K. Thakur, "Bioplastics - classification, production and their po-

tential food applications", *Journal of Hill Agriculture*, Vol. 8, No. 2, p. 118, 2017.

58. Gilbert, M., "Cellulose Plastics", *Brydson's Plastics Materials*, pp. 617–630, Elsevier, 2017.

59. Anal, A. K. and A. Tuladhar, "Biopolymeric micro-and nanoparticles: preparation, characterization and industrial applications", *Multifaceted Development and Application of Biopolymers for Biology, Biomedicine and Nanotechnology*, pp. 269–295, Springer, 2013.

60. van Beilen, J. B. and Y. Poirier, "Plants as factories for bioplastics and other novel biomaterials", *Plant Biotechnology and Agriculture*, pp. 481–494, Elsevier, 2012.

61. Mekonnen, T., M. Misra and A. Mohanty, "Processing, performance, and applications of plant and animal protein-based blends and their biocomposites", *Biocomposites*, pp. 201–235, Elsevier, 2015.

62. Song, Y. and Q. Zheng, "Ecomaterials based on food proteins and polysaccharides", *Polymer Reviews*, Vol. 54, No. 3, pp. 514–571, 2014.

63. Chronakis, I. S., "Gelation of edible blue-green algae protein isolate (Spirulina platensis strain pacifica): thermal transitions, rheological properties, and molecular forces involved", *Journal of agricultural and food chemistry*, Vol. 49, No. 2, pp. 888–898, 2001.

64. Fabra, M. J., M. Martínez-Sanz, L. G. Gómez-Mascaraque, R. Gavara and A. López-Rubio, "Structural and physicochemical characterization of thermoplastic corn starch films containing microalgae", *Carbohydrate Polymers*, Vol. 186, pp. 184–191, 2018.

65. Moreira, J. B., L. T. Lim, E. d. R. Zavareze, A. R. G. Dias, J. A. V. Costa and M. G. de Morais, "Antioxidant ultrafine fibers developed with microalga

compounds using a free surface electrospinning", *Food Hydrocolloids*, Vol. 93, pp. 131–136, 2019.

66. Morais, M. G. d., B. d. S. Vaz, E. G. d. Morais and J. A. V. Costa, "Biological effects of Spirulina (Arthrospira) biopolymers and biomass in the development of nanostructured scaffolds", *BioMed research international*, Vol. 2014, 2014.

67. Sabbah, M., C. V. L. Giosafatto, M. Esposito, P. Di Pierro, L. Mariniello and R. Porta, "Transglutaminase cross-linked edible films and coatings for food applications", *Enzymes in Food Biotechnology*, pp. 369–388, Elsevier, 2019.

68. Sorrentino, A., P. Di Pierro, R. Porta, L. Mariniello, G. Rossi Marquez and R. Villalonga, "Effect of Transglutaminase on the Mechanical and Barrier Properties of Whey Protein/Pectin Films Prepared at Complexation pH", *Journal of Agricultural and Food Chemistry*, Vol. 61, No. 19, pp. 4593–4598, 2013.

69. Porta, R., P. Di Pierro, G. Rossi-Marquez, L. Mariniello, M. Kadivar and A. Arabestani, "Microstructure and properties of bitter vetch (Vicia ervilia) protein films reinforced by microbial transglutaminase", *Food Hydrocolloids*, Vol. 50, pp. 102–107, 2015.

70. Pasternack, R., S. Dorsch, J. T. Otterbach, I. R. Robenek, S. Wolf and H.-L. Fuchsbauer, "Bacterial pro-transglutaminase from Streptoverticillium mobaraense: Purification, characterisation and sequence of the zymogen", *European Journal of Biochemistry*, Vol. 257, No. 3, pp. 570–576, 1998.

71. Andersen, R. A., *Algal culturing techniques*, Elsevier, 2005.

72. Ho, Y.-S. and G. McKay, "Pseudo-second order model for sorption processes", *Process biochemistry*, Vol. 34, No. 5, pp. 451–465, 1999.

73. Allen, S., G. McKay and K. Khader, "Intraparticle diffusion of a basic dye during adsorption onto sphagnum peat", *Environmental Pollution*, Vol. 56, No. 1, pp.

39–50, 1989.

74. Vijayaraghavan, K. and Y. Yun, "Bacterial biosorbents and biosorption", *Bacterial biosorbents and biosorption. Biotechnology Advances*, Vol. 26, pp. 266–291, 2008.

75. Khataee, A., F. Vafaei and M. Jannatkhah, "Biosorption of three textile dyes from contaminated water by filamentous green algal Spirogyra sp.: Kinetic, isotherm and thermodynamic studies", *International Biodeterioration & Biodegradation*, Vol. 83, pp. 33–40, 2013.

76. Ncibi, M., A. B. Hamissa, A. Fathallah, M. Kortas, T. Baklouti, B. Mahjoub and M. Seffen, "Biosorptive uptake of methylene blue using Mediterranean green alga Enteromorpha spp.", *Journal of Hazardous Materials*, Vol. 170, No. 2-3, pp. 1050–1055, 2009.

77. Safi, C., A. V. Ursu, C. Laroche, B. Zebib, O. Merah, P.-Y. Pontalier and C. Vaca-Garcia, "Aqueous extraction of proteins from microalgae: effect of different cell disruption methods", *Algal Research*, Vol. 3, pp. 61–65, 2014.

78. Kjeldahl, J., "Neue methode zur bestimmung des stickstoffs in organischen körpern", *Fresenius' Journal of Analytical Chemistry*, Vol. 22, No. 1, pp. 366–382, 1883.

79. Laemmli, U. K., "Cleavage of structural proteins during the assembly of the head of bacteriophage T4", *Nature*, Vol. 227, No. 5259, p. 680, 1970.

80. Aksu, Z. and S. Tezer, "Biosorption of reactive dyes on the green alga Chlorella vulgaris", *Process Biochemistry*, Vol. 40, No. 3-4, pp. 1347–1361, 2005.

81. Pathak, V. V., R. Kothari, A. Chopra and D. Singh, "Experimental and kinetic studies for phycoremediation and dye removal by Chlorella pyrenoidosa from textile wastewater", *Journal of environmental management*, Vol. 163, pp. 270–277,

2015.

82. Plazinski, W., J. Dziuba and W. Rudzinski, "Modeling of sorption kinetics: the pseudo-second order equation and the sorbate intraparticle diffusivity", *Adsorption*, Vol. 19, No. 5, pp. 1055–1064, 2013.

83. Saikia, J. and G. Das, "Framboidal vaterite for selective adsorption of anionic dyes", *Journal of Environmental Chemical Engineering*, Vol. 2, No. 2, pp. 1165–1173, 2014.

84. Goldberg, S., M. Tabatabai, D. Sparks, L. Al-Amoodi and W. Dick, "Equations and models describing adsorption processes in soils", *Soil Science Society of America Book Series*, Vol. 8, p. 489, 2005.

85. Malek, K., B. R. Wood and K. R. Bambery, "FTIR imaging of tissues: techniques and methods of analysis", *Optical spectroscopy and computational methods in biology and medicine*, pp. 419–473, Springer, 2014.

86. Ovchinnikov, O. V., A. V. Evtukhova, T. S. Kondratenko, M. S. Smirnov, V. Y. Khokhlov and O. V. Erina, "Manifestation of intermolecular interactions in FTIR spectra of methylene blue molecules", *Vibrational Spectroscopy*, Vol. 86, pp. 181–189, 2016.

87. Bartošová, A., L. Blinová, M. Sirotiak and A. Michalíková, "Usage of FTIR-ATR as non-destructive analysis of selected toxic dyes", *Research Papers Faculty of Materials Science and Technology Slovak University of Technology*, Vol. 25, No. 40, pp. 103–111, 2017.

88. Shi, B., L. Liang, H. Yang, L. Zhang and F. He, "Glycerol-plasticized spirulina–poly (vinyl alcohol) films with improved mechanical performance", *Journal of Applied Polymer Science*, Vol. 134, No. 20, 2017.

89. Matsumura, S., H. Kurita and H. Shimokobe, "Anaerobic biodegradability of

polyvinyl alcohol", *Biotechnology letters*, Vol. 15, No. 7, pp. 749–754, 1993.

90. Marušincová, H., L. Husárová, J. Ržička, M. Ingr, V. Navrátil, L. Buňková and M. Koutny, "Polyvinyl alcohol biodegradation under denitrifying conditions", *International Biodeterioration & Biodegradation*, Vol. 84, pp. 21–28, 2013.

91. Singh, P. and S. Kumar, "Microbial Enzyme in Food Biotechnology", *Enzymes in Food Biotechnology*, pp. 19–28, Elsevier, 2019.

92. Porta, R., L. Mariniello, P. Di Pierro, A. Sorrentino and C. V. L. Giosafatto, "Transglutaminase crosslinked pectin-and chitosan-based edible films: A review", *Critical reviews in food science and nutrition*, Vol. 51, No. 3, pp. 223–238, 2011.

93. Al-Hassan, A. and M. Norziah, "Effect of transglutaminase induced crosslinking on the properties of starch/gelatin films", *Food Packaging and Shelf Life*, Vol. 13, pp. 15–19, 2017.

94. Tang, C.-H., Y. Jiang, Q.-B. Wen and X.-Q. Yang, "Effect of transglutaminase treatment on the properties of cast films of soy protein isolates", *Journal of Biotechnology*, Vol. 120, No. 3, pp. 296–307, 2005.

95. Safi, C., M. Charton, O. Pignolet, F. Silvestre, C. Vaca-Garcia and P.-Y. Pontalier, "Influence of microalgae cell wall characteristics on protein extractability and determination of nitrogen-to-protein conversion factors", *Journal of applied phycology*, Vol. 25, No. 2, pp. 523–529, 2013.

96. Chronakis, I. S., A. N. Galatanu, T. Nylander and B. Lindman, "The behaviour of protein preparations from blue-green algae (Spirulina platensis strain Pacifica) at the air/water interface", *Colloids and Surfaces A: Physicochemical and Engineering Aspects*, Vol. 173, No. 1-3, pp. 181–192, 2000.

97. Lupatini, A. L., L. de Oliveira Bispo, L. M. Colla, J. A. V. Costa, C. Canan and E. Colla, "Protein and carbohydrate extraction from S. platensis biomass by

ultrasound and mechanical agitation", *Food research international*, Vol. 99, pp. 1028–1035, 2017.

98. Benelhadj, S., A. Gharsallaoui, P. Degraeve, H. Attia and D. Ghorbel, "Effect of pH on the functional properties of Arthrospira (Spirulina) platensis protein isolate", *Food Chemisty*, Vol. 194, pp. 1056–1063, 2016.

99. Simó, C., M. Herrero, C. Neusüß, M. Pelzing, E. Kenndler, C. Barbas, E. Ibáñez and A. Cifuentes, "Characterization of proteins from Spirulina platensis microalga using capillary electrophoresis-ion trap-mass spectrometry and capillary electrophoresis-time of flight-mass spectrometry", *Electrophoresis*, Vol. 26, No. 13, pp. 2674–2683, 2005.

100. Padyana, A. K., V. B. Bhat, K. Madyastha, K. Rajashankar and S. Ramakumar, "Crystal structure of a light-harvesting protein C-phycocyanin from Spirulina platensis", *Biochemical and biophysical research communications*, Vol. 282, No. 4, pp. 893–898, 2001.

101. Porta, R., P. Di, M. Sabbah, C. Regalado-gonzales and L. Mariniello, "Blend fi lms of pectin and bitter vetch (Vicia ervilia) proteins : Properties and effect of transglutaminase", Vol. 36, pp. 245–251, 2016.

102. Acevedo-Fani, A., L. Salvia-Trujillo, M. A. Rojas-Graü and O. Martín-Belloso, "Edible films from essential-oil-loaded nanoemulsions: Physicochemical characterization and antimicrobial properties", *Food Hydrocolloids*, Vol. 47, pp. 168–177, 2015.

APPENDIX A: SUPPORTING FIGURES

The full FT-IR spectra of *Chlorella* and *Scedenesmus* after MB, EBT and CR adsorptions along with full spectra of these dyes are given in this section.

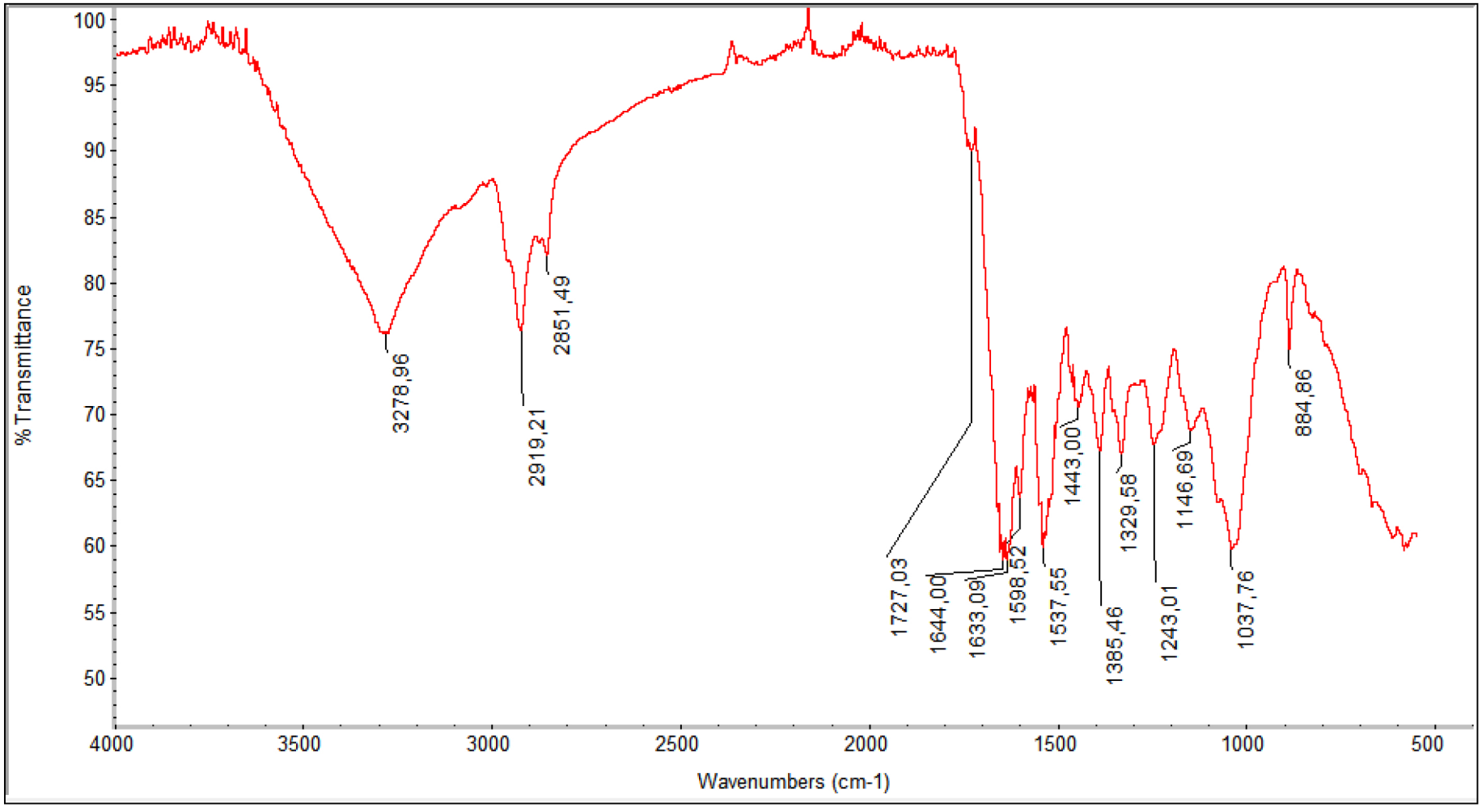

Figure A.1. Full FT-IR spectrum of *Chlorella*-MB.

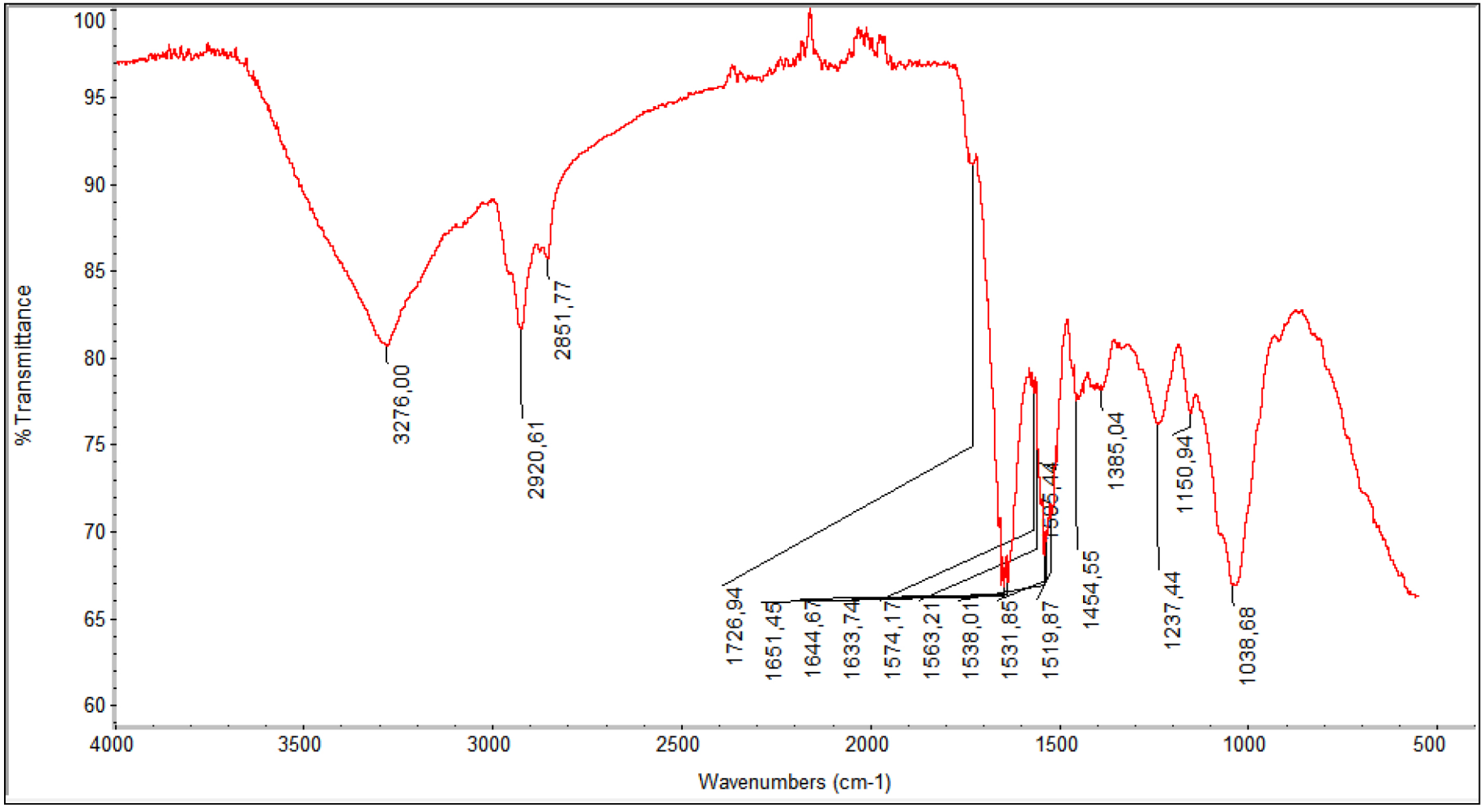

Figure A.2. Full FT-IR spectrum of *Chlorella*-EBT.

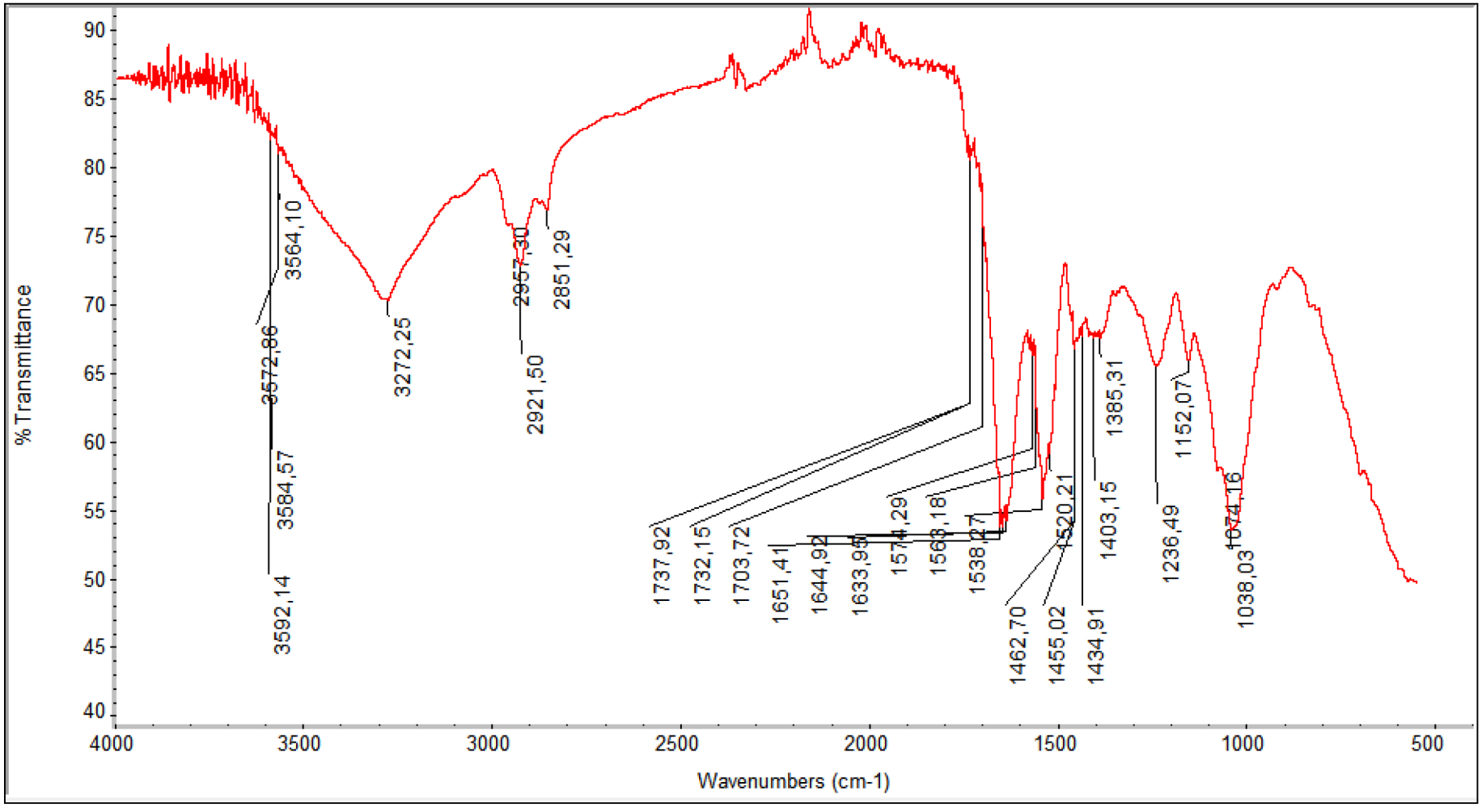

Figure A.3. Full FT-IR spectrum of *Chlorella*-CR.

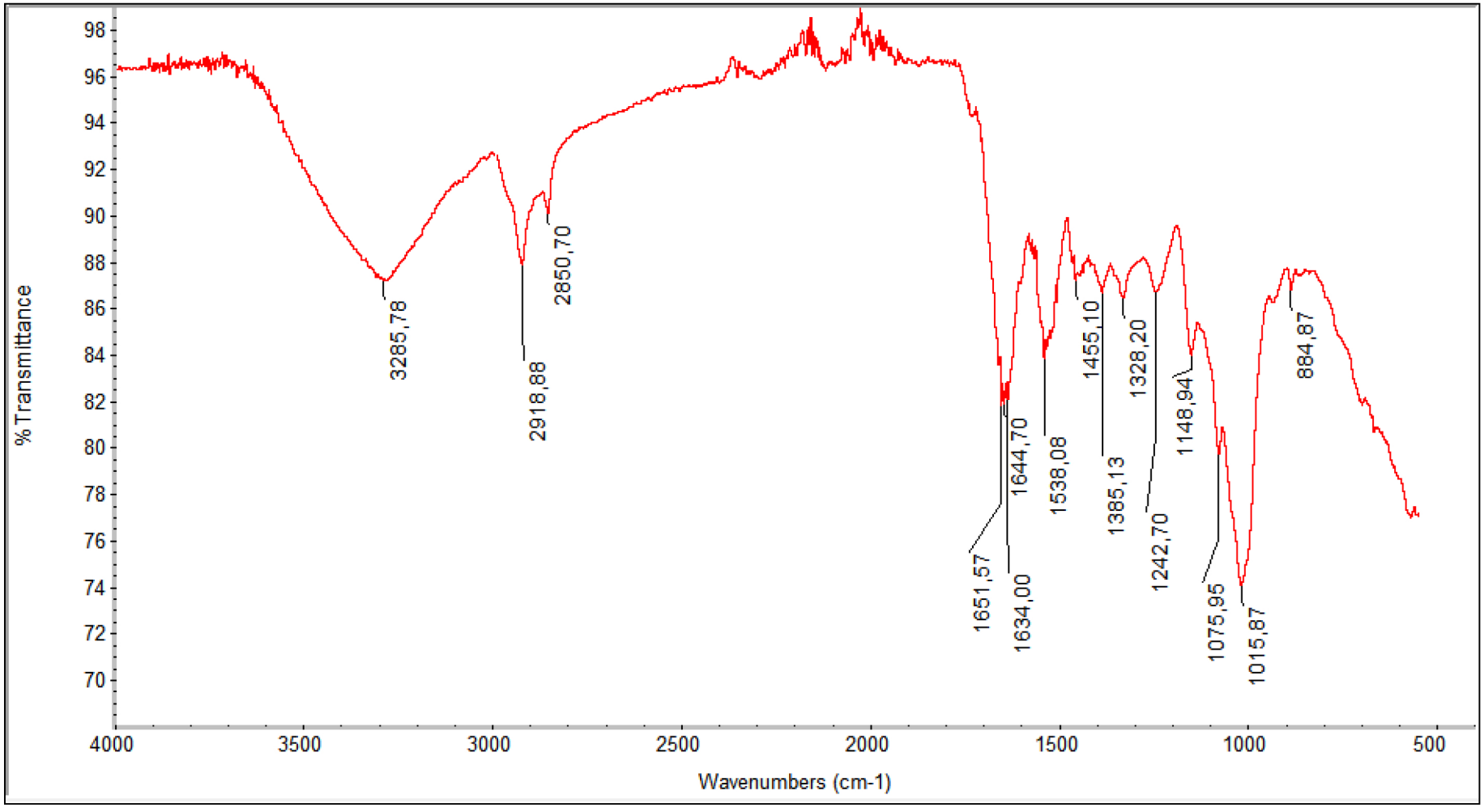

Figure A.4. Full FT-IR spectrum of *Scenedesmus*-MB.

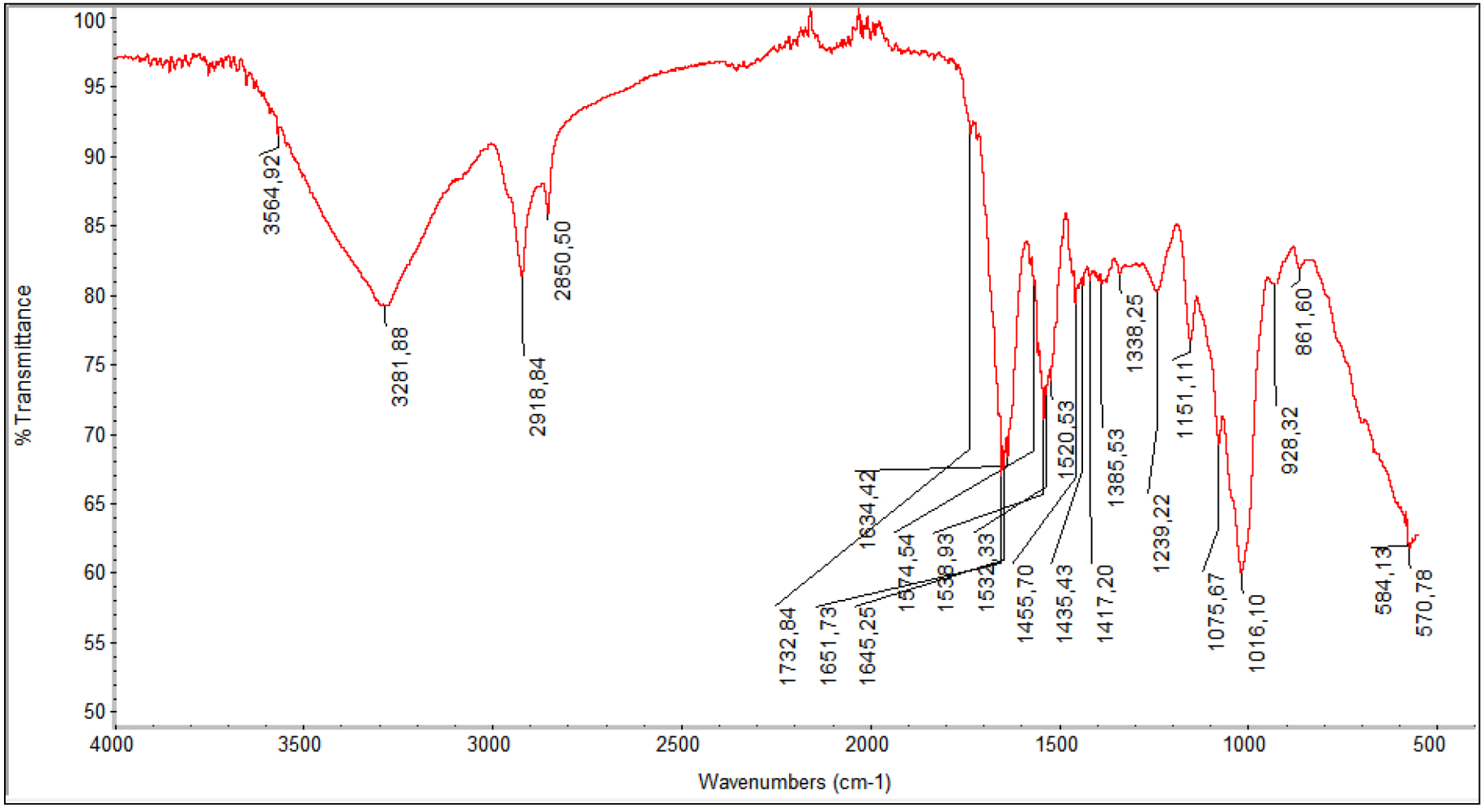

Figure A.5. Full FT-IR spectrum of *Scenedesmus*-EBT.

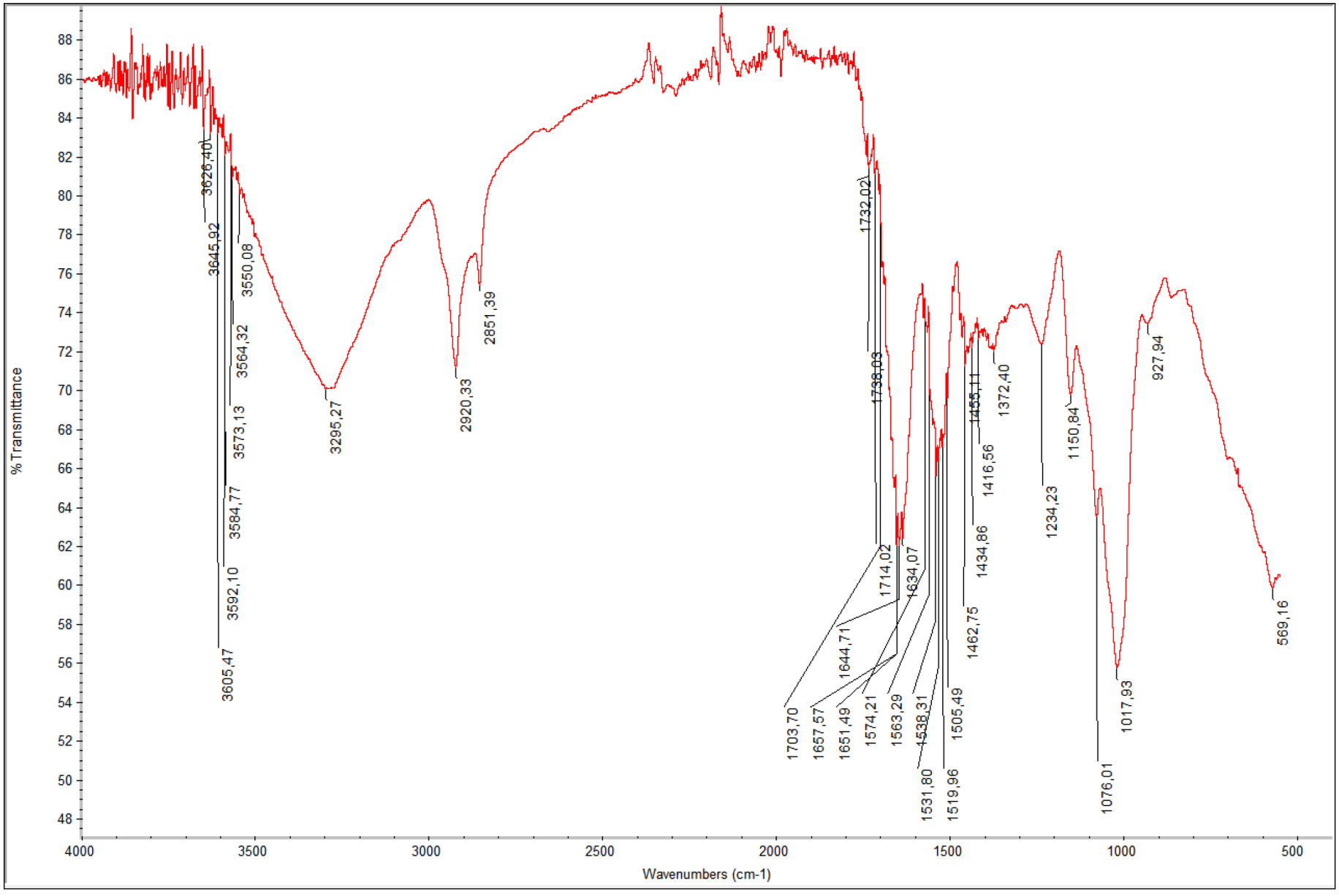

Figure A.6. Full FT-IR spectrum of *Scenedesmus*-CR.

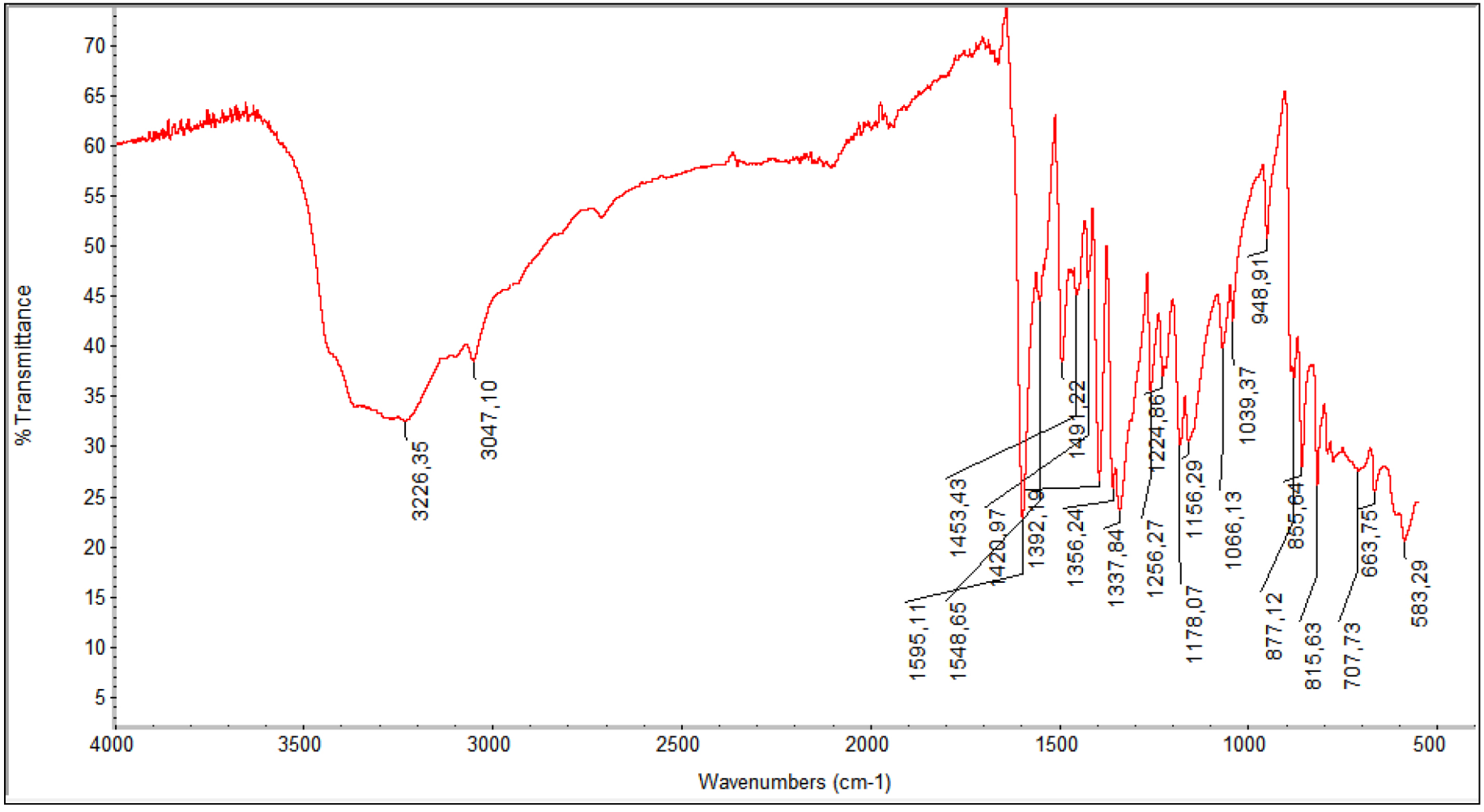

Figure A.7. Full FT-IR spectrum of MB.

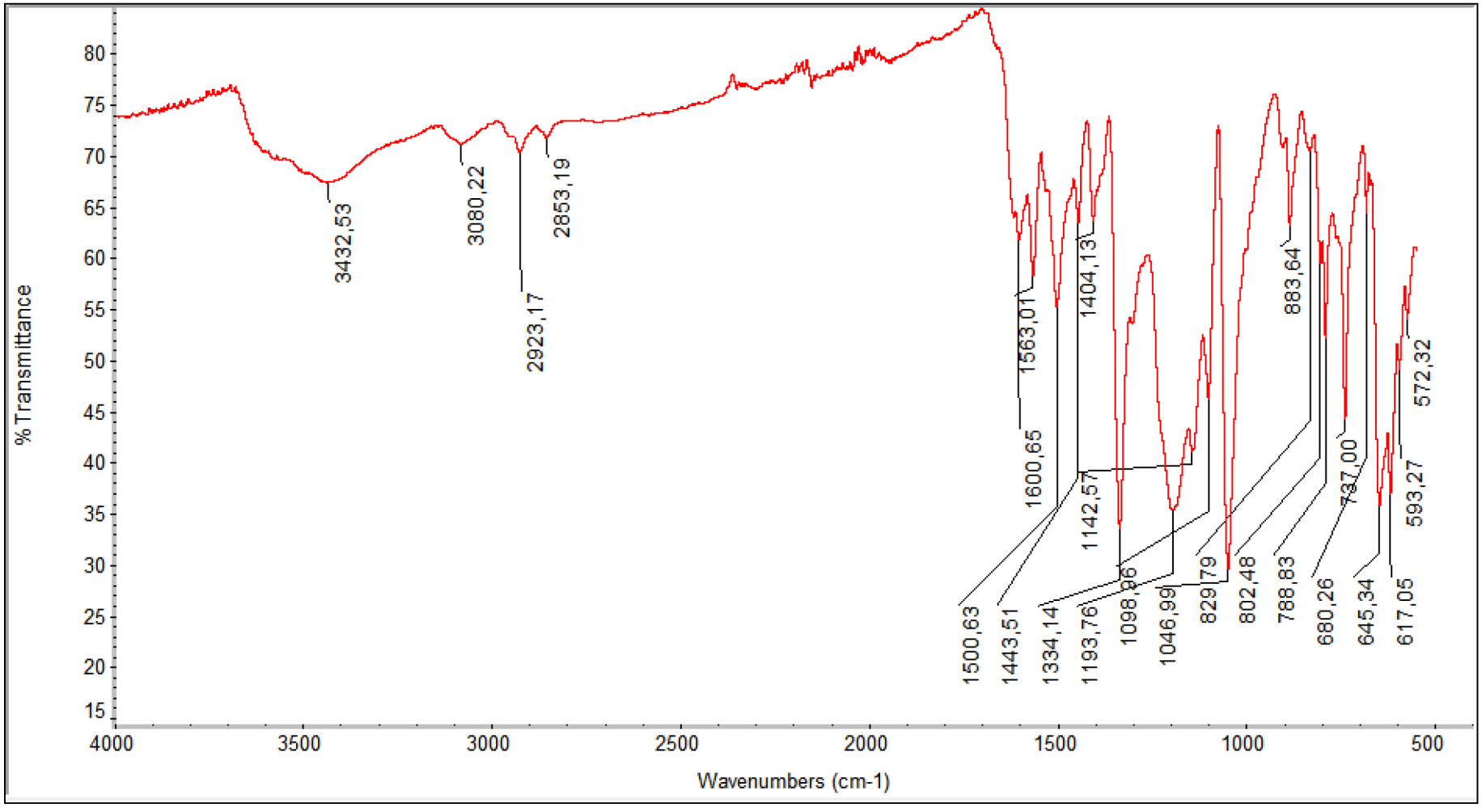

Figure A.87. Full FT-IR spectrum of EMBT.

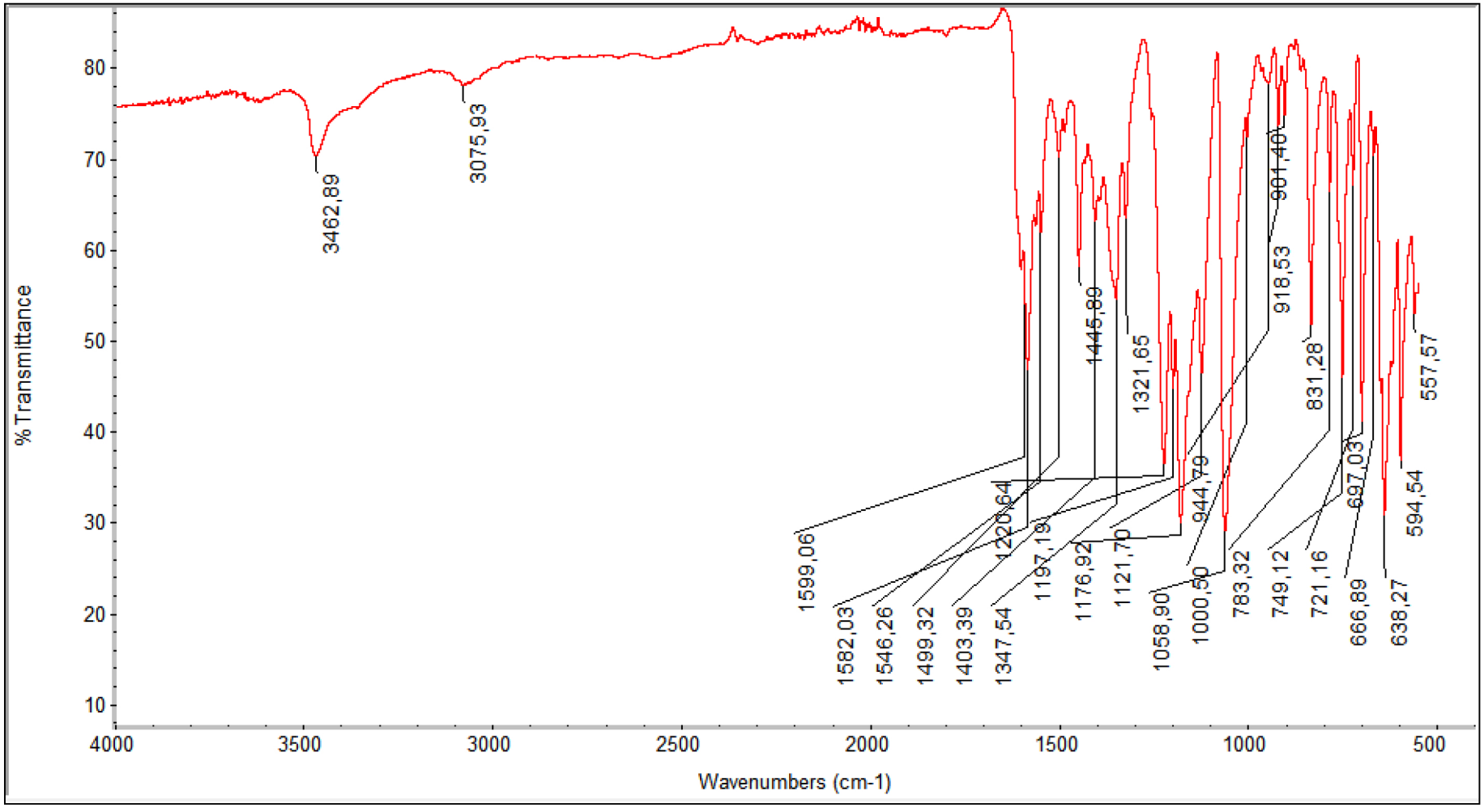

Figure A.9. Full FT-IR spectrum of CR.